# Amorphous Drug-Polymer Salts: Effect of Processing Conditions and Polymer Choice on Pharmaceutical Performance

by
Amy Lan Neusaenger

A dissertation submitted in partial fulfillment of

the requirements for the degree of

Doctor of Philosophy

(Pharmaceutical Sciences)

at the

UNIVERSITY OF WISCONSIN-MADISON

2025

Date of Final Oral Examination: May 22nd, 2025

The dissertation is approved by the following members of the Final Oral Committee:
Lian Yu, Professor, Pharmacy
Sandro Mecozzi, Professor, Pharmacy
Quanyin Hu, Associate Professor, Pharmacy
Mark Ediger, Professor, Chemistry

*To my family*

# Acknowledgements

As I reflect on the past five years, I am so deeply honored to recognize the multitude of people that have made this journey possible. I have zero doubts that without their support I would not have made it this far.

I sincerely thank Dr. Yu for his unwavering commitment to my journey as a scientist. His teachings both in and out of the lab are gifts I will carry with me for years to come, and I am confident that I am leaving UW-Madison with an unparalleled foundation for the rest of my career. I am grateful for the input and guidance of my committee members: Dr. Hu, Dr. Ediger, and Dr. Mecozzi, I cannot thank you enough for all that you've done to ensure my success.

Every day I am in awe of my luck to be a part of a lab whose members I respect and cherish so much. I could not have asked for a better start to my scientific career than that made possible by the endlessly patient and kind mentorship provided by Xin Yao, Junguang Yu, and Yuhui Li. You set a standard for leadership and teaching that I aspire toward to this day. I am so unbelievably thankful for each of my current lab members, who have played a monumental role in virtually every component of my Ph.D. career—I could not imagine a more incredible group of women to share a lab with. Kennedy, you are what I picture when I think of an ideal scientist and the kind I strive to be: honest, diligent, patient, and endlessly committed to her work. Thank you for helping me keep my head on straight these past five years. Caroline, I will sorely miss having you around. You are the perfect confidant, a wonderful friend, and a talented scientist whose resilience, humility, and intelligence I sincerely admire. Erika, I firmly believe you are the kind of person our field needs more of: you are curious, open-minded, and have the power to create sunshine in any room. I don't know where you'll end up after you graduate, but I know the people you surround yourself with will quickly realize they're incredibly lucky to have you. Yichun, I am so envious of your effortless kindness, patience, and strength and I hope you know how much we love having you around! You are an incredible person and scientist and so deserving of all the success that comes your way. Mayra and Xinran, I am. truly disappointed to have had so little time to get to know you both but it's already clear that you're both wonderful additions to the lab. I can't wait to see all that you accomplish in the next few years.

It is an impossible task to put into words the depth of my gratitude for my family, but I will attempt to do so. To my parents, I cannot fathom what I have done to deserve such unconditional support and constant encouragement over the years, but I am thankful anyway. I am certain I wouldn't have made it even half as far without you both, and I'm so lucky to know that no matter what, I can turn to you when I'm in need. Although unintentionally, Austin gave me the motivation to forge this career path; the choices that brought me to this point can be traced back to him. And to AJ, who has been by my side for almost my entire time in Madison, I cannot understate how important you have been to my ability to continue this journey even during its most difficult parts. You've been my rock through it all, and I only hope someday I can return the favor.

# Table of Contents

Acknowledgements…… iii
Abstract…… vii
Chapter 1. Introduction…… 1
1.1. Overview…… 2
1.2. Challenges in Oral Drug Delivery…… 3
1.3. Amorphous Solids…… 5
1.4. Amorphous Solid Dispersions…… 7
1.5. Contributions of this Thesis…… 15
1.6. References…… 17
Chapter 2. Amorphous drug-polymer salts: maximizing proton transfer to enhance stability and release…… 22
2.1. Abstract…… 23
2.2. Introduction…… 24
2.3. Materials & Methods…… 26
2.4. Results & Discussion…… 28
2.5. Conclusions…… 39
2.6. Acknowledgements…… 40
2.7. References…… 41
Chapter 3. Effect of polymer architecture and acidic group density on the degree of salt formation in amorphous solid dispersions…… 43
3.1. Abstract…… 44
3.2. Introduction…… 45
3.3. Materials & Methods…… 47
3.4. Results & Discussion…… 50
3.5. Conclusions…… 59
3.6. Acknowledgements…… 60
3.7. References…… 61
Chapter 4. Slurry conversion: A general method for formulating amorphous solid dispersions and fully integrating drug and polymer components…… 63

4.1. Abstract…… 64
4.2. Introduction…… 65
4.3. Materials & Methods…… 67
4.4. Results & Discussion…… 69
4.5. Conclusions…… 83
4.6. Acknowledgements…… 84
4.7. References…… 85
Chapter 5. Optimizing drug nanoparticle release from amorphous solid dispersions: exceptional performance of poly(acrylic acid) for releasing lumefantrine…… 89
5.1. Abstract…… 90
5.2. Introduction…… 91
5.3. Materials & Methods…… 94
5.4. Results…… 96
5.5. Discussion…… 107
5.6. Conclusions…… 111
5.7. Acknowledgements…… 112
5.8. References…… 113
Chapter 6. Conclusions and Future work…… 115
6.1. Synthesis and characterization of amorphous drug-polymer salts…… 116
6.2. Modified release of amorphous drug-polymer salts…… 121
6.3. References…… 123

## Abstract

This dissertation considers the formulation and performance of amorphous solid dispersions (ASDs), particularly amorphous drug-polymer salts.

An increasing number of newly identified drug candidates are poorly water soluble, creating a challenging bottleneck in the drug development pipeline that requires alternative formulation approaches to circumvent. ASDs are one of the most popular of these approaches, wherein a poorly soluble drug in its amorphous form is molecularly dissolved in a polymeric carrier. Previous work has shown that an amorphous drug-polymer salt can have significant performance advantages, including long-term stability under accelerated storage conditions and efficient drug release with sustained supersaturation.

Here we investigate the factors contributing to an effective amorphous drug-polymer salt, including 1) the manufacturing and processing conditions used to synthesize the formulation and 2) the structure and properties of the polymeric carrier. We find that in the case of lumefantrine (LMF) ASDs formulated with poly(acrylic acid) (PAA), efficient drug-polymer salt formation is facilitated by a simple slurry conversion synthesis procedure which outperforms other conventional ASD manufacturing methods including spray drying, hot melt extrusion, and rotary evaporation. This extensive salt formation is well-correlated with the performance of the formulation, with a compositionally identical melt-quenched ASD with a lower degree of salt formation underperforming that prepared by slurry conversion in both stability and dissolution tests. For LMF dispersed in other acidic polymers, the degree of salt formation achievable was found to be primarily determined by the polymer's acidic group density obtained from non-aqueous titration.

Additional study of the slurry conversion method and its generality reveals applicability to a majority of the poorly soluble drugs surveyed. In addition to the previously described LMF, 17 additional poorly soluble drugs including 15 basic, 1 neutral, and 1 acidic drug were formulated with PAA using the standard SC synthesis. Fully amorphous dispersions were successfully prepared under these synthesis conditions for 16 of the 18 drugs at 25% DL and 11 at 50% DL, with most formulations undergoing an observable "clearing" during stirring, indicating complete dissolution and amorphization prior to drying. Furthermore, it was shown that SC could be used

to prepare ternary ASDs (two drugs dispersed in PAA) and could also be scaled up at least 60-fold for LMF-PAA at 50% DL with only minor modifications to the stirring method. This demonstrated versatility of the slurry method is encouraging given its very low equipment cost, lower solvent usage than other solvent-based methods, and low energy consumption.

Work on ASD dissolution has observed the formation of drug-rich particles that may enhance drug release and supersaturation. For LMF-PAA ASDs dispersed in 0.1% sodium dodecyl sulfate (a common medium for dissolution testing), we find that PAA outperforms other polymers in releasing LMF as nanoparticles and reaching a high apparent solubility (AS), measured after filtration through a 0.2 μm filter. This outperformance of PAA over 9 other dispersion polymers (7 acidic and 2 neutral) persists from 25 to 50% DL, both releasing the greatest amount of LMF and producing the largest volume fraction of small-size (~10 nm) particles. These findings are especially notable considering the high degree of solid-state stability of these same LMF-PAA formulations, showing that if the solubility of a formulation is defined to include both true solubility and apparent solubility (of dispersed nanoparticles), an amorphous drug-polymer salt can be simultaneously stable and soluble. PAA's superior performance in this study suggests its potential viability as a new dispersion polymer and motivates further exploration of its dispersion capabilities.

# Chapter 1: Introduction

Amy Lan Neusaenger

## 1.1. Overview

Glasses are amorphous materials that can be found in a range of different industries with a variety of unique applications. Of particular interest to this work are pharmaceutical glasses, which can be used to overcome formulation obstacles presented by poorly soluble drugs.[1,2] The primary focus of this thesis will be on the preparation of these drugs as amorphous drug-polymer salts with enhanced solid-state stability and drug release properties. The goal of this chapter is to familiarize the reader with the fundamentals of amorphous solids and amorphous solid dispersions (ASDs) and the way they are generally utilized in conventional pharmaceutical manufacturing and drug delivery. Additionally, this chapter will provide an overview and discussion of recent progress in the formulation and performance of amorphous drug-polymer salts. Finally, this chapter will describe the current understanding of the phenomenon of nanoparticle formation during ASD dissolution, a behavior increasingly investigated as a method of solubility enhancement and potentially advantageous release mechanism that can be exploited to promote more efficient drug release and supersaturation.

In Chapter 2, we consider the influence of ionic drug-polymer interactions on the stability and release of a model ASD system. In Chapter 3, we expand on this work to investigate the role of polymer choice on this degree of salt formation in an ASD and how this property is influenced by the processing conditions used to manufacture the formulation. In Chapter 4, we turn to a broad selection of poorly soluble APIs, considering a general ASD synthesis method and the degree of salt formation it facilitates. Chapter 5 will in greater detail consider the dispersion of these ASDs in aqueous dissolution medium and the factors underlying high apparent ASD solubility and the role of polymer choice in promoting ASD solubility. Finally, Chapter 6 will discuss the primary conclusions of the work described in this thesis and potential future areas of further investigation.

## 1.2. Challenges in Oral Drug Delivery

Oral solid dosage forms are the most common drug delivery route due to their cost-effectiveness, storage stability, and ease of administration.[3] In order for an ingested active pharmaceutical ingredient (API) to reach its intended site of action, it must first attain sufficient dissolution and subsequent permeation in the gastrointestinal (GI) system.

The ability of a neat API to achieve these benchmarks can be broadly understood using the Biopharmaceutical Classification System (BCS), first introduced by Amidon et al. to categorize APIs into one of four classes based on their solubility and permeability (Fig. 1).[4] A drug is considered to have high solubility if its highest clinical dose strength is soluble in 250 mL or less of aqueous media between pH 1 – 7.5 at 37.5 deg. C.

With the introduction of high-throughput screening methods for potential APIs that tend to have higher molecular weights and greater lipophilicity,[5] poor aqueous solubility presents a challenging bottleneck in the drug development pipeline: approximately 90% of drugs in the R&D pipeline are poorly water-soluble.[6,7] Poor aqueous solubility can lead to insufficient efficacy, patient-to-patient variation, and erratic absorption if formulation is not carefully controlled.

**Fig. 1**. Biopharmaceutical classification system (BCS)

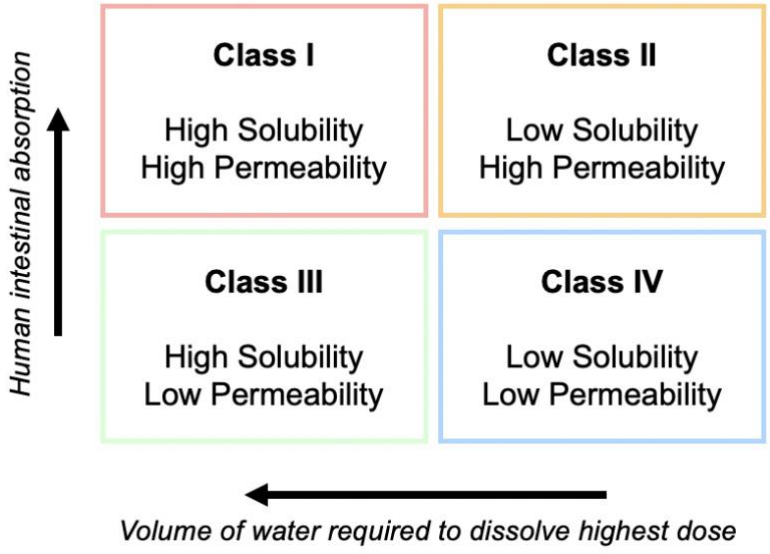

A number of approaches have been used to enhance the low aqueous solubility of BCS class II and IV APIs, including pH modulation,[8,9] particle size reduction,[10,11] solid dispersions,[12,13,14] cocrystals,[15,16] and cyclodextrin complexes.[17]

An alternative, increasingly common approach to the solubilization of these challenging APIs is amorphization, wherein the drug is formulated in its amorphous form rather than its crystalline form.[18] Most drug products contain a crystalline API due to their inherent stability and purity, but the high lattice energy barrier and low free energy of a crystalline material can significantly limit aqueous solubility. An amorphous state instead has no long-range molecular order, disrupting the stable crystal lattice and increasing its free energy, leading to higher solubility and subsequent absorption.[19] However, this solubility advantage is lost upon recrystallization of an amorphous drug, making the stabilization and crystallization inhibition of the formulation a critical step to ensure its optimal and consistent performance.[20]

A common approach to the stabilization of amorphous drugs is an amorphous solid dispersion, wherein the amorphous drug is molecularly dispersed in a suitable polymer that restricts molecular mobility, reduces the driving force for crystallization, and provides a stable carrier matrix.[21,22,23,24] An early example of marketed amorphous solid dispersion (ASD) was approved in 1985, consisting of the synthetic cannabinoid molecule nabilone dispersed in polyvinylpyrrolidone (PVP) under the brand name Cesamet®.[25] Since the introduction of this product, ASDs represent an increasingly popular formulation approach, with 48 drug products containing ASDs approved by the FDA between 2012 and 2023.[26] The growing popularity of ASDs as a drug delivery technology and increasing population of poorly soluble drug candidates necessitates careful consideration of the properties affecting ASD performance and how this performance can be optimized for particularly challenging APIs.

## 1.3. Amorphous Solids

Amorphous solids can be prepared in a number of ways depending on their glass-forming ability. An amorphous solid can form by cooling a melt, evaporating a solution, and mechanically damaging a crystal.[27,28] A crystalline drug undergoes melting at temperature $T_m$ generating a melt.[29] Slow cooling of this melt permits the molecules to rearrange into the preferred order, reforming the crystalline structure. Alternatively, rapid cooling of an effective glass-former may instead generate a metastable glassy state below the drug's characteristic glass transition temperature ($T_g$) as shown in Fig. 2).[30] At this temperature, the system undergoes a marked change in heat capacity (thermal expansion coefficient) causing a slope change of enthalpy (volume) and deviates from the equilibrium behavior (dotted line).[31] The glassy state has a liquid-like structure but is mechanically a solid. It is important to note that the glass transition is not a true thermodynamic phase transition and exhibits a dependence on the cooling rate. The solid nature of a glass

**Fig. 2.** Enthalpy and volume of a theoretical drug as a function of temperature. $T_m$ and $T_g$ represent melting temperature and glass transition temperature, respectively. The red star notes the change in slope that corresponds to glass formation.

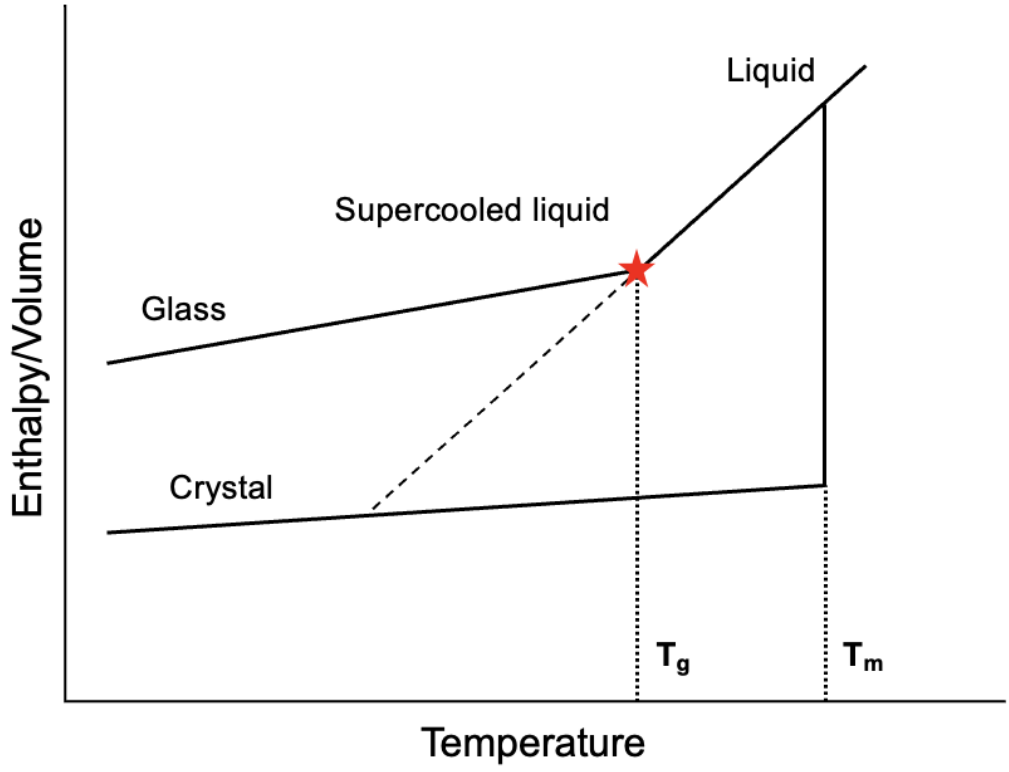

originates from the reduction in molecular mobility in this "frozen" state below $T_g$. An amorphous drug in this state has a higher free energy and solubility than its crystalline counterpart. This advantage can be better preserved via dispersion in a suitable carrier polymer, forming an amorphous solid dispersion (ASD) which reduce the molecular mobility, and the thermodynamic driving force required crystal nucleation and growth.[32]

**Fig. 3.** Illustration of relative chemical potential (μ) and activation energy required for drug crystallization ($E_A$) of amorphous drug and amorphous solid dispersions. The term ($\Delta\mu_1 - \Delta\mu_2$) represents the decrease of the thermodynamic driving force of crystallization by forming an amorphous solid dispersion. and subsequently enhanced solubility (not to scale).

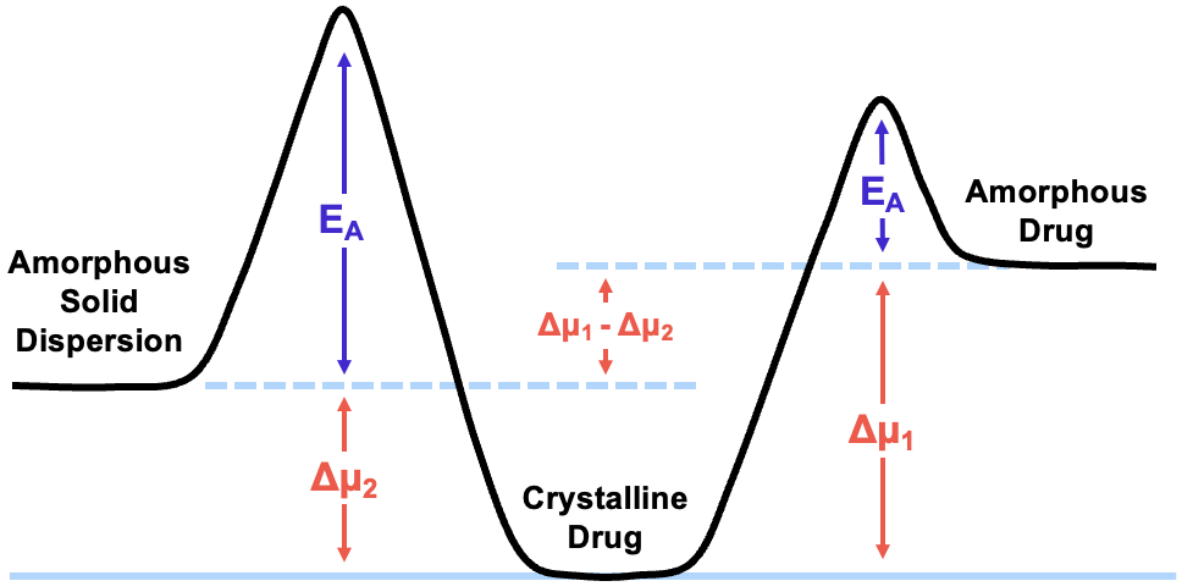

## 1.4. Amorphous Solid Dispersions

A successful ASD carrier polymer offers a variety of benefits including kinetic stabilization of the amorphous drug, elevating the formulation's $T_g$ and resistance to crystallization in the solid state as well as wettability and supersaturation during dissolution. The dissolution of a drug in a polymer lowers the chemical potential of the drug and increases the activation energy for its crystallization as shown in Fig. 3.[20,33,] Selection of the polymer matrix used to formulate an ASD is a critical formulation step and must take into account both the physicochemical properties of the drug as well as the desired manufacturing strategy and dissolution profile (i.e. gastric vs. intestinal release, controlled vs. rapid release). Carrier polymers must generally be chemically and pharmacologically inert and have Generally Recognized As Safe (GRAS) status. They must also be sufficiently miscible with the amorphous drug of choice with a sufficiently high $T_g$ to ensure stability at room temperature.[34] Additionally, qualities such as solubility in organic solvents or thermoplasticity may also be required depending on the manufacturing strategy chosen. More recently, specific interactions between drug and polymer have been shown to impact both the stability and release of an ASD, making the potential for a carrier polymer to form hydrogen or ionic bonds with the dispersed drug another important consideration.[35,36] Common polymers used in ASD formulation include vinyl pyrrolidone derivatives (polyvinylpyrrolidone (PVP),[37] vinyl pyrrolidone/vinyl acetate copolymer (PVPVA),[38] Crospovidone[39]), cellulose derivatives (hydroxypropylcellulose (HPC),[40] hydroxypropylmethylcellulose (HPMC),[41] hydroxypropylmethylcellulose acetate succinate (HPMCAS)),[42] and other synthetic polymers specifically designed for pharmaceutical applications (Eudragit® polymers, Soluplus®).[43,44]

### *1.4.1. ASD Manufacturing Methods*

ASDs have been successfully prepared in a variety of ways, the most common of which are hot melt extrusion (HME),[45,46] spray drying (SD),[47] and freeze drying.[48] Less common in industrial manufacturing but pharmaceutically relevant methods include mechanical activation,[49] rotary evaporation (RE),[50] antisolvent precipitation (AP),[51,52,53] and spray-freeze drying.[54] Selection of the appropriate manufacturing method can be based on logistical concerns (cost, equipment) and/or

**Table 1.** Examples of marketed FDA-approved products containing ASD.

| Product name | Drug | Manufacturer | Synthetic Method | Polymer | Indication | Year of FDA Approval |
|---|---|---|---|---|---|---|
| Cesamet® | Nabilone | Valeant | Solvent evaporation | PVP | Nausea and vomiting induced by cancer medications | 1985 |
| Prograf® | Tacrolimus | Fujisawa | Solvent evaporation | HPMC | Organ rejection prophylaxis | 1994 |
| Kaletra® | Ritonavir/ Lopinavir | Abbott | HME | PVPVA | HIV-1 infection | 2007 |
| Incivek® | Telaprevir | Vertex | Spray drying | HPMCAS | Chronic hepatitis C | 2011 |
| Belsomra® | Suvorexant | Merck | HME | PVPVA | Insomnia | 2014 |
| Orkambi® | Lumacaftor/ Ivacaftor | Vertex | Spray drying | HPMCAS | Cystic fibrosis | 2016 |
| Erleada™ | Apalutamide | Janssen | Spray drying | HPMCAS | Non metastatic castration resistant prostate cancer | 2018 |
| Paxlovid® | Nirmatrelvir/ Ritonavir | Pfizer | HME | PVPVA | COVID-19 | 2023 |

chemical compatibility (heat lability, limited solubility). Examples of FDA-approved ASDs and the manufacturing methods used to prepare them are shown in Table 1.[55,56] HME has been used to prepare several formulations on the market and is often favored due to its solvent-free processing but can be limited in its applicability by insufficient drug-polymer mixing and/or heat lability of ASD components.[57,58] For this reason, solvent-based methods (SD, RE) offer effective alternatives as the presence of solvent can reduce the processing temperature required to obtain sufficient drug-polymer mixing and subsequent amorphization. Of the solvent-based methods, SD is most commonly used due to its scalability and potential for continuous manufacturing but in some cases may be limited by a) component solubility in spray solvent and b) spray solution characteristics.[59] Solutions that exhibit high viscosity in the common solvent selected may be unsuitable for SD due to the strong influence of feed solution viscosity on spray pattern, droplet size, and droplet size distribution.[60] RE is less sensitive to solution viscosity, but

is used infrequently in commercial settings due to significantly higher solvent requirement and poor scalability.[61] In the recently described slurry conversion (SC)[62,63] synthesis method, a physical mixture of the drug and polymer is stirred at room temperature in the presence of a small volume of organic solvent which is subsequently removed. In contrast to HME, SC can be consistently performed at ambient temperature (25 °C), making it a viable alternative for heat labile drugs and polymers. Given the many ways to prepare an ASD, many have investigated whether they produce the same product in terms of internal structure and performance characteristics.[64,65,66,67] Despite work in this area, the current understanding remains limited.

### *1.4.2. Effect of Drug-Polymer Interactions on ASD Performance*

Drug-polymer interactions are strongly dependent on the characteristics of the drug and polymer chosen as well as the state of mixing achieved in each ASD. Recent work has identified the strength and extent of drug-polymer interaction within an ASD as an important factor in the performance of the formulation, necessitating thorough understanding of how this property is influenced by ASD preparation and subsequent effects on stability and release.

#### *1.4.2.1. Stability against Crystallization*

The presence of stronger or more extensive drug-polymer interactions has been shown to have a positive effect on the stability of an ASD and the inhibitory effect of the polymer on drug crystallization. In the case of indomethacin (IMC) dispersed in PVP, the stability of the dispersion against crystallization is attributed to hydrogen bonding between the two species' carboxylic acid groups.[68] Additionally, Mistry et al. demonstrated that for the weakly basic API ketoconazole, the strength of drug-polymer interaction correlates with the degree of molecular mobility measured via dielectric spectroscopy with the strongest interaction (ionic) leading to the greatest decrease in mobility and subsequent crystallization inhibition.[69]

#### *1.4.2.2. Dissolution and Drug Release*

The effect of drug-polymer interactions on both phases of dissolution is poorly understood, with system-to-system variability. Chen et al. investigated the dissolution performance of ketoconazole

dispersed in carrier polymers with differing degrees of drug-polymer interaction potential and found that strong interactions with hypromellose acetate succinate (HPMCAS) facilitated enhanced drug dissolution, likely due to more sustained supersaturation.[70] Similar behavior has been observed when comparing dispersions of griseofulvin in PVP (no hydrogen bonding) or HPMCAS (hydrogen bonding), where griseofulvin-HPMCAS dispersions prepared via ball milling exhibited significantly higher aqueous solubility.[71] Interestingly, this outperformance did not persist for dispersions prepared by spray drying, suggesting complex interplay between drug-polymer interaction and ASD processing on dissolution performance. Finally, Hiew et al. observed a "balance" between dissolution and stability for a series of drug-polymer systems, suggesting that strong drug-polymer interactions may lend themselves to an enhanced degree of solid-state stability while inhibiting drug release.[72] The varied observations concerning the effect of drug-polymer interactions on drug release from an ASD indicate the need for careful consideration in excipient selection and processing conditions to ensure desirable performance outcomes.

### *1.4.3. Amorphous Drug-Polymer Salts*

A drug-polymer salt is produced by an acid-base reaction between a small-molecule drug and an ionizable polymer (polyelectrolyte). Although salt formation is common in drug development, counterions are typically small inorganic ions or small organic ions, not charged polymers.[73,74,75] In the context of amorphous formulations, a salt formed with a polymeric counterion has greater resistance to crystallization than a salt formed with a small inorganic or organic counterion. This is a result of the awkward packing required for a drug and a polymer to crystallize together. Additionally, polyelectrolytes tend to be hydrophilic, and their incorporation into a drug formulation improves wetting and dispersion in water. A polymer has a lower solubility than its monomer or oligomers and provides stronger adhesion to solid surfaces. As a result, polyelectrolytes are often good coating materials, while low-molecular-weight materials could fail for this purpose. Table 2 summarizes previous reports of amorphous drug-polymer salts in the literature, including synthetic methods, formulation details, and performance metrics. When a comparison is possible, polymers that allow for salt formation with the drug appear to inhibit crystallization better than those that do not. For example, indomethacin is more stable when

formulated with Eudragit EPO, a salt former, than with HPMC, a neutral, non-salt-forming polymer.[76] Clofazimine and lumefantrine, both bases, are more stable when formulated with an acidic polymer than with a neutral polymer.[77,62,63] This confirms the importance of salt formation on the stability of amorphous drug–polymer formulations.

**Table 2.** Examples of amorphous drug-polymer salts reported in the literature.

| API, % Loading | Polymer Counterion | Synthetic Method | Physical Stability | Other Benefits |
|---|---|---|---|---|
| Naproxen, 42%[78] | Eudragit® EPO | Hot melt extrusion | Stable at 20 ◦C/60% RH for 12 mo. | Drug release triggered by inorganic salts |
| Lapatinib, 40%[79] Gefitinib, 40% | PSSA | Solvent evaporation, cryogenic grinding | Stable at 40 ◦C/75% RH for 6 mo. | Faster dissolution than crystalline form |
| Indomethacin, 30%[76] | Eudragit® EPO | Solvent evaporation, cryogenic grinding | Stable at 40 ◦C/75% RH for 100 d. Neutral ADSs less stable | Enhanced dissolution |
| Lumefantrine, 40%[77] | CAP, HPMCP, Eudragit® L100 | Solvent evaporation | Stable at 40 ◦C/75% RH for 6 mo. Neutral ASDs less stable | CAP dispersion has slow dissolution, others perform better |
| Clofazimine, 75%[62] | PAA | Slurry conversion | Stable at 40 ◦C/75% RH for 6 mo. Neutral ASDs less stable | Improved flow, tabletability, wettability, dissolution |
| Ciprofloxacin, 40%[80] | Eudragit® L | Ball milling | Stable at 25 ◦C/90% RH for 90 min. Improved stability over pure drug at 40 ◦C/75% RH | Improved solubility and drug permeability, persistent supersaturation |

### *1.4.4. Dissolution of Amorphous Solid Dispersions as Molecules and Nanoparticles*

The dissolution of ASDs is generally depicted as a "spring and parachute" process, where the "spring" refers to rapid initial drug dissolution and the "parachute" represents prolonged drug supersaturation (Fig.3).[81] This supersaturated state can only be generated from a high-free energy state (sufficient "spring") and occurs when the apparent concentration of the drug exceeds its equilibrium solubility.

Fig. 3. The spring-parachute depiction for ASD dissolution. $C_{aq}$ represents the crystalline solubility of the drug, reached after dissolution of neat crystalline drug or recrystallization and precipitation of the amorphous drug.

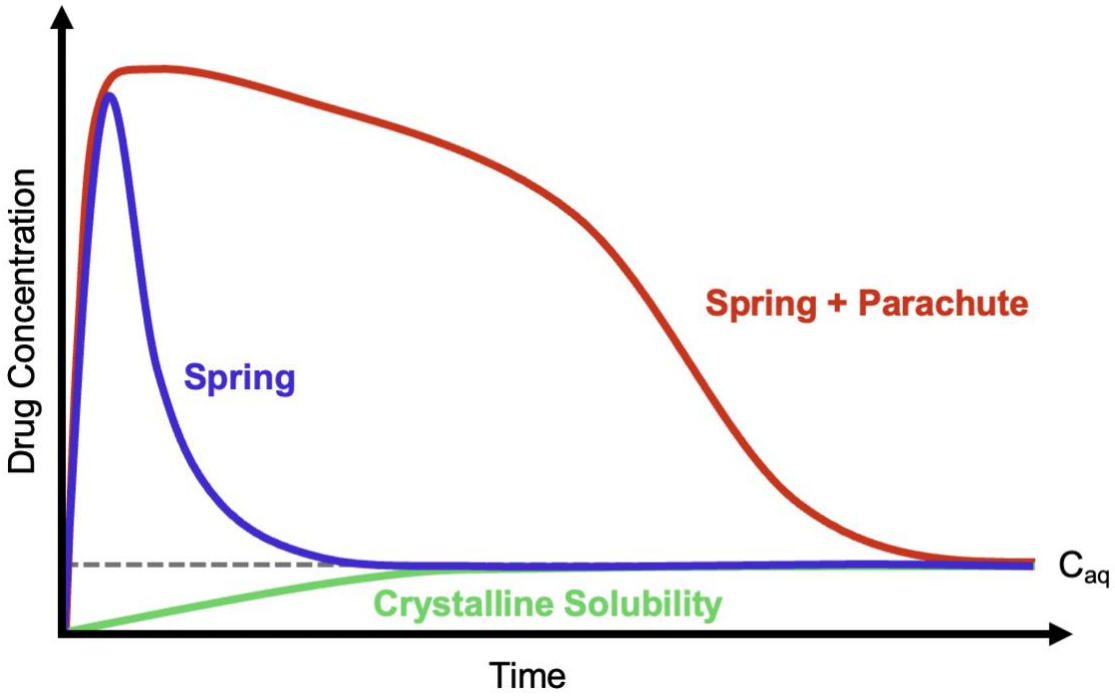


In addition to molecularly dissolved drug, the dissolution of some ASDs can generate colloidal particles of submicron size, leading to an apparent solubility that exceeds the true solubility. An early example of this phenomenon is β-carotene dispersed in PVP[82] and additional examples are shown in Table 3.

| Drug | Polymer | Preparation Method | Particle Size | Dissolution medium | Other Comments |
|---|---|---|---|---|---|
| β-carotene[82] | PVP | Solvent evaporation | ~100 nm | Water | Particle size obtained via filtration through various pore size filters |
| Itraconazole[83] | HPMCAS | Spray drying | ~300 nm | FaSSGF, FaSSIF | Colloids only formed in FaSSGF. ASDs with lower drug loading formed higher concentration of drug-rich colloid |
| Anacetrapib[84] | PVPVA + TPGS (surfactant) | HME | ~50 to ~200 nm | Water | Higher wt% TPGS in the formulation decreased particle size range from ~200 to ~50 nm for 2% to 10% TPGS, respectively |
| Ritonavir[85] | PVP, PVPVA, HPMCAS | Rotary Evaporation | ~200 nm, ~250 nm, ~315 nm for PVPVA, HPMCAS, PVP respectively | Phosphate buffer, pH 6.8 | Only 10:90 RTV-polymer ASDs formed observable colloidal species |
| Probucol[86] | HPMCAS | Spray drying | ~30 nm, ~70nm, ~180 nm for 10%, 25%, 50% probucol ASDs, respectively (mean volume diameter) | Phosphate buffered saline | Higher drug loading of probucol led to delayed NP formation and probucol dissolution relative to low-drug loading ASDs |
| Fenofibrate[87] | HPMC | Spray drying | ~160 nm (mean volume diameter) | Phosphate buffered saline | Fenofibrate-rich NPs correlated with enhanced intestinal absorption *in vivo* |

**Table 3.** Examples of previously studied systems shown to generate nanoparticles upon dissolution.

These studies demonstrated the dual-phase nature of ASD dissolution, wherein both the molecularly dissolved drug (corresponding to the neat amorphous solubility) and an amorphous drug nanoparticle phase both contribute to the overall "apparent solubility" (AS). These amorphous drug nanoparticles (NPs) have been shown in certain cases to act as "reservoirs," consistently replenishing the supply of molecularly dissolved drug to maintain a concentration gradient across a permeable membrane. The complex behavior of ASDs in solution and this behavior's dependence on a wide variety of formulation and physiological factors indicates this as a necessary focus of further investigation to ensure robust ASDs with reliable, consistent performance.

## 1.5. Contributions of this Thesis

In Chapter 2 and 3, the effect of polymer choice and processing conditions on salt formation in lumefantrine (LMF)-based ASDs was quantified by measuring the degree of proton transfer between LMF and an acidic polymer using x-ray photoelectron spectroscopy (XPS). Chapter 2 shows that the enhanced degree of proton transfer between LMF and the acidic polymer poly(acrylic acid) (PAA) facilitated by SC enhances the stability and release of the formulation. Compared to a melt-quench synthesis processing that mimics the conventional HME process, formulations prepared via SC attained significantly higher degree of protonation with subsequent 6x enhancement in apparent solubility in simulated gastric fluid and greatly increased stability at 40C/75% RH. In contrast to antisolvent precipitation, SC demonstrated highly tunable drug loading and a degree of acid-base reaction well-described by an equilibrium reaction model, indicating the ability of SC to attain the equilibrium state of the LMF-PAA reaction.

In Chapter 3, we instead focus on the degree of salt formation attainable via SC synthesis for LMF prepared with a variety of other acidic polymers and determined the polymer characteristics that dictate the ability of a given acidic polymer to form a salt with LMF. The polymers tested included cellulosic polymers (hypromellose phthalate (HPMCP), hypromellose acetate succinate (HPMCAS), cellulose acetate phthalate (CAP)) and acrylic/methacrylic polymers (PAA, Eudragit® L100, Eudragit® L100-55). The polymers studied showed very different degrees of LMF protonation for a given drug loading, however this discrepancy was largely eliminated when the results are instead plotted against the acidic group (COOH) density of each polymer as determined by a colorimetric non-aqueous titration. This indicates that the degree of salt formation in these ASDs is primarily dependent on this acidic group density and is largely insensitive to the individual polymers' architectures. Furthermore, these results were compared against three alternative methods used to synthesize LMF ASDs found in the literature. For a given LMF-acidic polymer ASD with identical composition, SC either outperforms (4 of 6 polymers) or attains the same extent of protonation as spray drying (2 of 6 polymers). This detailed understanding of the factors dictating the degree of intimate mixing and molecular-level structure in a multicomponent ASD, demonstrating the need for careful consideration of both the excipients and manufacturing conditions used to formulate an ASD with the desired physicochemical properties and pharmaceutical performance.

In Chapter 4, SC was further investigated as a general approach to formulate a variety of poorly soluble basic drugs with the polymer PAA. 18 drugs were formulated as binary and/or ternary ASDs and analyzed for amorphous character in addition to proton transfer if appropriate. At 25% drug loading, 16 of 18 drugs were successfully amorphized while at 50% drug loading, 11 of 18 drugs were amorphized. XPS analysis revealed a LMF protonation trend approximately correlated with basic strength, with aliphatic amines attaining the highest degree of protonation by PAA. For each drug whose protonation was quantifiable by XPS, a smooth trend of decreasing protonation with increasing drug loading was observed. This suggests the consistent ability of SC to facilitate a reaction equilibrium state where intimate molecular-level mixing is ensured.

In Chapter 5, the previously reported enhanced dissolution behavior of LMF-PAA ASDs was further investigated. LMF was formulated with 10 different pharmaceutical polymers (8 acidic polymers, mentioned above in addition to PVP and PVPVA) and its subsequent release in 0.1% SDS solution quantified. PAA was demonstrated to outperform all other polymers tested when prepared at both 25 and 50 wt% drug loading with a high degree of supersaturation that is stable for at least 8 hours. This superior performance of PAA as a dispersion polymer suggests its underutilization in ASD formulation excipient and indicates its use in more general pharmaceutical contexts warrants further study in additional drug systems and dissolution conditions. The future directions of these amorphous drug-polymer salts and their use in the delivery of poorly soluble drugs are discussed in Chapter 6.

Overall, this thesis considers the preparation, optimization, and performance of amorphous drug-polymer salts for a variety of drug-polymer systems, particularly focusing on the formulation of poorly soluble basic drugs prepared with oppositely charged acidic polymers. The findings in this thesis are relevant to the continued development of amorphous drug formulations for the increasing population of low-solubility drug candidates and offers new approaches for their efficient delivery and long-term stability.

## 1.6. References


[1] Forster, A.; Hempenstall, J.; Rades, T. Characterization of Glass Solutions of Poorly Water-Soluble Drugs Produced by Melt Extrusion with Hydrophilic Amorphous Polymers. *Journal of Pharmacy and Pharmacology* **2001**, *53* (3), 303–315.
[2] Yu, L. Amorphous Pharmaceutical Solids: Preparation, Characterization and Stabilization. *Advanced Drug Delivery Reviews* **2001**, *48* (1), 27–42.
[3] Aulton, M. E.; Taylor, K. *Aulton's Pharmaceutics : The Design and Manufacture of Medicines*, 5th ed.; Elsevier: London, 2018.
[4] Shah, V. P.; Amidon, G. L. G.L. Amidon, H. Lennernas, V.P. Shah, and J.R. Crison. A Theoretical Basis for a Biopharmaceutic Drug Classification: The Correlation of in Vitro Drug Product Dissolution and in Vivo Bioavailability, Pharm Res 12, 413–420, 1995—Backstory of BCS. *The AAPS Journal* **2014**, *16* (5), 894–898.
[5] Lipinski, C. A.; Lombardo, F.; Dominy, B. W.; Feeney, P. J. Experimental and Computational Approaches to Estimate Solubility and Permeability in Drug Discovery and Development Settings. *Advanced Drug Delivery Reviews* **2012**, *64*, 4–17.
[6] Benet, L. Z.; Broccatelli, F.; Oprea, T. I. BDDCS Applied to over 900 Drugs. *The AAPS Journal* **2011**, *13* (4), 519–547.
[7] Ku, M. S. Use of the Biopharmaceutical Classification System in Early Drug Development. *The AAPS Journal* **2008**, *10*(1), 208–212.
[8] Taniguchi, C.; Kawabata, Y.; Wada, K.; Yamada, S.; Onoue, S. Microenvironmental PH-Modification to Improve Dissolution Behavior and Oral Absorption for Drugs with PH-Dependent Solubility. *Expert Opinion on Drug Delivery***2014**, *11* (4), 505–516.
[9] Tran, P. H.-L.; Tran, T. T.-D.; Lee, K.-H.; Kim, D.-J.; Lee, B.-J. Dissolution-Modulating Mechanism of PH Modifiers in Solid Dispersion Containing Weakly Acidic or Basic Drugs with Poor Water Solubility. *Expert Opinion on Drug Delivery***2010**, *7* (5), 647–661.
[10] Khadka, P.; Ro, J.; Kim, H.; Kim, I.; Kim, J. T.; Kim, H.; Cho, J. M.; Yun, G.; Lee, J. Pharmaceutical Particle Technologies: An Approach to Improve Drug Solubility, Dissolution and Bioavailability. *Asian Journal of Pharmaceutical Sciences* **2014**, *9* (6), 304–316.
[11] Kumar, R.; Thakur, A. K.; Chaudhari, P.; Banerjee, N. Particle Size Reduction Techniques of Pharmaceutical Compounds for the Enhancement of Their Dissolution Rate and Bioavailability. *Journal of Pharmaceutical Innovation* **2021**.
[12] Sekiguchi, K.; Obi, N. Studies on Absorption of Eutectic Mixture. I. A Comparison of the Behavior of Eutectic Mixture of Sulfathiazole and that of Ordinary Sulfathiazole in Man. *CHEMICAL & PHARMACEUTICAL BULLETIN* **1961**, *9*(11), 866–872.
[13] Cid, A. G.; Simonazzi, A.; Palma, S. D.; Bermúdez, J. M. Solid Dispersion Technology as a Strategy to Improve the Bioavailability of Poorly Soluble Drugs. *Therapeutic Delivery* **2019**, *10* (6), 363–382.
[14] Sareen, S.; Joseph, L.; Mathew, G. Improvement in Solubility of Poor Water-Soluble Drugs by Solid Dispersion. *International Journal of Pharmaceutical Investigation* **2012**, *2* (1), 12.
[15] Kumari Sugandha; Santanu Kaity; Mukherjee, S.; Isaac, J.; Ghosh, A. Solubility Enhancement of Ezetimibe by a Cocrystal Engineering Technique. *Crystal Growth & Design* **2014**, *14* (9), 4475–4486.
[16] Elder, D. P.; Holm, R.; Diego, H. L. de. Use of Pharmaceutical Salts and Cocrystals to Address the Issue of Poor Solubility. *International journal of pharmaceutics* **2013**, *453* (1), 88–100.
[17] Carrier, R. L.; Miller, L. A.; Ahmed, I. The Utility of Cyclodextrins for Enhancing Oral Bioavailability. *Journal of Controlled Release* **2007**, *123* (2), 78–99.
[18] Hancock, B. C.; Parks, M. What Is the True Solubility Advantage for Amorphous Pharmaceuticals? *Pharmaceutical Research* **2000**, *17* (4), 397–404.
[19] Babu, N. J.; Nangia, A. Solubility Advantage of Amorphous Drugs and Pharmaceutical Cocrystals. *Crystal Growth & Design* **2011**, *11* (7), 2662–2679.

[20] Murdande, S. B.; Pikal, M. J.; Shanker, R. M.; Bogner, R. H. Solubility Advantage of Amorphous Pharmaceuticals: I. A Thermodynamic Analysis. *Journal of Pharmaceutical Sciences* **2010**, *99* (3), 1254–1264.
[21] Leuner, C. Improving Drug Solubility for Oral Delivery Using Solid Dispersions. *European Journal of Pharmaceutics and Biopharmaceutics* **2000**, *50* (1), 47–60.
[22] Kennedy, M.; Hu, J.; Gao, P.; Li, L.; Ali-Reynolds, A.; Chal, B.; Gupta, V.; Ma, C.; Mahajan, N.; Akrami, A.; Surapaneni, S. Enhanced Bioavailability of a Poorly Soluble VR1 Antagonist Using an Amorphous Solid Dispersion Approach: A Case Study. *Molecular Pharmaceutics* **2008**, *5* (6), 981–993.
[23] Jung, J.-Y.; Yoo, S. D.; Lee, S.-H.; Kim, K.-H.; Yoon, D.-S.; Lee, K.-H. Enhanced Solubility and Dissolution Rate of Itraconazole by a Solid Dispersion Technique. *International Journal of Pharmaceutics* **1999**, *187* (2), 209–218.
[24] Vasconcelos, T.; Sarmento, B.; Costa, P. Solid Dispersions as Strategy to Improve Oral Bioavailability of Poor Water Soluble Drugs. *Drug Discovery Today* **2007**, *12* (23), 1068–1075.
[25] Thakkar, A. L.; Hirsch, C. A.; Page, J. G. Solid Dispersion Approach for Overcoming Bioavailability Problems due to Polymorphism of Nabilone, a Cannabinoid Derivative. *Journal of Pharmacy and Pharmacology* **1977**, *29* (1), 783–784.
[26] Moseson, D. E.; Tran, T. B.; Karunakaran, B.; Rohan Ambardekar; Tze Ning Hiew. Trends in Amorphous Solid Dispersion Drug Products Approved by the U.S. Food and Drug Administration between 2012 and 2023. *International Journal of Pharmaceutics X* **2024**, *7*, 100259–100259.
[27] Hancock, B. C.; Zografi, G. Characteristics and Significance of the Amorphous State in Pharmaceutical Systems. *Journal of Pharmaceutical Sciences* **1997**, *86* (1), 1–12.
[28] Craig, D. The Relevance of the Amorphous State to Pharmaceutical Dosage Forms: Glassy Drugs and Freeze Dried Systems. *International Journal of Pharmaceutics* **1999**, *179* (2), 179–207.
[29] J Zarzycki. *Glasses and the Vitreous State*; Cambridge University Press: Cambridge ; New York, 1991.
[30] Suga, H.; Seki, S. Thermodynamic Investigation on Glassy States of Pure Simple Compounds. *Journal of Non-Crystalline Solids* **1974**, *16* (2), 171–194.
[31] Kawakami, K.; Pikal, M. J. Calorimetric Investigation of the Structural Relaxation of Amorphous Materials: Evaluating Validity of the Methodologies. *Journal of Pharmaceutical Sciences* **2005**, *94* (5), 948–965.
[32] Bhattacharya, S.; Raj Suryanarayanan. Local Mobility in Amorphous Pharmaceuticals—Characterization and Implications on Stability. *Journal of Pharmaceutical Sciences* **2009**, *98* (9), 2935–2953.
[33] Murdande, S. B.; Pikal, M. J.; Shanker, R. M.; Bogner, R. H. Solubility Advantage of Amorphous Pharmaceuticals: II. Application of Quantitative Thermodynamic Relationships for Prediction of Solubility Enhancement in Structurally Diverse Insoluble Pharmaceuticals. *Pharmaceutical Research* **2010**, *27* (12), 2704–2714.
[34] Qian, F.; Huang, J.; Hussain, M. A. Drug–Polymer Solubility and Miscibility: Stability Consideration and Practical Challenges in Amorphous Solid Dispersion Development. *Journal of Pharmaceutical Sciences* **2010**, *99* (7), 2941–2947.
[35] Meng, F.; Trivino, A.; Prasad, D.; Chauhan, H. Investigation and Correlation of Drug Polymer Miscibility and Molecular Interactions by Various Approaches for the Preparation of Amorphous Solid Dispersions. *European Journal of Pharmaceutical Sciences* **2015**, *71*, 12–24.
[36] Amponsah-Efah, K. K.; Mistry, P.; Eisenhart, R.; Raj Suryanarayanan. The Influence of the Strength of Drug–Polymer Interactions on the Dissolution of Amorphous Solid Dispersions. *Molecular Pharmaceutics* **2020**, *18* (1), 174–186.
[37] Jahangiri, A.; Barzegar-Jalali, M.; Garjani, A.; Javadzadeh, Y.; Hamishehkar, H.; Rameshrad, M.; Adibkia, K. Physicochemical Characterization and Pharmacological Evaluation of Ezetimibe-PVP K30 Solid Dispersions in Hyperlipidemic Rats. *Colloids and Surfaces B: Biointerfaces* **2015**, *134*, 423–430.
[38] Yang, F.; Su, Y.; Zhang, J.; DiNunzio, J.; Leone, A.; Huang, C.; Brown, C. D. Rheology Guided Rational Selection of Processing Temperature to Prepare Copovidone–Nifedipine Amorphous Solid Dispersions via Hot Melt Extrusion (HME). *Molecular Pharmaceutics* **2016**, *13* (10), 3494–3505.

[39] Shibata, Y.; Fujii, M.; Suzuki, A.; Koizumi, N.; Kanada, K.; Yamada, M.; Watanabe, Y. Effect of Storage Conditions on the Recrystallization of Drugs in Solid Dispersions with Crospovidone. *Pharmaceutical Development and Technology***2013**, *19* (4), 468–474.
[40] Sarode, A. L.; Malekar, S. A.; Cote, C.; Worthen, D. R. Hydroxypropyl Cellulose Stabilizes Amorphous Solid Dispersions of the Poorly Water Soluble Drug Felodipine. *Carbohydrate Polymers* **2014**, *112*, 512–519.
[41] Fan, N.; He, Z.; Ma, P.; Wang, X.; Li, C.; Sun, J.; Sun, Y.; Li, J. Impact of HPMC on Inhibiting Crystallization and Improving Permeability of Curcumin Amorphous Solid Dispersions. *Carbohydrate Polymers* **2018**, *181*, 543–550.
[42] Arun Butreddy. Hydroxypropyl Methylcellulose Acetate Succinate as an Exceptional Polymer for Amorphous Solid Dispersion Formulations: A Review from Bench to Clinic. *European Journal of Pharmaceutics and Biopharmaceutics***2022**, *177*, 289–307.
[43] Li, J.; Il Woo Lee; Gye Hwa Shin; Chen, X.; Hyun Jin Park. Curcumin-Eudragit® E PO Solid Dispersion: A Simple and Potent Method to Solve the Problems of Curcumin. *European Journal of Pharmaceutics and Biopharmaceutics* **2015**, *94*, 322–332.
[44] Caron, V.; Hu, Y.; Tajber, L.; Erxleben, A.; Corrigan, O. I.; McArdle, P.; Healy, A. M. Amorphous Solid Dispersions of Sulfonamide/Soluplus® and Sulfonamide/PVP Prepared by Ball Milling. *AAPS PharmSciTech* **2013**, *14* (1), 464–474.
[45] Repka, M. A.; Majumdar, S.; Kumar Battu, S.; Srirangam, R.; Upadhye, S. B. Applications of Hot-Melt Extrusion for Drug Delivery. *Expert Opinion on Drug Delivery* **2008**, *5* (12), 1357–1376.
[46] Repka, M. A.; Shah, S.; Lu, J.; Maddineni, S.; Morott, J.; Patwardhan, K.; Mohammed, N. N. Melt Extrusion: Process to Product. *Expert Opinion on Drug Delivery* **2011**, *9* (1), 105–125. .
[47] Paudel, A.; Worku, Z. A.; Meeus, J.; Guns, S.; Van den Mooter, G. Manufacturing of Solid Dispersions of Poorly Water Soluble Drugs by Spray Drying: Formulation and Process Considerations. *International Journal of Pharmaceutics* **2013**, *453* (1), 253–284.
[48] Tang, X. (Charlie); Pikal, M. J. Design of Freeze-Drying Processes for Pharmaceuticals: Practical Advice. *Pharmaceutical Research* **2004**, *21* (2),191–200.
[49] Crowley, K. J.; Zografi, G. Cryogenic Grinding of Indomethacin Polymorphs and Solvates: Assessment of Amorphous Phase Formation and Amorphous Phase Physical Stability. *Journal of Pharmaceutical Sciences* **2002**, *91* (2), 492–507.
[50] Hiew, T. N.; Zemlyanov, D. Y.; Taylor, L. S. Balancing Solid-State Stability and Dissolution Performance of Lumefantrine Amorphous Solid Dispersions: The Role of Polymer Choice and Drug–Polymer Interactions. *Molecular Pharmaceutics* **2021**.
[51] Bhujbal, S. V.; Pathak, V.; Zemlyanov, D. Y.; Taylor, L. S.; Zhou, Q. (Tony). Physical Stability and Dissolution of Lumefantrine Amorphous Solid Dispersions Produced by Spray Anti-Solvent Precipitation. *Journal of Pharmaceutical Sciences* **2020**..
[52] Strotman, N. A.; Schenck, L. Coprecipitated Amorphous Dispersions as Drug Substance: Opportunities and Challenges. *Organic Process Research & Development* **2021**, *26* (1), 10–13.
[53] Armstrong, M.; Wang, L.; Ristroph, K.; Tian, C.; Yang, J.; Ma, L.; Santipharp Panmai; Zhang, D.; Karthik Nagapudi; Prud'homme, R. K. Formulation and Scale-up of Fast-Dissolving Lumefantrine Nanoparticles for Oral Malaria Therapy. *Journal of Pharmaceutical Sciences* **2023**, *112*(8), 2267–2275.
[54] Adeli, E. The Use of Spray Freeze Drying for Dissolution and Oral Bioavailability Improvement of Azithromycin. *Powder Technology* **2017**, *319*, 323–331.
[55] Pandi, P.; Bulusu, R.; Kommineni, N.; Khan, W.; Singh, M. Amorphous Solid Dispersions: An Update for Preparation, Characterization, Mechanism on Bioavailability, Stability, Regulatory Considerations and Marketed Products. *International Journal of Pharmaceutics* **2020**, *586*, 119560.
[56] Jermain, S. V.; Brough, C.; Williams, R. O. Amorphous Solid Dispersions and Nanocrystal Technologies for Poorly Water-Soluble Drug Delivery – an Update. *International Journal of Pharmaceutics* **2018**, *535* (1-2), 379–392.
[57] Patil H, Tiwari RV, Repka MA. Hot-Melt Extrusion: from Theory to Application in Pharmaceutical Formulation. *AAPS PharmSciTech*. 2015;(1):20-42. 7

[58] Repka MA, Shah S, Lu J, et al. Melt extrusion: process to product. *Expert Opinion on Drug Delivery*. 2011;(1):105-125.
[59] Singh A, Van den Mooter G. Spray drying formulation of amorphous solid dispersions. *Advanced Drug Delivery Reviews*. Published online May 2016:27-50.
[60] Li J, Patel D, Wang G. Use of Spray-Dried Dispersions in Early Pharmaceutical Development: Theoretical and Practical Challenges. *The AAPS Journal*. 2016;(2):321-333.
[61] Vasconcelos T, Marques S, das Neves J, Sarmento B. Amorphous solid dispersions: Rational selection of a manufacturing process. *Advanced Drug Delivery Reviews*. Published online May 2016:85-101.
[62] Gui Y, McCann EC, Yao X, Li Y, Jones KJ, Yu L. Amorphous Drug–Polymer Salt with High Stability under Tropical Conditions and Fast Dissolution: The Case of Clofazimine and Poly(acrylic acid). *Molecular Pharmaceutics*. 2021;(3):1364-1372. 0
[63] Yao X, Kim S, Gui Y, et al. Amorphous Drug–Polymer Salt with High Stability under Tropical Conditions and Fast Dissolution: The Challenging Case of Lumefantrine-PAA. *Journal of Pharmaceutical Sciences*. 2021;(11):3670-3677.
[64] Haser, A.; Cao, T.; Lubach, J.; Listro, T.; Acquarulo, L.; Zhang, F. Melt Extrusion vs. Spray Drying: The Effect of Processing Methods on Crystalline Content of Naproxen-Povidone Formulations. *European Journal of Pharmaceutical Sciences* **2017**, *102*, 115–125.
[65] Tau, R.; Ong, C. K.; Cheng, S.; Ng, W. K. Amorphization of Crystalline Active Pharmaceutical Ingredients via Formulation Technologies. *Powder Technology* **2017**, *311*, 175–184.
[66] Dedroog, S.; Huygens, C.; Van den Mooter, G. Chemically Identical but Physically Different: A Comparison of Spray Drying, Hot Melt Extrusion and Cryo-Milling for the Formulation of High Drug Loaded Amorphous Solid Dispersions of Naproxen. *European Journal of Pharmaceutics and Biopharmaceutics* **2019**, *135*, 1–12.
[67] Martynek, D.; Ridvan, L.; Sivén, M.; Šoóš, M. Stability and recrystallization of amorphous solid dispersions prepared by hot-melt extrusion and spray drying. *International Journal of Pharmaceutics* **2025**, journal pre-proof.
[68] Chauhan, H.; Kuldipkumar, A.; Barder, T.; Medek, A.; Gu, C.-H.; Atef, E. Correlation of Inhibitory Effects of Polymers on Indomethacin Precipitation in Solution and Amorphous Solid Crystallization Based on Molecular Interaction. *Pharmaceutical Research* **2013**, *31* (2), 500–515.
[69] Mistry, P.; Mohapatra, S.; Gopinath, T.; Vogt, F. G.; Suryanarayanan, R. Role of the Strength of Drug–Polymer Interactions on the Molecular Mobility and Crystallization Inhibition in Ketoconazole Solid Dispersions. *Molecular Pharmaceutics* **2015**, *12* (9), 3339–3350.
[70] Chen, Y.; Liu, C.; Chen, Z.; Su, C.; Hageman, M. J.; Hussain, M. A.; Haskell, R.; Stefanski, K.; Qian, F. Drug–Polymer–Water Interaction and Its Implication for the Dissolution Performance of Amorphous Solid Dispersions. *Molecular Pharmaceutics* **2015**, *12* (2), 576–589.
[71] Hisham Al-Obaidi; Lawrence, M. J.; Shah, S.; Henna Moghul; Noor Al-Saden; Bari, F. Effect of Drug–Polymer Interactions on the Aqueous Solubility of Milled Solid Dispersions. *International Journal of Pharmaceutics* **2013**, *446* (1-2), 100–105.
[72] Hiew, T. N.; Zemlyanov, D. Y.; Taylor, L. S. Balancing Solid-State Stability and Dissolution Performance of Lumefantrine Amorphous Solid Dispersions: The Role of Polymer Choice and Drug–Polymer Interactions. *Molecular Pharmaceutics* **2021**, *19* (2).
[73] Stahl, P.H.; Wermuth, C.G. (Eds.) *Pharmaceutical Salts: Properties, Selection and Use*; John Wiley & Sons: Hoboken, NJ, USA, 2002.
[74] Serajuddin, A. T. M. Salt Formation to Improve Drug Solubility. *Advanced drug delivery reviews* **2007**, *59* (7), 603–616.
[75] Sun, C. C. Cocrystallization for Successful Drug Delivery. *Expert Opinion on Drug Delivery* **2012**, *10* (2), 201–213.
[76] Xie, T.; Gao, W.; Taylor, L. S. Impact of Eudragit EPO and Hydroxypropyl Methylcellulose on Drug Release Rate, Supersaturation, Precipitation Outcome and Redissolution Rate of Indomethacin Amorphous Solid Dispersions. *International Journal of Pharmaceutics* **2017**, *531* (1), 313–323.

[77] Trasi, N. S.; Bhujbal, S. V.; Zemlyanov, D. Y.; Zhou, Q. (Tony); Taylor, L. S. Physical Stability and Release Properties of Lumefantrine Amorphous Solid Dispersion Granules Prepared by a Simple Solvent Evaporation Approach. *International Journal of Pharmaceutics: X* **2020**, *2*, 100052.
[78] Kindermann, C.; Matthée, K.; Strohmeyer, J.; Sievert, F.; Breitkreutz, J. Tailor-Made Release Triggering from Hot-Melt Extruded Complexes of Basic Polyelectrolyte and Poorly Water-Soluble Drugs. *European Journal of Pharmaceutics and Biopharmaceutics* **2011**, *79* (2), 372–381.
[79] Song, Y.; Dmitry Zemlyanov; Chen, X.; Nie, H.; Su, Z.; Fang, K.; Yang, X.; Smith, D.; Byrn, S.; Lubach, J. W. Acid–Base Interactions of Polystyrene Sulfonic Acid in Amorphous Solid Dispersions Using a Combined UV/FTIR/XPS/SsNMR Study. *Molecular Pharmaceutics* **2015**, *13* (2), 483–492.
[80] Mesallati, H.; Umerska, A.; Paluch, K. J.; Tajber, L. Amorphous Polymeric Drug Salts as Ionic Solid Dispersion Forms of Ciprofloxacin. *Molecular Pharmaceutics* **2017**, *14* (7), 2209–2223.
[81] Brouwers, J.; Brewster, M. E.; Augustijns, P. Supersaturating Drug Delivery Systems: The Answer to Solubility-Limited Oral Bioavailability? *Journal of Pharmaceutical Sciences* **2009**, *98* (8), 2549–2572.
[82] Tachibana, T.; Nakamura, A. A Methode for Preparing an Aqueous Colloidal Dispersion of Organic Materials by Using Water-Soluble Polymers: Dispersion OfB-Carotene by Polyvinylpyrrolidone. *Colloid and Polymer Science* **1965**, *203* (2), 130–133.
[83] Nunes, P. D.; Pinto, J. F.; Henriques, J.; Paiva, A. M. Insights into the Release Mechanisms of ITZ:HPMCAS Amorphous Solid Dispersions: The Role of Drug-Rich Colloids. *Molecular Pharmaceutics* **2021**, *19* (1), 51–66.
[84] Harmon, P.; Galipeau, K.; Xu, W.; Brown, C.; Wuelfing, W. P. Mechanism of Dissolution-Induced Nanoparticle Formation from a Copovidone-Based Amorphous Solid Dispersion. *Molecular Pharmaceutics* **2016**, *13* (5), 1467–1481.
[85] Purohit, H. S.; Taylor, L. S. Phase Behavior of Ritonavir Amorphous Solid Dispersions during Hydration and Dissolution. *Pharmaceutical Research* **2017**, *34* (12), 2842–2861.
[86] Ricarte, R. G.; Li, Z.; Johnson, L. M.; Ting, J. M.; Reineke, T. M.; Bates, F. S.; Hillmyer, M. A.; Lodge, T. P. Direct Observation of Nanostructures during Aqueous Dissolution of Polymer/Drug Particles. *Macromolecules* **2017**, *50* (8), 3143–3152. h
[87] Yoshikawa, E.; Ueda, K.; Hakata, R.; Higashi, K.; Moribe, K. Quantitative Investigation of Intestinal Drug Absorption Enhancement by Drug-Rich Nanodroplets Generated via Liquid–Liquid Phase Separation. *Molecular Pharmaceutics* **2024**, *21* (4), 1745–1755.

# Chapter 2. Amorphous drug-polymer salts: maximizing proton transfer to enhance stability and release

Amy Lan Neusaenger, Xin Yao, Junguang Yu, Soojin Kim, Ho-Wah Hui, Lian Huang, Chailu Que, Lian Yu

As published in:
*Molecular Pharmaceutics* **2023**
DOI: 10.1021/acs.molpharmaceut.2c00942

## 2.1. Abstract

An amorphous drug-polymer salt (ADPS) can be remarkably stable against crystallization at high temperature and humidity (e.g., 40°C/75 % RH) and provide fast release. Here we report that process conditions have a strong influence on the degree of proton transfer (salt formation) between a drug and a polymer and in turn the product's stability and release. For lumefantrine (LMF) formulated with poly(acrylic acid) (PAA), we first show that the amorphous materials prepared by slurry conversion and antisolvent precipitation produce a single trend in which the degree of drug protonation increases with PAA concentration from zero for pure LMF to ~100 % above 70 wt % PAA, independent of PAA's molecular weight (1.8, 450, and 4000 kg/mol). This profile describes the equilibrium for salt formation. Relative to this equilibrium, the literature methods of hot-melt extrusion (HME) and rotary evaporation (RE) reached significantly lower degrees of salt formation. For example, at 40 wt % drug loading, HME reached 5 % salt formation and RE 15 %, both substantially lower than the equilibrium value of 85 %. This is disconcerting given the common use of HME and RE in manufacturing amorphous formulations, indicating a need to carefully control the process conditions to ensure the full interactions between the drug and the polymer molecules. This need arises due to the low mobility of macromolecules and the mutual hindrance of adjacent reaction sites. We find that a high degree of salt formation enhances drug stability and release. For example, at 50 % drug loading, an HME-like formulation with 19 % salt formation crystallized faster and released only 20 % of the drug relative to a slurry-prepared formulation with 70 % salt formation. Based on this work, we recommend slurry conversion as the method for preparing ADPS for its ability to complete salt formation and continuously adjust drug loading. While this work focused on salt formation, the impact of process conditions on the molecular-level interactions between a drug and a polymer is likely a general issue for amorphous solid dispersions, with consequences on product stability and drug release.

## 2.2. Introduction

An amorphous solid is more soluble than its crystalline counterpart.[1,2] In recent years, this principle has been applied to develop amorphous solid dispersions (ASDs) to deliver poorly soluble drugs.[3,4,5] An ideal ASD provides enhanced solubility over its crystalline counterpart and high resistance to crystallization to maintain its solubility advantage. A recent progress in this area is the formulation of amorphous drug-polymer salts (ADPS).[6,7] An ADPS is formed by the acid-base reaction between a small-molecule drug and an oppositely changed polyelectrolyte. Relative to an

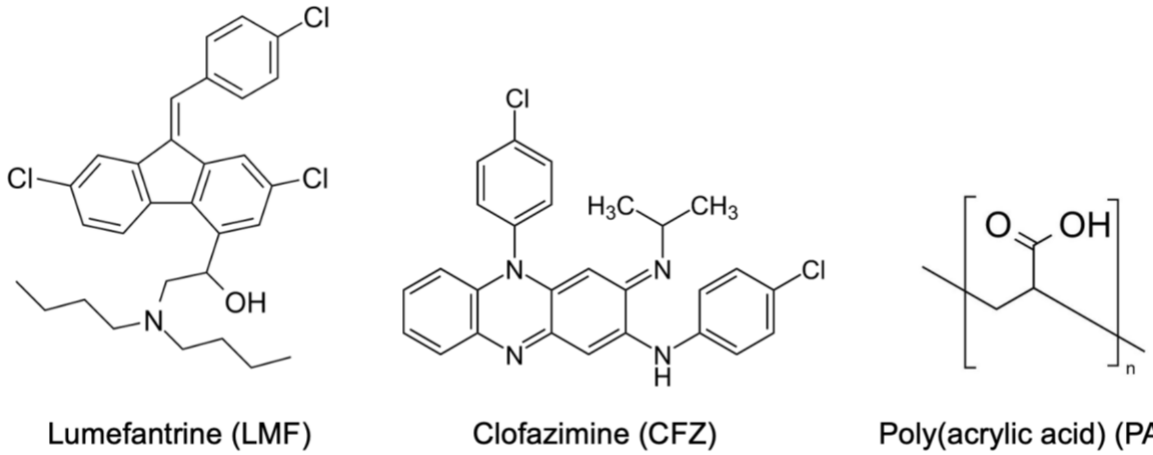


**Scheme 1**. Structures of lumefantrine (LMF), clofazimine (CFZ), and poly(acrylic acid) (PAA).

ASD containing unionized drug and polymer, an ADPS is more stable in a hot and humid environment, a need for many medicines for global health. This enhanced stability results from the strong ionic interaction between a drug and a polymer, which reduces the driving force for crystallization, while it is difficult (perhaps impossible) for the drug and the polymer to form a co-crystal. The increase of thermodynamic stability, at first glance, suggests reduced solubility, but both lumefantrine (LMF) and clofazimine (CFZ) when formulated with poly(acrylic acid) (PAA) show excellent dissolution in biorelevant media (see Scheme 1 for the structures of LMF, CFZ, and PAA).[6,7]

For an ADPS, the extent of acid-base reaction is a critical quality attribute. For a basic drug like LMF and CFZ, this refers to the fraction of the molecules that are protonated by an acidic polymer. Song et al. reported significant variation in the fraction of LMF molecules protonated by acidic

polymers.[8] For example, in formulations prepared with PAA at 40 wt % drug loading, LMF was 5 % protonated if prepared by hot-melt extrusion (HME) and 15 % protonated by rotary evaporation (RE). These values indicate very low degrees of salt formation and a significant influence of process conditions. Given the large size and low mobility of polymers, this is perhaps to be expected since a drug-polymer salt could be slower to form than a salt of small ions. In this work, we show that process conditions play a critical role in completing the salt formation between a drug and a polymer and for the LMF-PAA system, nearly complete salt formation is possible under proper conditions.

Many methods have been used to prepare ASDs, including HME[9,10] spray drying[11] (SD), and RE.[12,13] Our recent work introduced a low-cost slurry conversion method for synthesizing ADPS.[6] In this method, a physical mixture of the drug and the polymer is stirred in the presence of a small amount of solvent, which is subsequently removed. Compared to SD and RE, this method uses less solvent and does not require complete dissolution of the reactants; compared to HME, it uses a lower temperature, thus avoiding the decomposition of thermally labile polymers such as PAA. In this work, we apply the slurry method to prepare the amorphous salt of LMF and PAA and compare the product with those prepared by HME and RE.[8] In addition, antisolvent precipitation is tested as another method of preparation.[14,15]

Lumefantrine (LMF), the model drug of this study, is a low-solubility WHO Essential Medicine and first-line antimalarial. Jain et al. have shown that the bioavailability of LMF can be improved by formulating it as an ASD.[16] Being a malaria medicine, LMF formulations should be stable under tropical conditions since many regions afflicted by malaria are hot and humid. This requirement can potentially be met using the approach of amorphous drug-polymer salts. Being a weak base, LMF can be protonated by an acidic polymer like PAA.[8] Hiew et al. investigated the stability and release of amorphous LMF formulated with several polymers.[17] Their work did not investigate PAA or the impact of process conditions on LMF protonation, which are the focus of this study.

We report that the amorphous formulations of LMF and PAA prepared by slurry conversion and antisolvent precipitation form a single profile where the degree of drug protonation increases with PAA concentration from zero for pure LMF to ~100 % above 70 wt % PAA. This profile holds regardless of the synthetic method and PAA MW (1.8, 450, and 4000 kg/mol) and thus describes

the equilibrium condition for salt formation. Remarkably, the degree of salt formation obtained by slurry conversion greatly exceeds those by HME and RE,[8] indicating the important role of process conditions in completing the proton transfer between the drug and the polymer. We also report that a high degree of salt formation leads to improved stability and drug release.

## 2.3. Materials & Methods

### Materials

Poly(acrylic acid) (PAA, Carbomer, MW = 1.8, 450, 4000 kg/mol) was purchased from Sigma-Aldrich (St. Louis, MO), lumefantrine (LMF) from Nanjing Bilatchem Industrial Co. (Nanjing, China), dichloromethane (ChromAR grade) from Thermo Fisher Scientific (Fair Lawn, NJ), and ethanol from Decon Laboratories (King of Prussia, PA). All materials were used as received.

### Amorphous Formulations of LMF and PAA

*Slurry Conversion.* The slurry synthesis of amorphous LMF-PAA has been described by Yao et al.[6] In this work, a reduced synthesis temperature of 25 °C (from the original 75 °C) was tested; the products prepared after 30 min of reaction showed similar degrees of protonation as those prepared at the original temperature. The products were ground in an agate mortar with a pestle to a fine uniform powder prior to further analysis. For PAA of higher MW (450 and 4000 kg/mol), reaction with LMF was performed using both the standard slurry method[6] and an amended method involving ball milling to facilitate mixing. In this latter method, a physical mixture of LMF and PAA at a chosen drug loading (25, 50, 75 wt %) was combined with the solvent (dichloromethane/ethanol, 1:1 by volume) at a 4:1 solvent/solid ratio. The resulting paste was milled in a ball mill (MM400, Retsch GmbH, Haan, Germany). The container of the mill was a 25 mL-capacity steel jar with five 5-mm stainless steel balls. The mill operated at 20 Hz and the milling time was 30 minutes. The milling was performed at room temperature, and the internal temperature was measured immediately post-milling with an IR thermometer. The increase of internal temperature was less than 5°C.

*Melt Quenching*

To assess the effect of the degree of salt formation on formulation performance, amorphous LMF-PAA was prepared using a melt-quench method to simulate HME. A physical mixture of LMF and PAA 450 kg/mol was prepared at 50 wt % drug and heated to 135 °C while stirring with a stainless-steel spatula to mimic HME. The heating time was ~4 min. The product was ground in an agate mortar with a pestle to a fine powder before further analysis.

*Antisolvent Precipitation*

A solution of LMF in acetone (50 mg/mL) was added into an aqueous solution of PAA (3.5 mg/mL), causing precipitation. The precipitant was filtered using Whatman Grade 2 Qualitative Filter Paper and dried under vacuum overnight at room temperature and ground in an agate mortar with a pestle to a fine powder before further analysis.

**Powder X-ray Diffraction**

X-ray diffraction patterns were collected using a Bruker D8 Advance X-ray diffractometer with a Cu Kα source operating at a tube load of 40 kV and 40 mA. A powder sample of approximately 10 mg was spread evenly and flattened on a Si (510) zero-background holder and scanned between 3° and 40° (2θ) at a step size of 0.02° and a scan rate of 1 s/step.

**X-Ray Photoelectron Spectroscopy (XPS)**

The details of XPS measurement and data analysis have been described previously.[18] For an amorphous LMF-PAA formulation, approximately 5 mg of a powder was pressed into a tablet using a stainless-steel press. For a sample of pure LMF, approximately 1 mg of LMF powder was melted on a glass coverslip and quenched to room temperature by contact with an Al block. The samples were stored in a sealed plastic tube filled with Drierite before XPS analysis. The high-resolution spectrum of the N atom was used to measure the fraction protonated of LMF. For each sample, the N spectrum was recorded in duplicate in two separate regions. Curve fitting was performed using the program Origin following smart baseline subtraction.

**Dissolution**

Solubility tests were performed in simulated gastric fluid (SGF). The details of sample preparation, data collection and analysis have been described previously.[6]

## 2.4. Results & Discussion

### *Amorphous Formulations of LMF and PAA by Slurry Conversion*

Fig. 1 shows the typical XPS spectra of the N atom collected to determine the degree of proton transfer (salt formation). These materials were prepared at different drug loading with PAA 450 kg/mol using the slurry-conversion method and confirmed amorphous by XRD. The pure drug, a free base, shows a single peak at 399 eV, corresponding to the unprotonated amine N. With increasing PAA concentration (decreasing drug loading), this peak decreases and a new peak emerges at 401.5 eV. The new peak corresponds to the protonated amine group of higher electron binding energy.[8,19] Together, the spectra in Fig. 1 indicate an increase of the protonated fraction of the drug with increasing PAA concentration.

The fraction protonated of LMF is calculated from an XPS spectrum as follows:

$$\%\ N\ protonated = \frac{A_P}{A_P + A_N} \times 100$$

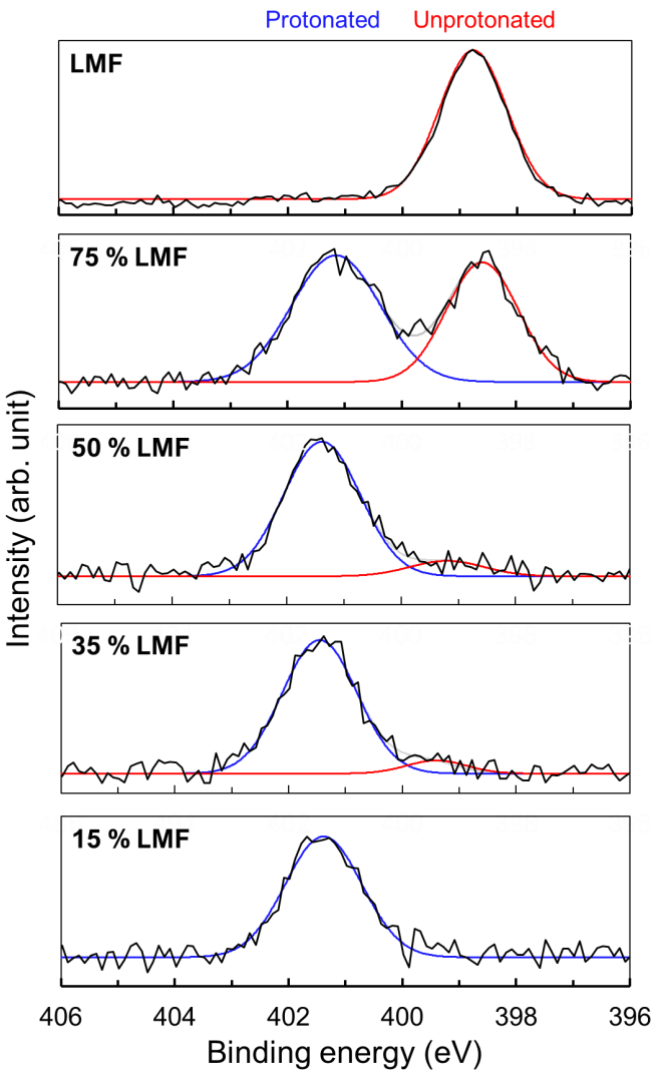


**Fig. 1**. Typical XPS N spectra of amorphous LMF-PAA. These materials were prepared by slurry conversion using PAA 450 kg/mol. With increasing PAA concentration (decreasing drug loading), the unprotonated N peak decreases and the protonated N peak increases. The curves are Gaussian fits of the peaks.

where $A_P$ and $A_N$ are the areas of the protonated and neutral nitrogen peaks, respectively, obtained by curve fitting (Fig. 1).

Because XPS is a surface analytical tool with a probe depth of several nanometers,[18] it is important to establish that the degree of salt formation measured by XPS is representative of the entire material, not just the surface region. For this purpose, we compare in Fig. 2 the drug concentrations in the bulk and at the surface for a series of materials prepared by slurry conversion. The bulk concentration was obtained from the initial amounts of LMF and PAA used for slurry synthesis. Since neither component was lost in this one-pot synthesis, the overall concentration of the product can be obtained from the initial amounts. The surface concentration was measured by XPS as follows:[18]

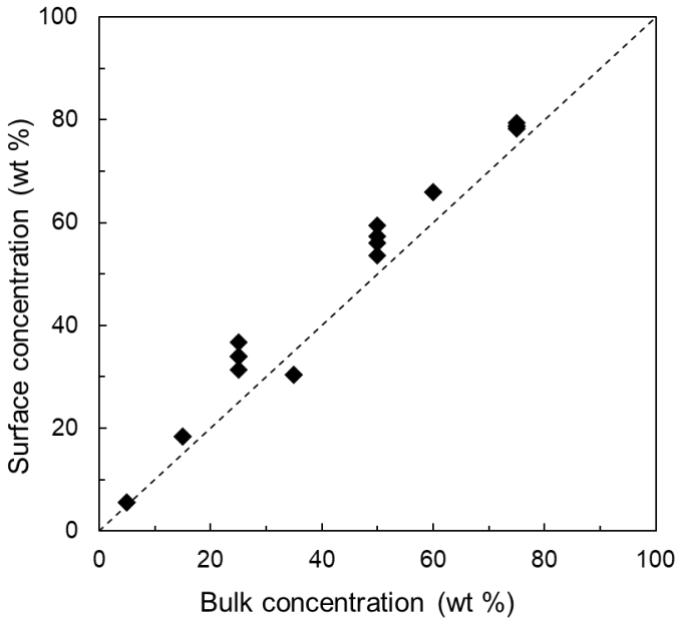


**Fig. 2**. Surface concentration of LMF as a function of bulk concentration. The diagonal line indicates perfect agreement of the two concentrations.

$$w_{LMF} = \frac{2k/M_P}{\frac{2k}{M_P} + \frac{1-k}{M_{LMF}}}$$

where $w_{LMF}$ is the weight fraction of LMF, $k$ is the measured N/O ratio, $M_P$ is the molecular weight of the PAA monomer, and $M_{LMF}$ is the molecular weight of LMF.

Fig. 2 indicates that there is no significant difference between the drug concentrations at the surface and in the bulk. This is not surprising because before XPS analysis, each sample was ground to fine particles, exposing fresh surfaces that had the bulk composition. According to Yu et al.,[20] the time for the surface composition to equilibrate is determined by the rate of polymer diffusion through the bulk and can be years or longer below the glass transition temperature. That is, even if a thermodynamic driving force exists for component segregation in the surface region, the kinetics is too slow to have a significant effect on our results and the degree of salt formation from XPS is representative of the bulk material.

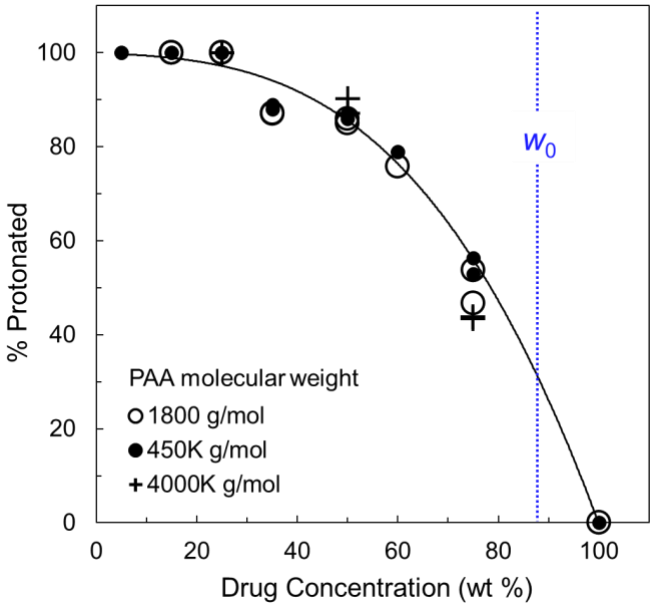


**Fig. 3.** Fraction protonated of LMF in amorphous formulations with PAA of different MW. For PAA 450 and 4000 kg/mol, some results were obtained with more vigorous mixing. A single trend is observed regardless of PAA MW, indicating the reaction had reached equilibrium. The vertical line at $w_0$ = 88 wt % corresponds to one LMF molecule (MW = 528.9 g/mol) per PAA monomer (MW = 72.1 g/mol). The curve is a guide to the eye.

Fig. 3 shows the fraction of LMF molecules that are protonated in the amorphous formulations with PAA of three MWs (1.8, 450, and 4000 kg/mol) prepared by slurry conversion. For each MW series, the fraction protonated is plotted against drug loading. For PAA 1800 g/mol, the results correspond to the products of the standard slurry synthesis.[6] For higher-MW PAA grades, the results correspond either to the products of standard synthesis or to those prepared with more vigorous mixing. As discussed below, for formulations of high polymer content (low drug loading), enhanced mixing was needed to complete the proton transfer. The data in Fig. 3 form a single trend with no significant difference between PAA of different MWs. This indicates that the acid-base reaction between LMF and PAA had reached equilibrium under the slurry conditions used. If, on the other hand, the degree of salt formation was limited by kinetics, the larger, less mobile polymer

would be slower to react and show lower degree of salt formation. The simplest explanation for the "master curve" in Fig. 3 is that slurry synthesis allowed the reaction to reach equilibrium.

Fig. 3 shows that the fraction of LMF molecules that are protonated increases as the PAA concentration increases (as drug loading decreases). The fraction is zero for the pure drug (a free base) and rises with the PAA concentration, approaching 100 % above 70 wt % PAA. This trend is sensible since at a low PAA concentration, not enough acidic groups are available to neutralize all the basic drug molecules. The vertical line at $w_0$ = 88 wt % corresponds to one LMF molecule (MW = 528.9 g/mol) per PAA monomer (MW = 72.1 g/mol). The observed profile indicates that even when PAA monomers are in excess, not every monomer can react with a drug molecule.

As noted above, some formulations required more vigorous mixing to reach reaction equilibrium than utilized in the standard slurry synthesis.[6] This occurred at higher PAA MW and higher PAA concentration. We illustrate this in Fig. 4 for PAA 4000 kg/mol. For this MW grade, significant gelling occurred upon addition of the solvent and stirring became difficult. As a result, the reaction was slower and less reproducible. In Fig. 4, we compare the protonation profiles of amorphous LMF prepared with PAA 4000 kg/mol using the standard slurry synthesis (open symbols) and with enhanced mixing in a Retsch mill (solid symbols). The products of the standard synthesis showed less complete proton transfer and larger scatter, whereas the products formed with enhanced mixing had higher and tighter degrees of salt formation. For this reason, the PAA 4000 kg/mol results in Fig. 3 correspond to those obtained with enhanced mixing.

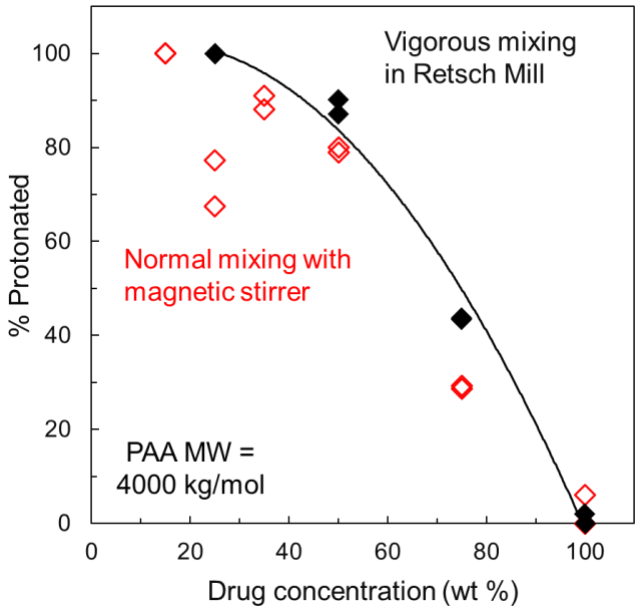


**Fig. 4.** Fraction protonated in amorphous LMF-PAA prepared with PAA 4000 kg/mol using the standard slurry method (open symbols) and with enhanced mixing (solid symbols). The latter show higher and tighter degrees of protonation due to more complete reaction. The curve is a guide to the eye.

A 4000 kg/mol polymer is massive and it is not surprising that better mixing is required to complete the reaction with the drug. For PAA 450 kg/mol, the effect described above is less severe and noticeable only at high polymer concentrations (above 50 wt %). When a significant effect is noted, the results plotted in Fig. 3 correspond to those obtained with enhanced mixing.

***Amorphous Formulations of LMF and PAA by Antisolvent Precipitation***

To expand the survey of synthetic methods, we investigated antisolvent precipitation as an alternative approach to preparing amorphous LMF-PAA. This method is analogous to "coprecipitated amorphous dispersion" (cPAD) of Strotman and Schenck.[14] In this method, each component was dissolved first (LMF in acetone and PAA in water) and the mixing of the two solutions induced precipitation. The precipitant was confirmed amorphous by XRD. As in the case of slurry conversion, antisolvent precipitation was performed using PAA of different MWs (1.8, 450, 4000 kg/mol) at different drug/polymer ratios that corresponded to 25, 50, and 75 % drug loading. This "bottom-up" method could, in principle, achieve more complete mixing of the reactants than a "top-down" method like HME and slurry conversion. An issue with the precipitation method, however, is the unknown composition of the precipitant, since it is separated from the supernatant which can contain dissolved reactants. In contrast, the composition of a slurry-prepared product is known from the initial amounts of the ingredients because no ingredient is lost during synthesis. For this reason,

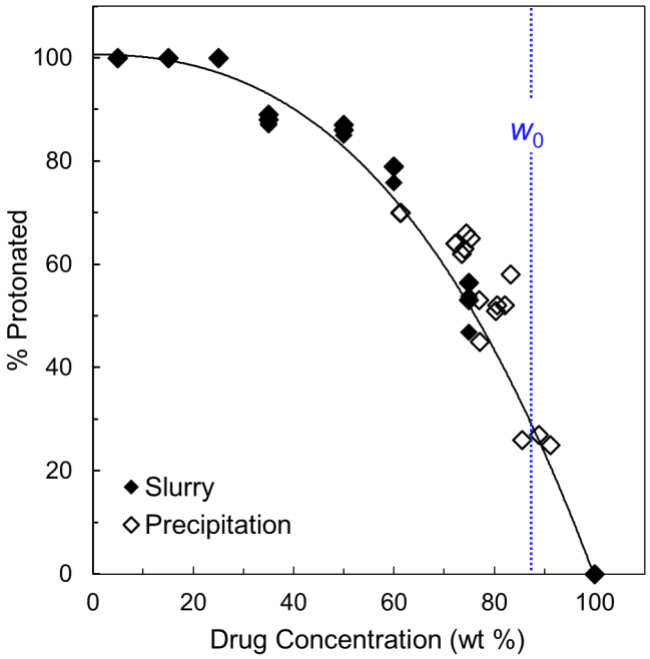


**Fig. 5.** Protonated fraction of LMF vs. drug concentration. The materials were prepared by slurry conversion (solid symbols) and antisolvent precipitation (open symbols) using PAA of different MWs, which are not distinguished. Within experimental error, the materials prepared by the two methods form a single trend. The vertical line at $w_0$ has the same meaning as that in Fig. 3. The curve is a guide to the eye.

the drug concentration in a precipitated product must be determined and we did so by XPS from the N/O atomic ratios as described previously (Fig. 2).[18]

In Fig. 5, we compare the protonation profiles of the products of antisolvent precipitation (open symbols) and slurry conversion (solid symbols). For the slurry products, the results are the same as those in Fig. 3 but we do not distinguish the PAA MWs since the data cluster together. Similarly, for the precipitated products, the PAA MW had no significant effect on the degree of protonation observed and we simply plot the results together without distinguishing the PAA MWs. Fig. 5 shows that relative to slurry conversion, antisolvent precipitation consistently yielded products of high drug loading (70 – 90 wt %), regardless of the initial drug/polymer ratio. This means a significant fraction of PAA did not coprecipitate with LMF but remained dissolved in the solution. This is caused by the high aqueous solubility of PAA. For this reason, the actual drug concentration in the precipitant did not correspond to the initial drug loading and must be determined post-isolation by XPS. It is interesting that the precipitated materials all had a composition close to $w_0$ (one LMF molecule per PAA monomer).

Despite their narrower range of composition, the products of antisolvent precipitation join the same trend as those prepared by slurry conversion. This single trend strongly supports the idea that both methods reached the equilibrium for the acid-base reaction between the drug and the polymer. Between the two methods, slurry conversion provided continuous tunability of drug loading whereas antisolvent precipitation yielded products of only high drug loading. For this reason, slurry conversion is the more versatile of the two and the method of choice for the remainder of this work.

In Fig. 6, we compare the degrees of salt formation in the amorphous materials of LMF and PAA prepared by different methods, including slurry conversion used in this work and HME and RE used by Song et al.[8] In addition, a melt-quench formulation from this work is included. For a fair comparison, all these materials were prepared with PAA of the same MW (450 kg/mol). All the % protonated values in Fig. 6 were obtained by XPS and prior to XPS analysis, each sample was milled to ensure that the internal composition was analyzed (Fig. 2). It is noteworthy that the slurry-

prepared formulations reached significantly higher degrees of salt formation than those by RE and HME. At 40 % drug loading, the slurry method reached 85 % drug protonation, while HME and RE 5 % and 15 %, respectively. This indicates that the drug-polymer reaction was incomplete in the latter two cases. This is startling since HME and RE are standard methods for ASD manufacturing and reached very low degrees of salt formation relative to what is possible.

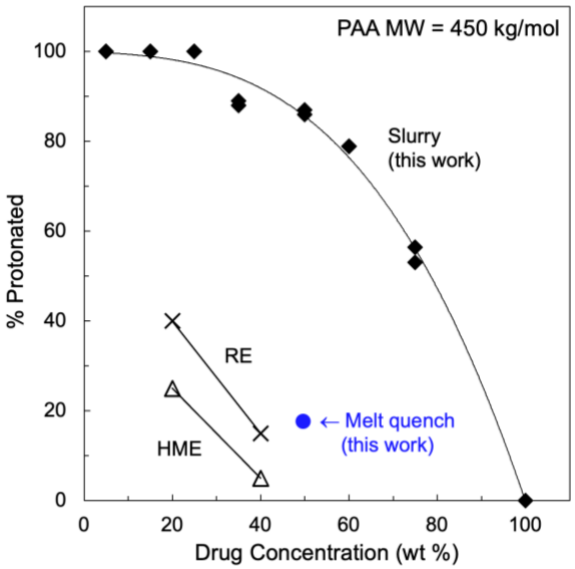


**Fig. 6.** Comparison of protonation profiles in amorphous LMF formulated with PAA 450 kg/mol by different methods. At the same drug loading, slurry conversion (solid diamonds) achieved significantly more complete salt formation than HME and RE used by Song et al.[8] and a melt-quench method used in this work. The curve is a guide to the eye.

To investigate salt formation by HME, we prepared an amorphous formulation of LMF and PAA under conditions that mimic HME. This formulation was prepared at 50 % drug loading using PAA 450 kg/mol; the ingredients were melted together and stirred in the molten state. This formulation reached 19 % protonation (Fig. 6), which is broadly consistent with Song et al.'s HME values but significantly lower than the level reached by slurry synthesis. This comparison confirms the low degree of salt formation by HME and indicates the significant role of manufacturing methods and process conditions in completing the reaction between a drug and a polymer.

Why is the proton transfer between LMF and PAA less complete in HME than in slurry conversion? In an HME process, LMF and PAA are mixed through heat and mechanical agitation without the aid of a solvent. This might suggest that a solvent could facilitate the reaction, perhaps by reducing the kinetic barrier for reaction. This notion is consistent with the Song et al.'s observation of a higher degree of salt formation by RE than by HME. However, it cannot explain the large discrepancy between their RE product and our slurry product (Fig. 6). The RE process of Song et al. used more solvent (50:1 liquid/solid ratio) than our slurry method (4:1). In the RE

process, LMF and PAA were initially dissolved in a single solvent (DCM/methanol), which was then removed under vacuum. The larger amount of solvent used could increase the drying time and the likelihood of phase separation during drying. Despite these differences, the general similarity between RE and slurry conversion suggests that the RE conditions could be modified to achieve more complete salt formation. Overall, the results presented in Fig. 6 highlight the importance of process conditions in preparing amorphous formulations that have a consistent internal state of drug-polymer interactions. In the next section, we explore the effect of a varying degree of salt formation on drug stability and release.

***Effect of Salt Formation on Stability and Drug Release.*** To investigate the effect of salt formation on formulation performance, we studied the stability and dissolution of two amorphous LMF-PAA formulations that had identical drug loading (50 wt %) and PAA MW (450K g/mol), but different degrees of salt formation. By slurry synthesis, we prepared a material with 70 % protonation, and by melt quench, a material with 19 % protonation. Figure 7a shows the XPS spectra of the two materials, where the slurry-prepared material exhibits a larger

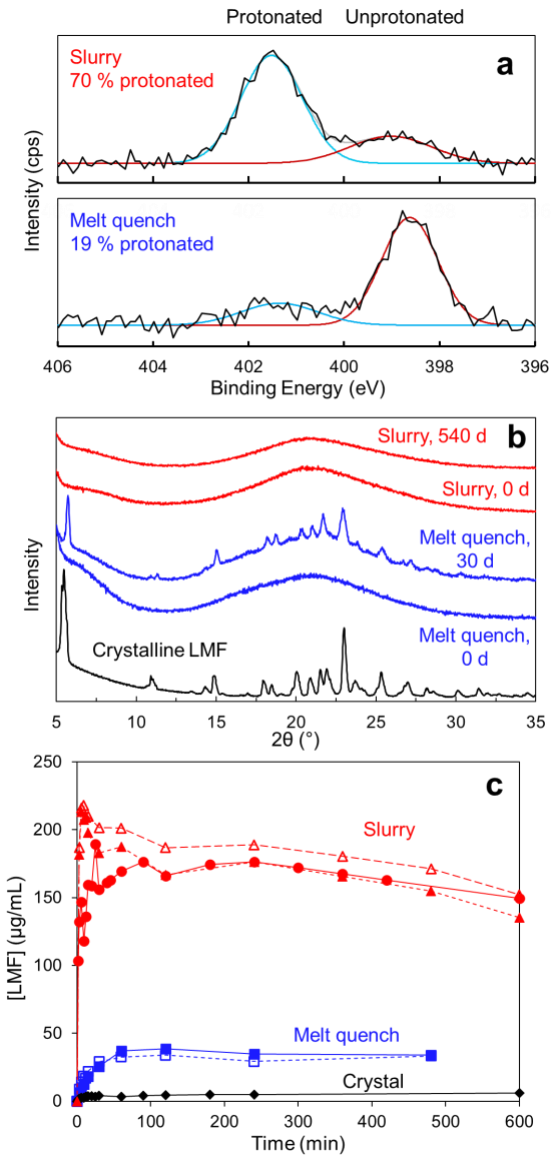


**Fig. 7.** (a) XPS spectra of two amorphous LMF formulations prepared by slurry conversion and melt quench. Both were prepared with PAA MW 450 kg/mol at 50 % drug loading but had different degrees of salt formation. (b) Stability of the two formulations in (a) at 40 °C and 75 % RH. The melt-quenched formulation crystallized faster than the slurry-prepared formulation. (c) Dissolution curves of the two formulations in (a) and crystalline LMF. For each sample, the different symbols indicate results on independent batches. The melt-quenched material reached higher concentration than the crystals, but much lower value than the slurry-prepared material.

protonated N peak and the melt-quenched material a larger unprotonated N peak. Both materials were amorphous as-prepared according to XRD.

Figure 7b shows the stability of these two materials against crystallization at 40°C and 75 % R.H. The slurry-prepared formulation remained amorphous after 540 d,[6] whereas the melt-quenched material crystallized significantly after 30 d. This is fully consistent with our understanding of the effect of drug-polymer salt formation on stability. The strong ionic interactions reduce the crystallization driving force to a greater extent than possible by the mixing of the neutral drug and polymer molecules or the molecules ionized to a lesser extent. This comparison indicates the positive effect of more complete salt formation on stability.

Fig. 7c shows the dissolution curves for the two amorphous formulations above in simulated gastric fluid (SGF). For comparison, the result is also shown for the crystalline drug. Relative to the crystals, both amorphous formulations show elevated concentrations for at least 8 h, but the slurry-prepared formulation reached significantly higher concentration (by a factor of 5) than the melt-quenched formulation. In light of the different degrees of protonation (70 % and 19 %, respectively), these results indicate a positive effect of salt formation on drug solubilization. It is noteworthy that the comparisons in Figs. 7b and 7c are between two materials that are identical in every respect except for the degree of salt formation. This strengthens the conclusion that more complete salt formation improves the stability and the drug release of an amorphous formulation of LMF and PAA.

That the salt formation between LMF and PAA can simultaneously enhance stability and drug release might seem counterintuitive, since stability often leads low solubility. But this dual enhancement has been observed for both LMF[6] and CFZ[7] formulated with PAA. Hiew et al. recently investigated the amorphous formulations of LMF with a series of polymers (excluding PAA) prepared by RE[17] and noted that formulations containing protonated LMF tend to be more stable against crystallization but have worse dissolution performance. Their conclusion agrees with ours with respect to stability but not dissolution. To understand this, we note that the polymer of our formulation, PAA, was not in their study and could be exceptional. In addition, the dissolution medium is SGF in this study, but a phosphate buffer in their study. Further work is warranted to develop a unified understanding of the wide range of observations.

***Greater Protonating Power of PAA "Dimer".*** The results in Fig. 3 indicate that PAA of different MWs (1.8 – 4000 kg/mol) have similar ability to protonate LMF. We now show that at a lower MW, PAA could have a greater protonating power. Fig. 8 shows the degree of salt formation as a function of PAA MW at a fixed drug loading of 75 %. At this drug loading, the polymer formulations show a similar degree of salt formation, ~50 %. We use maleic acid (MW = 116.07 g/mol) as a mimic for a dimer of PAA. An amorphous salt of LMF and maleic acid was prepared using a solvent evaporation method[21] and was found to contain LMF that was 85 % protonated. This suggests a possible increase of protonating power below MW ~ 1 kg/mol. One explanation for this effect is that LMF is a larger molecule than a PAA monomer and binding to one monomer on a polymer chain blocks the access to the adjacent segments. For a free-moving dimer, however, this crowding effect is less severe. Despite this potential increase of protonating power at low MW, we do not advocate the use of small-molecule counterions for salt formation because we would lose the stabilizing benefit of a polyelectrolyte. Yao et al. showed that amorphous particles of LMF formulated with PAA 450 kg/mol at 50 wt % drug loading remained free-flowing after 540 days at 40 °C and 75 % R.H.[6] In contrast, the same formulation prepared with maleic acid became a viscous liquid after 1 day under the same condition. This is a consequence of a large increase of the glass transition temperature by the polyelectrolyte while the same stabilizing effect is not achieved with a small counterion.

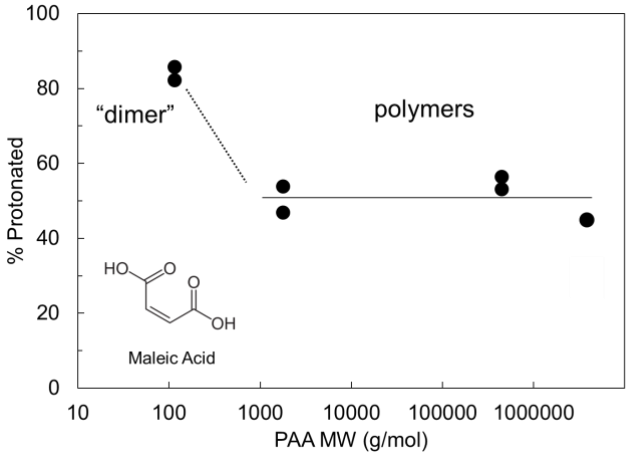


**Fig. 8**. Fraction of LMF molecules in amorphous LMF-PAA that are protonated as a function of PAA MW. For this comparison, the drug loading was fixed at 75 %. Maleic acid, a dicarboxylic acid, is used to mimic a PAA dimer. For the polymers, the ability to protonate LMF is insensitive to MW (horizontal line), while the protonating power could increase for oligomers (sloping line).

***Salt Formation in LMF-PAA and CFZ-PAA.*** Figure 9 compares the degrees of salt formation in the LMF-PAA system and in the CFZ-PAA system.[7] Both formulations were prepared using the slurry method with PAA 450 kg/mol. Gui et al. determined the degree of salt formation in CFZ-PAA by visible absorption spectroscopy, taking advantage of the color change of CFZ upon protonation. At the same drug loading, CFZ is protonated to a greater extent than LMF. CFZ is almost fully protonated below 60 wt % drug loading, whereas LMF does so below 30 wt % drug loading. This demonstrates the important role of the drug molecule in the degree of salt formation that can be reached. It is unclear why CFZ is more easily protonated by PAA than LMF. The literature $pK_a$ values for the two molecules are: 8.5 for LMF,[8] 8.4 (Ref. [22]) and 9.3 (Ref. [23]) for CFZ. While the high $pK_a$ value of CFZ (9.3) is consistent with its more complete salt formation with PAA, the low value (8.4) is not. (Note that the 9.3 value was calculated, not measured.[23]) CFZ is a marginally smaller molecule than LMF, which could "fit" around a PAA chain more easily, perhaps facilitating salt formation. There is some evidence from spectroscopy[22] and computer model[23] that CFZ can be doubly protonated (see illustration at the bottom of Fig. 9). Keswani et al. assign a $pK_a$ of 2.3 to this site,[23] which suggests that it could not be protonated by PAA ($pK_a$ = 4.5). In the crystal structure of CFZ with citric acid, this site is observed to form a hydrogen bond with a carboxylic acid group without ionization,

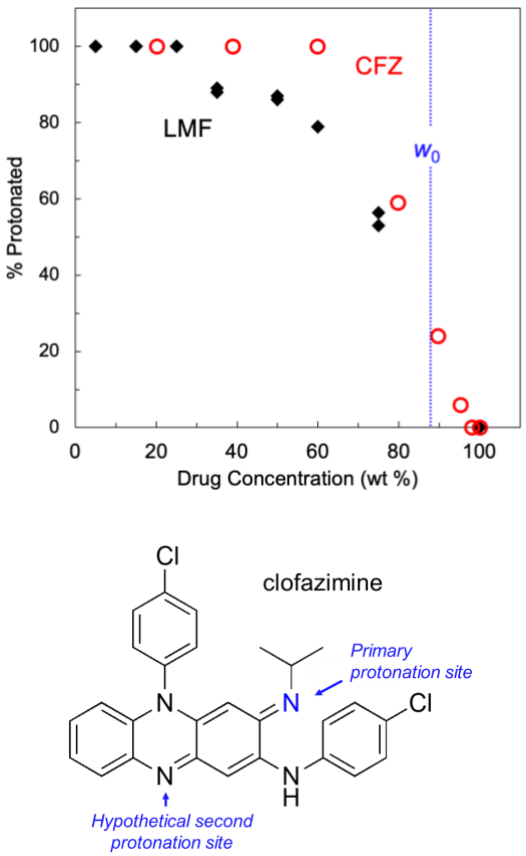


**Fig. 9.** Comparison of the degrees of salt formation in LMF-PAA and in CFZ-PAA prepared with PAA 450 kg/mol. At the same drug loading, salt formation is more complete for CFZ than LMF. The vertical line at $w_0$ corresponds to 1 drug molecule per PAA monomer (MW = 72.06 g/mol) with $w_0$ = 88 wt % for LMF (MW = 528.9 g/mol) and 87 % for CFZ (MW = 473.4 g/mol), indistinguishable at the scale used.

while the primary site is protonated and forms a hydrogen-bonded ion pair with a carboxylate ion.[24] Similar multi-site interactions could occur in CFZ-PAA, possibly aiding salt formation. It is interesting to note that in the crystals, the protonated LMF and CFZ each form a cyclic hydrogen-bonded ion pair with a carboxylate ion. In the fumarate salt of LMF, the ammonium group and the adjacent OH group form a cyclic hydrogen bond with both oxygen atoms of the carboxylate ion.[24] In the carboxylate salts of CFZ, the imine N and the adjacent NH group are both hydrogen bonded with one of the O atoms of the carboxylate ion.[25] It is possible that similar hydrogen-bonded ion pairs occur in the amorphous phase of LMF-PAA and CFZ-PAA.

## 2.5. Conclusions

This study investigated the effects of different synthetic methods and process conditions on the degree of salt formation between the basic drug LMF and the acidic polymer PAA. The products of slurry conversion and antisolvent precipitation form a single trend where the degree of salt formation systematically increases with increasing PAA concentration, regardless of PAA's molecular weight (Figure 3). This is a strong indication that the master trend observed represents the equilibrium for salt formation since a kinetically hindered reaction would be less complete for PAA of higher molecular weight. Remarkably, the literature methods of HME and RE[8] reached far lower degrees of salt formation than the reaction equilibrium (Figure 5). This is significant since both HME and RE are standard methods for manufacturing amorphous solid dispersions. Their inability to complete the salt formation between a drug and a polymer calls for careful control of process conditions and characterization of the final product for quality control. We find that a high degree of salt formation has a positive effect on drug stability and release (Figure 7). This justifies future work to optimize reaction conditions to achieve maximal and reproducible salt formation. Based on this work, we recommend slurry conversion as the method for preparing amorphous drug-polymer salts for its low cost, its ability to complete salt formation, and its ability to continuously adjust drug loading. There is certainly room for further development in this area and a deeper understanding of the effect of salt formation on drug performance.

The results of this work have given a vivid illustration of the extremely different physical states that an amorphous drug-polymer formulation can have because of a change in the method of

preparation and process conditions. The amorphous nature of a formulation might give the impression that the ingredients are uniformly mixed at the molecular level. But for the system studied here, the drug and the polymer can be almost fully reacted to form a salt or barely reacted at all, depending on the method of preparation (Figure 6). This translates to a significant difference in drug stability and release (Figure 7). The extreme variability of physical states attained by a drug-polymer formulation stems from the low mobility of macromolecules and the linking in a chain of reaction sites. Relative to a small counterion, reaction with a polyelectrolyte could be significantly slower.[26] Consistent with this view, in our slurry method, PAA of the highest MW (4000 kg/mol) required more vigorous agitation to complete salt formation, especially when polymer concentration was high. Although this work focused on a system in which the drug and the polymer can ionize each other, the state of mixing is likely a general issue in developing amorphous solid dispersions whether or not salt formation occurs, with strong impact on product performance.

## 2.6. Acknowledgements

The part of this work to develop amorphous drug-polymer salts was supported by the Bill and Melinda Gates Foundation (OPP1160408) and benefitted from helpful discussions with Niya Bowers, David Monteith, and Paco Alvarez. We acknowledge the support from BMS to develop the XPS method to measure the surface composition of amorphous formulations and the access to the characterization facility of the NSF-supported University of Wisconsin Materials Research Science and Engineering Center (DMR-1720415). We thank the Zeeh Pharmaceutical Experiment Station and the Analytical Instrumentation Center in School of Pharmacy at University of Wisconsin-Madison for analytical support.

## 2.7. References


[1] Babu, N. Jagadeesh, and Ashwini Nangia. Solubility Advantage of Amorphous Drugs and Pharmaceutical Cocrystals. *Crystal Growth & Design* **2011**, *11* (7), 2662–2679.
[2] Murdande, Sharad B., et al. Solubility Advantage of Amorphous Pharmaceuticals: I. A Thermodynamic Analysis." *Journal of Pharmaceutical Sciences* **2010**, *99* (3), 1254–1264.
[3] Kennedy, Michael, et al. Enhanced Bioavailability of a Poorly Soluble VR1 Antagonist Using an Amorphous Solid Dispersion Approach: A Case Study. *Molecular Pharmaceutics* **2008** *5* (6), 981–993.
[4] Van den Mooter, Guy. The Use of Amorphous Solid Dispersions: A Formulation Strategy to Overcome Poor Solubility and Dissolution Rate. *Drug Discovery Today: Technologies* **2012** *9* (2), e79–8e5.
[5] Brough, Chris, and R. O. Williams. Amorphous Solid Dispersions and Nano-Crystal Technologies for Poorly Water-Soluble Drug Delivery. *International Journal of Pharmaceutics* **2013**, *453* (1) 157–66.
[6] Yao, X.; Kim, S.; Gui, Y.; Chen, Z.; Yu, J.; Jones, K. J.; Yu, L. Amorphous Drug–Polymer Salt with High Stability under Tropical Conditions and Fast Dissolution: The Challenging Case of Lumefantrine-PAA. *Journal of Pharmaceutical Sciences* **2021**, *110* (11), 3670–3677.
[7] Gui, Y.; McCann, E. C.; Yao, X.; Li, Y.; Jones, K. J.; Yu, L. Amorphous Drug–Polymer Salt with High Stability under Tropical Conditions and Fast Dissolution: The Case of Clofazimine and Poly(Acrylic Acid). *Molecular Pharmaceutics* **2021**, *18* (3), 1364–1372.
[8] Song, Y.; Zemlyanov, D.; Chen, X.; Su, Z.; Nie, H.; Lubach, J. W.; Smith, D.; Byrn, S.; Pinal, R. Acid-Base Interactions in Amorphous Solid Dispersions of Lumefantrine Prepared by Spray-Drying and Hot-Melt Extrusion Using X-Ray Photoelectron Spectroscopy. *International Journal of Pharmaceutics* **2016**, *514* (2), 456–464.
[9] Maniruzzaman, M.; Boateng, J. S.; Snowden, M. J.; Douroumis, D. A Review of Hot-Melt Extrusion: Process Technology to Pharmaceutical Products. *ISRN Pharmaceutics* **2012**, *2012*, 1–9.
[10] Patil, H.; Tiwari, R. V.; Repka, M. A. Hot-Melt Extrusion: From Theory to Application in Pharmaceutical Formulation. *AAPS PharmSciTech* **2015**, *17* (1), 20–42.
[11] Sollohub, K.; Cal, K. Spray Drying Technique: II. Current Applications in Pharmaceutical Technology. *Journal of Pharmaceutical Sciences* **2010**, *99* (2), 587–597.
[12] Taylor, L.S, Zografi, G. Spectroscopic Characterization of Interactions Between PVP and Indomethacin in Amorphous Molecular Dispersions. *Pharm. Res*. 1997, *14* (12), 1691-1698.
[13] Trasi, N. S.; Bhujbal, S. V.; Zemlyanov, D. Y.; Zhou, Q. (Tony); Taylor, L. S. Physical Stability and Release Properties of Lumefantrine Amorphous Solid Dispersion Granules Prepared by a Simple Solvent Evaporation Approach. *International Journal of Pharmaceutics: X* **2020**, *2*, 100052.
[14] Strotman, N. A.; Schenck, L. Coprecipitated Amorphous Dispersions as Drug Substance: Opportunities and Challenges. *Org. Process Res. Dev*. **2022**, *26*, 10−13.
[15] Frank, Derek S., et al. Densifying Co-Precipitated Amorphous Dispersions to Achieve Improved Bulk Powder Properties. *Pharmaceutical Research* **2022.**
[16] Jain, J. P.; Leong, F. J.; Chen, L.; Kalluri, S.; Koradia, V.; Stein, D. S.; Wolf, M.-C.; Sunkara, G.; Kota, J. Bioavailability of Lumefantrine Is Significantly Enhanced with a Novel Formulation Approach, an Outcome from a Randomized, Open-Label Pharmacokinetic Study in Healthy Volunteers. *Antimicrobial Agents and Chemotherapy* **2017**, *61* (9).
[17] Hiew, T. N.; Zemlyanov, D. Y.; Taylor, L. S. Balancing Solid-State Stability and Dissolution Performance of Lumefantrine Amorphous Solid Dispersions: The Role of Polymer Choice and Drug–Polymer Interactions. *Molecular Pharmaceutics* **2021**.
[18] Yu, J.; Li, Y.; Yao, X.; Que, C.; Huang, L.; Hui, H.-W.; Gong, Y.; Qian, F.; Yu, L. Surface Enrichment of Surfactants in Amorphous Drugs: An X-Ray Photoelectron Spectroscopy Study. *Molecular Pharmaceutics* **2022**, *19* (2), 654–660.
[19] NIST X-ray Photoelectron Spectroscopy Database, NIST Standard Reference Database Number 20, *National Institute of Standards and Technology* **2000**

[20] Yu, J.; Yao, X.; Que, C.; Huang, L.; Hui, H.-W.; Gong, Y.; Qian, F.; Yu, L. Kinetics of Surface Enrichment of a Polymer in a Glass-Forming Molecular Liquid. *Molecular Pharmaceutics* **2022**, *19* (9), 3350–3357.
[21] Tomar, D.; Lodagekar, A.; Gunnam, A.; Allu, S.; Chavan, R. B.; Tharkar, M.; Ajithkumar, T. G.; Nangia, A. K.; Shastri, N. R. The Effects of *Cis* and *Trans* Butenedioic Acid on the Physicochemical Behavior of Lumefantrine. *CrystEngComm* **2022**, *24* (1), 156–168.
[22] O'Connor, R.; O'Sullivan; J. F.; O'Kennedy, R. The Pharmacology, Metabolism, and Chemistry of Clofazimine. *Drug Metabolism Reviews* **1995***, 27(4),* 591-614.
[23] Keswani, R. K.; Tian, C.; Peryea, T.; Girish, G.; Wang, X.; Rosania, G. R. Repositioning Clofazimine as a Macrophage-Targeting Photoacoustic Contrast Agent. *Sci. Rep.* **6**, 23528; doi: 10.1038/srep23528 (2016).
[24] Bannigan, P. et al. CCDC 1559559. *Experimental Crystal Structure Determination* **2018**.
[25] Bannigan, P.; Durack, E.; Madden, C.; Lusi, M.; Hudson, S. P. Role of Biorelevant Dissolution Media in the Selection of Optimal Salt Forms of Oral Drugs: Maximizing the Gastrointestinal Solubility and in Vitro Activity of the Antimicrobial Molecule, Clofazimine. *ACS Omega* **2017**, *2*, 8969−8981.
[26] Gregor, H. P.; Luttinger, L. B.; Loebl, E. M. Metal–Polyelectrolyte Complexes. I. The Polyacrylic Acid–Copper Complex. *The Journal of Physical Chemistry* **1955**, *59* (1), 34–39.

# Chapter 3. Effect of polymer architecture and acidic group density on the degree of salt formation in amorphous solid dispersions

Amy Lan Neusaenger, Caroline Fatina, Junguang Yu, and Lian Yu

As published in:
*Molecular Pharmaceutics* **2024**
DOI: 10.1021/acs.molpharmaceut.4c00089

## 3.1. Abstract

Recent work has shown that an amorphous drug-polymer salt (ADPS) can be highly stable against crystallization under hot and humid conditions (e.g., 40°C/75% RH) and provide fast release and that these advantages depend on the degree of salt formation. Here we investigate the salt formation between the basic drug lumefantrine (LMF) and several acidic polymers: poly(acrylic acid) (PAA), hypromellose phthalate (HPMCP), hypromellose acetate succinate (HPMCAS), cellulose acetate phthalate (CAP), Eudragit L100, and Eudragit L100-55. Salt formation was performed by "slurry synthesis" where dry components were mixed at room temperature in the presence of a small quantity of an organic solvent, which was subsequently removed. This method has been shown to achieve more complete salt formation than the conventional methods of hot-melt extrusion and rotary evaporation. The acidic group density of a polymer was determined by non-aqueous titration in the same solvent used for slurry synthesis; the degree of LMF protonation was determined by X-ray Photoelectron Spectroscopy (XPS). The polymers studied show very different abilities to protonate LMF when compared at a common drug loading, following the order: PAA > (HPMCAS ~ CAP ~ L100 ~ L100-55) > HPMCAS, but the difference largely disappears when the degree of protonation is plotted against the concentration of the available acidic groups for reaction. This indicates that the extent of salt formation is mainly controlled by the acidic group density and less insensitive to the polymer architecture. Our results are relevant for selecting the optimal polymer to control the degree of ionization in amorphous solid dispersions.

## 3.2. Introduction

The use of an amorphous solid dispersion (ASD) to deliver poorly soluble drugs[1,2,3] takes advantage of the higher solubility of an amorphous solid relative to its crystals.[4,5,6,7] For any ASD, the stability against crystallization is essential since crystallization negates its advantages.[8,9] In this context, salt formation between a drug and a polymer is an especially effective approach to inhibiting crystallization under hot and humid conditions.[10,11,12,13,14,15] For clofazimine[10] and lumefantrine,[11] the amorphous salts with poly(acrylic acid) also improve release.

The amorphous formulations of the basic drug lumefantrine (LMF) and the acidic polymer poly(acrylic acid) (PAA) have been prepared using different methods[16,17] and the results indicate a strong dependence of salt formation on the preparation methods, with direct impact on drug stability and release. Using hot-melt extrusion (HME) and rotary evaporation (RE), Song et al. prepared amorphous formulations in which the protonated fractions of LMF molecules were 5% and 15%, respectively, at 40 wt% drug loading.[16] In comparison, a simple slurry-conversion method[10,11] reached 85% protonation at the same drug loading.[17] It was found that more complete protonation of LMF led to higher stability against crystallization and more complete release into a simulated gastric fluid.[17] These results indicate the critical role of process conditions in preparing ASDs to control their molecular-level structure and performance.

In this work, we build on the previous results to investigate the salt formation between LMF and a series of acidic polymers. Our two main questions are: (1) How does the degree of salt formation depend on the polymer structure and properties? and (2) Does the simple slurry method achieve more complete salt formation than the alternative methods for the wide range of polymers? LMF is the model basic drug because of its importance as a WHO Essential Medicine for the first-line treatment of malaria. The low solubility of LMF (BCS Class IV) makes it a candidate for the approach of amorphous formulations to enhance bioavailability.[18] With malaria being more prevalent in tropical and subtropical countries, product stability under hot and humid conditions is required, making drug-polymer salts a potentially useful tool. The polymers chosen for this study include: PAA, Eudragit L100, Eudragit L100-55, hypromellose phthalate (HPMCP), cellulose acetate phthalate (CAP), and hypromellose acetate succinate (HPMCAS); see Scheme 1 for their structures. Among these, PAA, L100, and L100-55 form one group where the polymer backbone

is a carbon chain to which the acidic COOH group is directly attached, and the other polymers have a more complex carbohydrate backbone and the COOH group is attached to a sidechain phthalyl group (HPMCP and CAP) or succinyl group (HPMCAS). The diversity of these polymers helps evaluate the role of polymer architecture and acidic group density on salt formation with LMF. We find that the acidic group density of a polymer has a controlling effect on the degree of salt formation at a given drug loading, whereas the polymer architecture plays a minor role. In addition, the simple slurry method achieves significantly more complete salt formation for all the polymers tested than the alternative methods of HME, RE, and spray drying (SD). These results are relevant for selecting polymers for preparing ADPS and predicting the degree of salt formation and formulation performance.

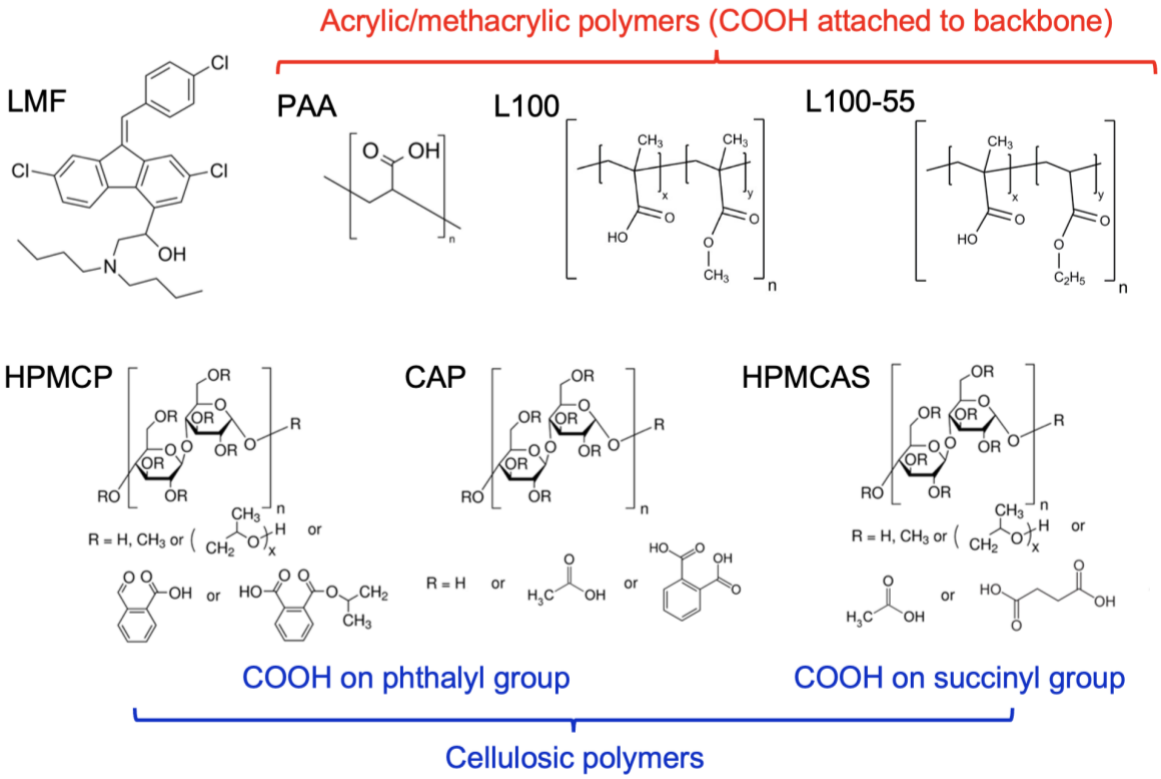


**Scheme 1**. Structures of lumefantrine (LMF) and the acidic polymers used for salt formation. The polymers fall into two groups: (1) the acrylic/methacrylic group (PAA, Eudragit L100 and L100-55), where COOH is attached to the polymer backbone, and (2) the cellulosic group, for which COOH is on the sidechain phthalyl group (HPMCP and CAP) or succinyl group (HPMCAS). Eudragit L100 and L100-55 are random copolymers where the x:y ratio is approximately 1.

## 3.3. Materials & Methods

### Materials

Poly(acrylic acid) (PAA, Carbomer, MW = 450,000 g/mol), cellulose acetate phthalate (CAP, MW = 2,500 g/mol), anhydrous potassium hydroxide (KOH), and phenol red were purchased from Sigma-Aldrich (St. Louis, MO). Eudragit L100 (MW = 125,000 g/mol) and L100-55 (MW = 320,000 g/mol) were purchased from Evonik Industries (Essen, Germany).[19] Hypromellose phthalate (HPMCP-55, MW = 45,600 g/mol) and hypromellose acetate succinate (HPMCAS-LF, HPMCAS-MF, HPMCAS-HF; MW = 17,000 – 20,000 g/mol) were purchased from Shin-Etsu Chemical Company Ltd. (Tokyo, Japan). Lumefantrine was purchased from VWR International (Radnor, PA), dichloromethane (ChromAR grade) from Thermo Fisher Scientific (Fair Lawn, NJ), and ethanol from Decon Laboratories (King of Prussia, PA). All materials were used as received.

### Slurry Synthesis

The slurry synthesis of amorphous LMF-polymer salts was adapted from the method of Yao et al.[11] and conducted at a reduced temperature of 25 °C (from the original 75 °C). The powders of LMF and a polymer were mixed at a target drug loading (typically 25, 50, 75 wt%, other values as needed) and a mixed solvent of dichloromethane (DCM) and ethanol (1:1 v/v) was added at a solid/liquid ratio of 1:4 (w/w). To prevent gelling of the powder, DCM was added first and then ethanol. Each formulation batch contained 400 mg in solid mass. The mixture was stirred

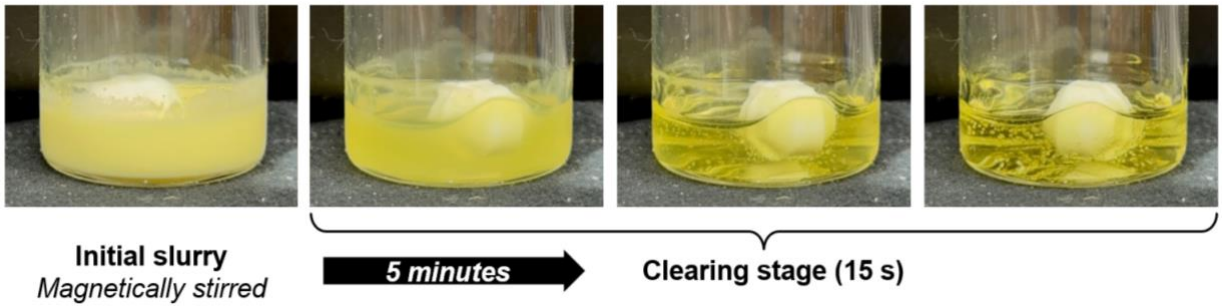


**Scheme 2**. Typical progression of the reaction between LMF and PAA. The left image shows the initial slurry being magnetically stirred. For approximately 5 min, the slurry maintained the same appearance and then abruptly clears. The three images on the right show the abrupt clearing in roughly 15 s. For this preparation, the drug loading was 50 wt%. Similar progression was observed for LMF reacting with other polymers.

magnetically at 25 °C for up to 20 min. During stirring, the initial free-flowing slurry became clear, indicating complete dissolution and amorphization (Scheme 2). The viscous clear solution was dried under vacuum at room temperature for 1 day, resulting in a glassy, brittle foam. This material was ground in an agate mortar with a pestle to a fine powder for further analysis.

**Powder X-ray Diffraction**

X-ray diffraction was performed with a Bruker D8 Advance X-ray diffractometer with a Cu Kα source operating at a tube load of 40 kV and 40 mA. A powder sample of approximately 10 mg was spread and flattened on a Si (510) zero-background holder and scanned between 3° and 40° (2θ) at a step size of 0.02° and a scan rate of 1 s/step.

**X-Ray Photoelectron Spectroscopy (XPS)**

The details of XPS measurement and data analysis have been described previously.[20] For a LMF formulation, approximately 3 mg of a powder was pressed onto a carbon tape fixed to the XPS sample holder. For pure LMF, approximately 1 mg of powder was melted on a glass coverslip and quenched to room temperature by contact with an Al block. The samples were stored in a sealed plastic tube filled with Drierite before XPS analysis. The high-resolution spectrum of the N atom was used to measure the protonated fraction of LMF. For each sample, the spectrum was recorded in duplicate in two separate regions. Curve fitting was performed using the program Origin following smart baseline subtraction.

**Non-aqueous titration**

Colorimetric titration was used to measure the COOH density of each polymer.[21] To be relevant for understanding the drug-polymer reaction, titrations were performed in the same organic solvent used for slurry synthesis. Our method is similar to the USP analysis for phthalyl content in HPMCP. 12.5 mg of each polymer was dissolved in 25 mL of a 1:1 mixture of DCM and ethanol. To this solution approximately 1 mg of the colorimetric indicator phenol red was added and non-aqueous titration was performed in the standard manner with a 0.05 M KOH solution in ethanol as the

titrant and the endpoint identified by the color change from yellow to orange.[21,22] Each titration was performed in duplicate.

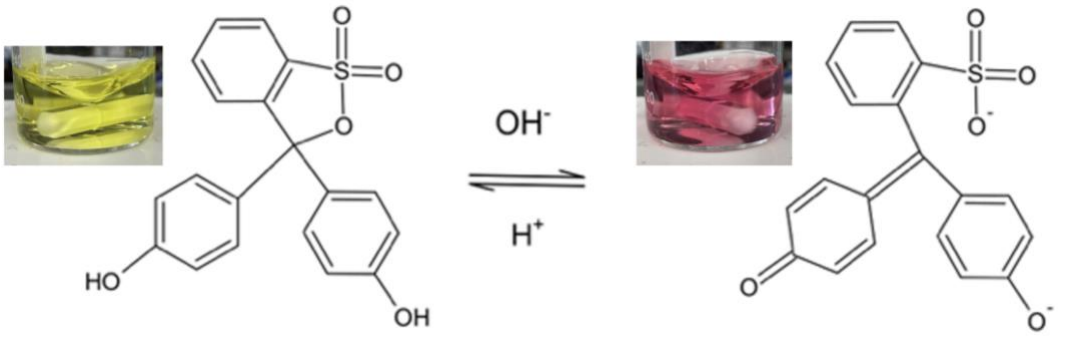


**Scheme 3**. Phenol red as indicator for non-aqueous acid-base titration. The acidic form of the indicator (left) is yellow and the basic form (right) pink.

## 3.4. Results and Discussion

Figure 1 shows the typical XPS spectra of the N atom in LMF in formulations with different acidic polymers (Scheme 1). For this comparison, the drug loading was 50 wt%. These spectra allowed determination of the extent of salt formation between LMF and the polymer. The pure drug shows a single peak at a binding energy (BE) of 399 eV, corresponding to the unprotonated N atom in LMF.[23] Upon reaction with an acidic polymer, a second peak emerges at a higher BE (401.5 eV), corresponding to the protonated N atom in LMF. At the fixed DL of 50 wt%, PAA is the most effective in protonating LMF, followed by L100, L100-55, HPMCP, and CAP (no strong differentiation between the latter 4 polymers), and by HPMCAS (three grades). Among the three grades of HPMCAS, the ability to protonate LMF follows the order LF (highest) > MF > HF (lowest).

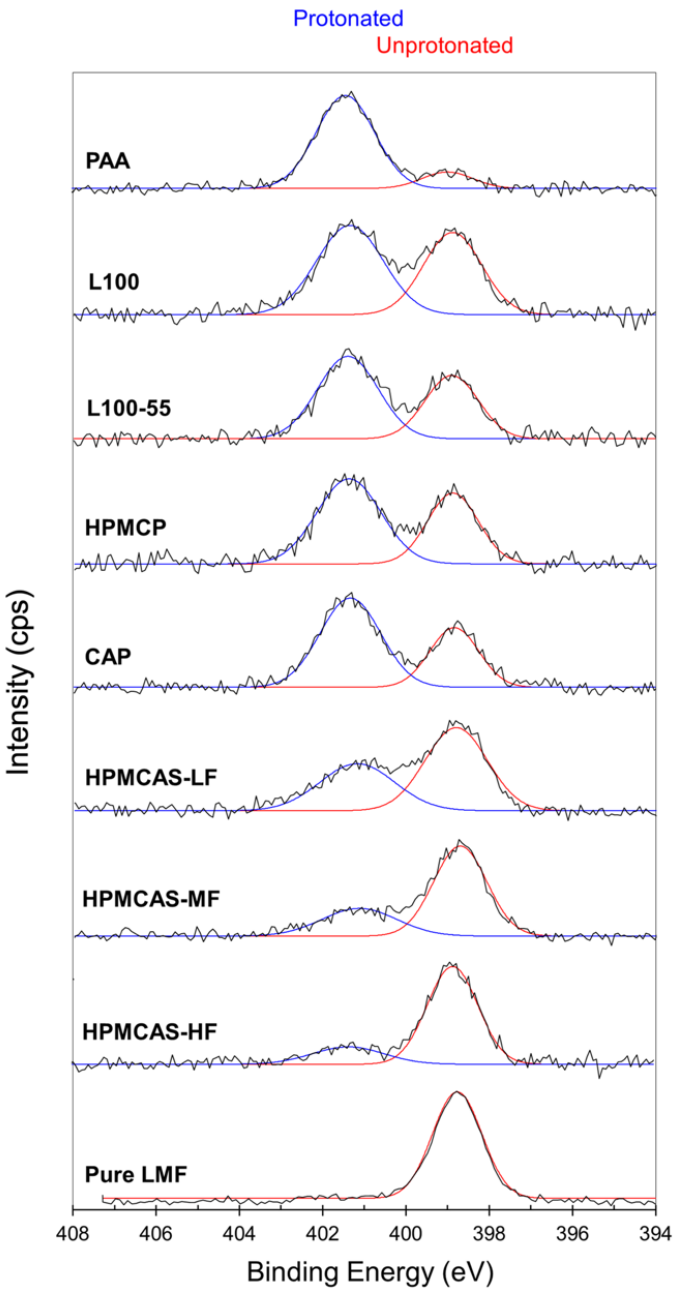


**Figure 1**. Typical XPS spectra of the N atom in LMF formulated with different acidic polymers. For this comparison, drug loading was fixed at 50 wt%. The 399 eV peak corresponds to unprotonated N and the 401.5 eV peak to protonated N. The areas of these peaks areas were used to calculate the degree of protonation of LMF (eq. 1).

The degree of protonation (extent of acid-base reaction) is given by:

$$\%\ N\ protonated = \frac{A_P}{A_P + A_N} \times 100 \qquad (1)$$

where $A_P$ and $A_N$ are the areas of the protonated and unprotonated (neutral) nitrogen peaks, respectively. We obtain the peak areas by fitting each spectrum as a sum of two Gaussian functions (red and blue curves in Figure 1). Although XPS is a surface-analysis tool, previous work has shown that on the timescale of this measurement, the surface composition is identical to the bulk value (no surface enrichment effect).[20]

Figure 2a shows the protonated fraction of LMF as a function of DL in the formulations with the different polymers. For each polymer, the % protonation decreases as DL increases. [17] This is because at higher DL, more LMF molecules compete for each reaction site on the polymer chain and the probability of success is reduced. We observe a large difference between the polymers in their ability to protonate LMF. For example, at 50 wt% DL, the degree of protonation is 20% for the reaction with HPMCAS-HF and 87% with PAA. At any DL, PAA is either the most effective in protonating the drug or ties with CAP. The two polymers

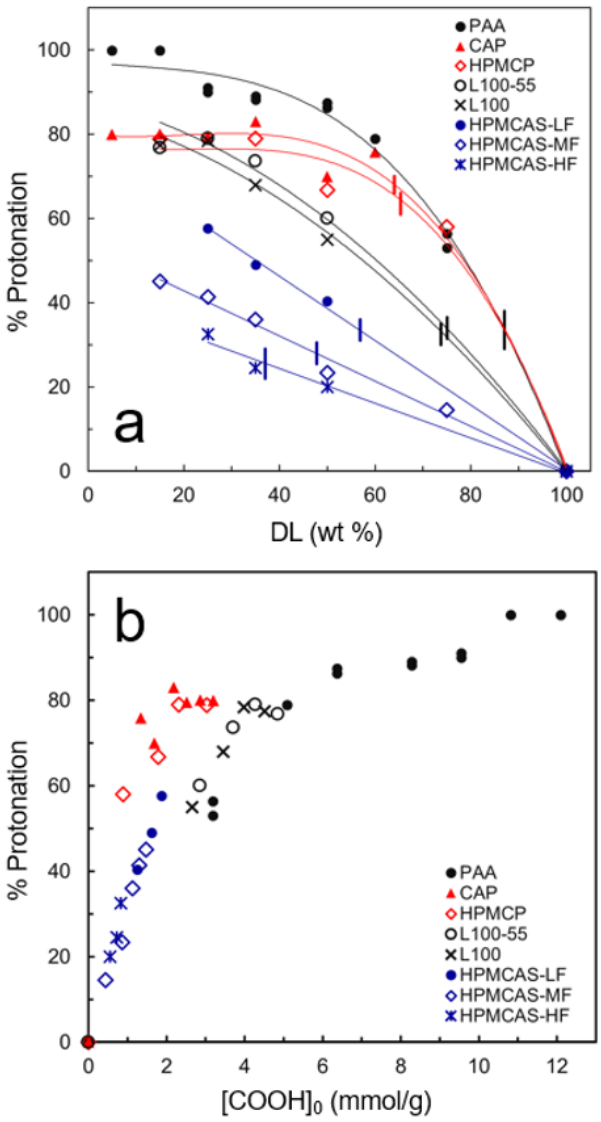


**Figure 2**. (a) Protonated fraction of LMF vs. DL in different polymer formulations. The curves are guide to the eye. The vertical line on each curve indicates the DL, $w_0$, at which LMF and the polymer's COOH have the same molar concentration; see Table 1 for the values of $w_0$. (b) Protonated fraction of LMF vs. the COOH concentration available for reaction.

with PAA-like structures, L100 and L100-55 (see Scheme 1), are significantly less effective than PAA in protonating the drug when compared at the same DL. Of the polymers tested, the HPMCAS group (three grades) is the least effective in protonating the drug at a given DL, and within this group, the ranking is LF > MF > HF. For the cellulosic polymers, those with COOH on a phthalyl group (HPMCP and CAP) are more able to protonate than those with COOH on a succinyl group (HPMCAS). In Figure 2a, the short vertical line on each curve indicates the DL at which the drug and the polymer's COOH group have equal molar concentrations. This quantity, $w_0$, is calculated from the acidic group density of the polymer as discussed below.

In Figure 2b, the % protonation values in Figure 2a are replotted as a function of $[COOH]_0$, the COOH concentration in each formulation given by:

$$[COOH]_0 = (1 - DL)\,[COOH]_P \qquad (2)$$

where DL is the wt% of LMF and $[COOH]_P$ is the COOH density of the polymer determined by non-aqueous titration (see below). In this format, the scattered data points in Figure 2a largely coalesce to a single trend, indicating the polymer's acidic group density plays a major role in the degree of salt formation while its architecture a minor role. Below we first discuss the titration results and then return to Figure 2 for further discussion.

Table 1 shows the COOH densities of the polymers determined by non-aqueous titration. From the titrant volume at the endpoint (Column 2), the COOH density was calculated (Column 3). The titrations were performed in the same organic solvent as used for slurry synthesis (1:1 DCM-ethanol) rather than the standard medium of water to ensure accurate measurement of accessible acidic groups in the reaction medium. This is important as the strength of an acid or base depends on its solvent environment.[21] For a polymer, the solvent has a strong influence on its conformation and accessible reaction sites.[24,25] For the polymers tested, PAA has the highest COOH density, and the two structurally similar polymers, L100 and L100-55, have lower densities, as expected. For the cellulosic polymers, HPMCP and CAP have higher COOH densities than HMPCAS. The measured COOH density for PAA, 12.7 (0.09) mmol/g, is reasonably close to the theoretical value of 13.9 mmol/g and the small difference could result from deviations from the ideal polymer structure (e.g., small degree of crosslinking present in commercial PAA). Of the three HPMCAS grades, the COOH densities follow the order LF > MF > HF and are in *quantitative* agreement

with their succinyl contents.[26] Since the COOH groups in HPMCAS reside on the succinyl sidechain, its density should be proportional to the succinyl content. This is indeed observed (Figure 3) and validates our titration method to determine the acidic group density in a polymer.

Knowing the acidic group density of each polymer, $[COOH]_p$, it is possible to calculate the DL at which the drug has the same molar concentration as the COOH group in the polymer:

$$w_0 = 100\, M_0\, [COOH]_p / (1 + M_0\, [COOH]_p) \qquad (3)$$

where $M_0$ is the molar mass of the drug LMF (528.9 g/mol). The calculated values are given in Table 1. These values provide further validation of the titration method. For example, for PAA, $w_0$ can be calculated from the molar masses of LMF and the AA monomer (72.1 g/mol). The result, 88 wt %, agrees with the value from titration (87 wt %). The difference could be a result of the experimental error and/or deviation of the actual polymer structure from the ideal structure.

In Figure 2a, we indicate the $w_0$ value for each polymer formulation with a short vertical line. At DL < $w_0$, there are enough COOH groups to neutralize all the drug molecules; at DL > $w_0$, the opposite is true. The data do not indicate any sharp transition as DL traverses $w_0$ and even when the COOH groups in excess, it is generally impossible to fully protonate the drug.

**Table 1**. COOH densities of polymers determined by non-aqueous titration in the same solvent used for slurry synthesis.

| Polymer | V KOH (µL) | $[COOH]_p$ (mmol/g) | Succinyl Content (%) | $w_0$ (wt %) |
|---|---|---|---|---|
| PAA | 3183 (24) | 12.7 (0.09) | - | 87 |
| Eudragit L100-55 | 1425 (20) | 5.70 (0.08) | - | 75 |
| Eudragit L100 | 1328 (8) | 5.31 (0.03) | - | 74 |
| HPMCP | 890 (29) | 3.56 (0.04) | - | 65 |
| CAP | 840 (11) | 3.36 (0.04) | - | 64 |
| HPMCAS-LF | 622 (9) | 2.49 (0.03) | 14 – 18 | 57 |
| HPMCAS-MF | 433 (13) | 1.73 (0.05) | 10 – 14 | 48 |
| HPMCAS-HF | 277 (14) | 1.11 (0.06) | 4 – 8 | 37 |

In Figure 2b, we plot the same data in Figure 2a against $[COOH]_0$, the COOH concentration available for reaction calculated from the titration results using eq. 2. In this format, the scatter seen in Figure 2a mostly disappears and the data points cluster around a single trend. This indicates that the degree to which LMF is protonated is mainly controlled by the COOH density of the polymer and is less sensitive to its architecture. This conclusion is by no means obvious. For example, if we compare the structures of PAA, L100 and L100-55 (Scheme 1), we might speculate that the larger spacing between COOH groups in L100 and L100-55 allow these polymers to react more efficiently with the drug, leading to higher % protonation at the same $[COOH]_0$. But we observe no such effect in Figure 2b (black symbols): the three polymers reach approximately the same % protonation at a common $[COOH]_0$ (e.g., 5 mmol/g). Thus, despite their different architectures, each COOH in these polymers has approximately the same reactivity toward LMF.

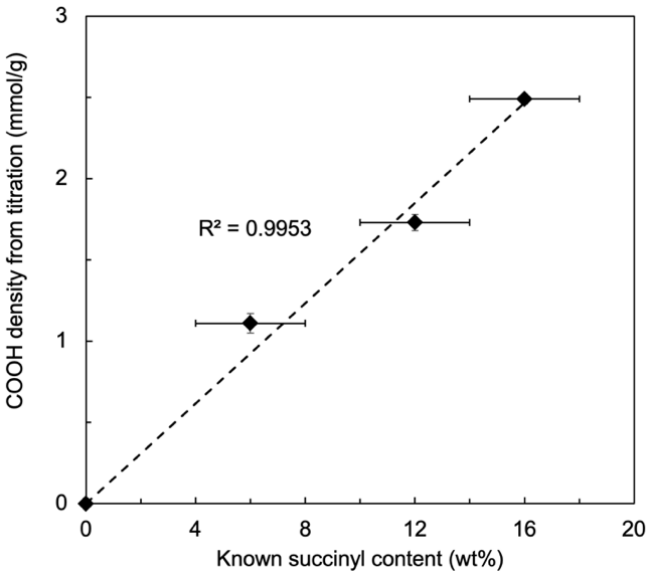


**Figure 3**. $[COOH]_P$ of each HPMCAS grade (LF, MF, or HF) plotted against its succinyl content (range indicated as horizontal bar). The two quantities are proportional to each other, as expected, indicating the titration method correctly determines the acidic group density.

The trend formed by PAA, L100, and L100-55 appears to smoothly join the data points for HPMCAS (3 grades). This further indicates that the polymer's architecture plays a relatively minor role in its reaction with LMF. In PAA, L100, and L100-55, the COOH group is directly attached to the polymer's carbon chain, whereas in HPMCAS, the COOH group is attached to a succinyl side chain of a complex cellulose backbone. Despite this difference, each COOH group has a similar reactivity toward LMF. Interestingly, relative to this trend, HPMCP and CAP appear to be more potent protonators when compared at the same $[COOH]_0$. In these polymers, COOH is attached to a phthalyl sidechain of the cellulose backbone. Overall, the main conclusion from Figure 2b is that the polymer's COOH density has a controlling effect on the salt formation with

LMF, while its architecture plays a smaller role. It would be of interest to model these systems by molecular simulations to learn how the molecules organize themselves to achieve this.

To complete the characterization of our systems, in Figures 4, we show the fraction of the COOH groups that are deprotonated in each formulation as a function of DL. This quantity is calculated from:

$$\% \text{ deprotonation} = [\text{LMF}]_0 (\% \text{ protonation}) / [\text{COOH}]_0 \qquad (4)$$

where $[\text{LMF}]_0$ is the initial concentration of the drug, % protonation is the protonated fraction of LMF after reaction, and $[\text{COOH}]_0$ is the initial concentration of COOH (eq. 2). For each system, increasing the DL increases the % deprotonation of the polymer. These results complement those in Figure 2a, which indicate a decrease of the % protonation of the drug with increasing DL. Note in Figure 4 that at the same DL, the acrylic/methacrylic polymers (PAA, L100, and L00-55, in black symbols) show lower % deprotonation than the cellulosic polymers (red and blue symbols). Within the cellulosic polymers, those with the COOH on a phthalyl group (CAP and HPMCP) are deprotonated to a greater extent at DL > 50% than those with the COOH on a succinyl group (HPMCAS in three grades). At DL = 75 wt %, HPMCP is almost fully deprotonated, while HPMCAS-MF is 50% deprotonated. This difference is consistent with the view that HPMCP and CAP are slightly stronger acids than HPMCAS, consistent with their greater protonating power seen in Figure 2b near $[\text{COOH}]_0$ = 2 mmol/g.

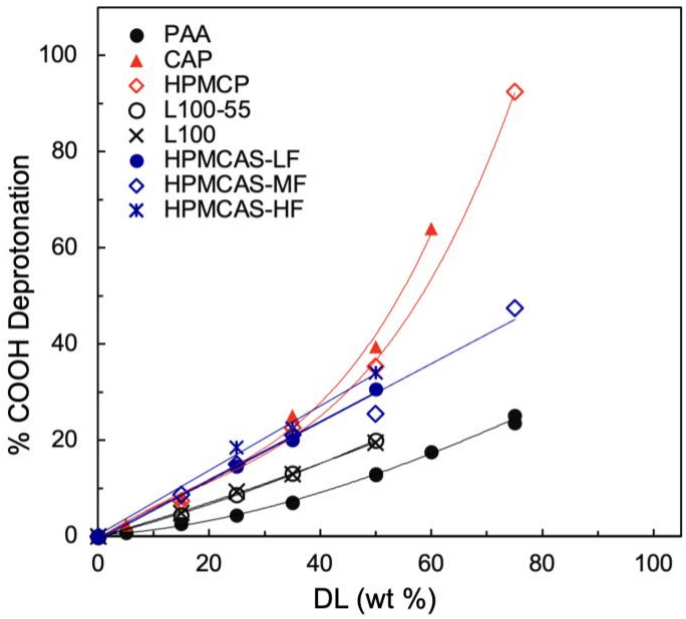


**Figure 4**. % deprotonation of the polymer when formulated with LMF as a function of DL.

**Comparison of ASD Manufacturing Methods.** Several methods have been used to prepare amorphous LMF-polymer formulations, including HME,[16] SD,[16] RE,[16,27,13] and slurry conversion

(SC).[11,17] Table 2 summarizes the attributes of these methods and Figure 5 compares the degrees of salt formation reached by them. Among these methods, HME does not require any solvent and its later removal, while the others do. For the solvent-based methods, SC uses less solvent (4:1 solvent/solid ratio) than SD and RE (50:1). As for the reaction temperature, HME employs a higher temperature (130 °C) than the solvent-based methods (room temperature, though reaction can also occur during spray drying at elevated temperature). In the drying stage, SD requires a higher temperature than RE and SC and between the latter two methods, drying is significantly faster for SC since less solvent must be removed.

**Table 2**. Comparison of the methods used to prepare amorphous LMF-polymer formulations.

| | Hot melt extrusion (HME)[16] | Spray drying (SD)[16] | Rotary evaporation (RE)[27,16] | Slurry conversion (SC)[11,17] |
|---|---|---|---|---|
| Solvent | None | DCM-methanol (1:1) | DCM-methanol (1:1 or 8:2), DCM-ethanol (1:1) | DCM-ethanol (1:1) |
| Solvent/solid ratio | NA | 50:1 | 50:1 | 4:1 |
| Reaction temperature | 130 °C | RT (higher T during drying) | RT (also at 45 °C during drying) | RT default, 75 °C also used |
| Drying temperature | NA | 75 °C inlet, 45 °C outlet | 45 °C under vacuum | RT under vacuum |

Note. RT: room temperature

Figure 5 compares the % protonation of LMF in polymer formulations prepared by the different methods. The PAA and L100-55 systems allow comparison of SC (solid circles) with HME (crosses) and we find that HME achieves less complete salt formation than SC, by a factor of 3 – 18. Similarly, we can use the L100-55, HPMCP, and HPMCAS-MF formulations to evaluate the relative performance of SC and SD (open circles). For the L100-55 and HPMCP systems, SD reaches similar degrees of salt formation as SC; for the HPMCAS-MF system, SD significantly underperforms SC, yielding no salt formation. Finally, every system in Figure 5 except for L100-55 allows a comparison of SC with RE (open triangles) and in every case, RE significantly

underperforms SC, by up to a factor of 2. Overall, these results indicate that SC has the best performance for completing the salt formation between LMF and an acidic polymer. Apart from this metric, SC has the advantage of lower solvent consumption than SD and RE and lower operating temperature than SD, making it a low-cost and green alternative to the current manufacturing platforms.

At present, the understanding is limited of why the different manufacturing methods reach such different degrees of salt formation between LMF and an acidic polymer. The underperformance of HME relative to the solution-based methods suggests the need for a solvent in completing the reaction. A solvent could be a mass-transfer aide that helps complete salt formation. Given that a liquid surfactant is commonly present in HME-prepared ASDs, it is of interest to learn whether the addition of a surfactant could promote salt formation. The outperformance of SC over other solvent-based methods is more puzzling since they all begin with a homogeneous solution and involve the drying of that solution. In SC, the initial solution is more concentrated than in SD and RE. A more concentrated solution could facilitate the formation of ion pairs, the principal species for ions in an organic solvent,[21] since ion pairs tend to dissociate in a dilute solution, reverting to neutral molecules. This hypothesis can be tested with NMR measurements. In the drying stage, it is possible that the system evolves before kinetic arrest (glass transition). It would thus be of interest to follow the evolution of the system during drying. Together these results may help explain why the different methods perform so differently in completing salt formation. With this understanding, it is conceivable that the different methods could be optimized to achieve comparable performance.

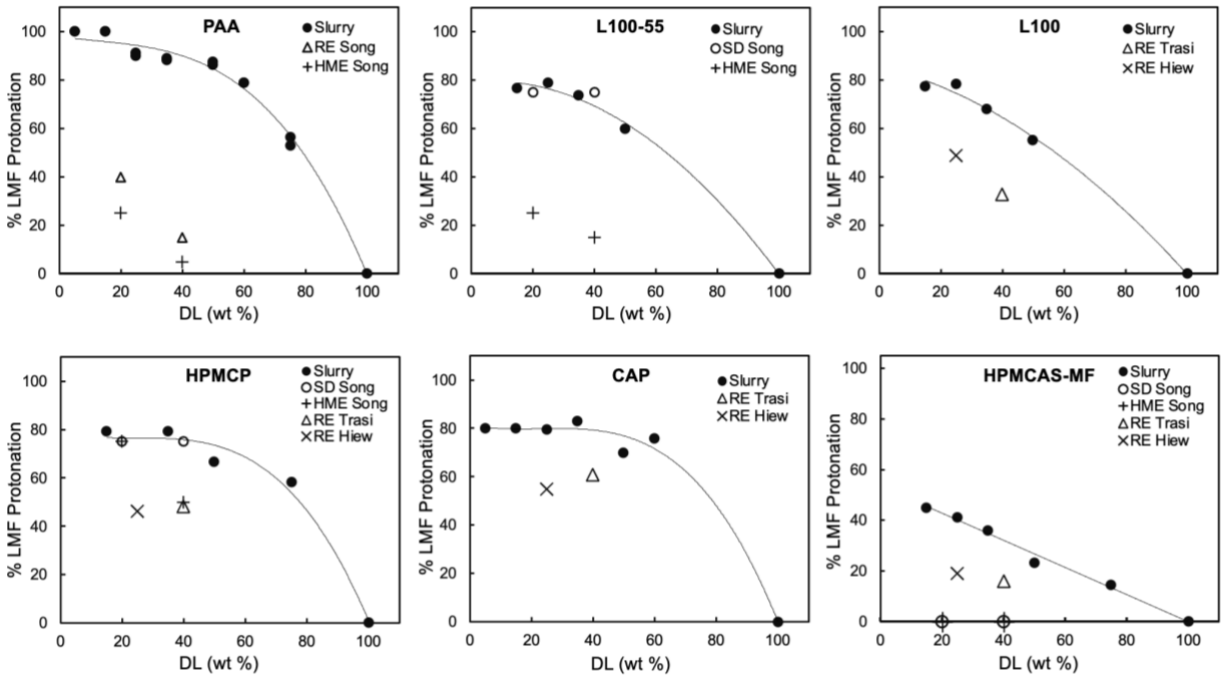


**Figure 5**. Comparison of % protonation of LMF in formulations with different polymers prepared using different methods. “Slurry” refers to the slurry conversion (SC) method used in this work. HME: hot melt extrusion. SD: spray drying. RE: rotary evaporation.

## 3.5. Conclusions

This study investigated the salt formation between the basic drug lumefantrine (LMF) and a series of acidic polymers based on acrylic/methacrylic and cellulosic backbones (Scheme 1). The polymers show very different abilities to protonate LMF when compared at the same drug loading (DL) (Figure 2a), but the difference largely disappears when the results are plotted against the COOH concentration available for reaction (Figure 2b). This indicates that for the polymers tested, the abilities to protonate LMF depend mainly on their acidic group densities and are less sensitive to their different architectures. For this analysis, the acidic group densities were determined by non-aqueous titration in the same medium used for slurry synthesis to accurately probe the accessible reaction sites. Had the aqueous titration results[13] been used in this analysis, data collapse would be less complete. Our finding that a polymer's COOH density outweighs its architecture in predicting salt formation with a basic drug is relevant for polymer selection in developing amorphous formulations. This conclusion is by no means obvious; it is even counterintuitive for PAA, L100, and L100-55 taken as a group, since the wider spacing of COOH groups in L100 and L100-55 might suggest higher reactivity with the drug, but this was not observed (Figure 2b). Future work is warranted to understand why the crowding effect is seemingly unimportant.

The second part of this work has compared the slurry synthesis used here with three other methods for manufacturing amorphous drug-polymer formulations. For LMF reacting with the 6 polymers, slurry conversion either achieves the most complete salt formation (4 of 6 polymers) or ties with spray drying for the first place (2 of 6). Compared to spray drying, slurry conversion has lower cost, lower solvent consumption, and lower drying temperature. This encourages further development of the method for broader applications as a platform to manufacture amorphous solid dispersions. A remarkable result from this comparison is that for a given amorphous formulation (with a specific polymer at a specific DL), the internal structure can vary widely, depending on the methods of preparation (Figure 5). The common method of hot-melt extrusion consistently yielded the lowest degree of salt formation. Spray drying showed comparable performance as slurry conversion for two polymers, but yielded no reaction for a third. Rotary evaporation, in principle a similar method to slurry conversion, consistently yielded less complete salt formation than slurry conversion. This is a vivid illustration that an "X-ray amorphous" formulation of fixed composition can have vastly different internal structures depending on the method of preparation. The

amorphousness of a multi-component formulation might suggest intimate mixing of its components, but a detailed analysis like the degree of protonation can reveal large structural differences. These differences could impact dissolution kinetics and stability for compositionally identical amorphous formulations. To obtain a consistent product with a reproducible molecular-level structure, a manufacturing process must be carefully chosen and controlled. This task is not unlike the control of polymorphism for crystalline materials and requires analytical tools that go beyond the amorphous halo of X-ray diffraction.

## 3.6 Acknowledgements

This work was supported by the Bill and Melinda Gates Foundation (OPP1160408) and we acknowledge the helpful discussions with Niya Bowers, David Monteith, and Paco Alvarez. Under the grant conditions of the Foundation, a Creative Commons Attribution 4.0 Generic License has already been assigned to the Author Accepted Manuscript version that might arise from this submission. The data that support the findings of this study are openly available in Mendeley Data at doi:10.17632/ s23j9y3mc8.1. The authors acknowledge the use of the characterization facility of the NSF-supported University of Wisconsin Materials Research Science and Engineering Center (DMR- 2309000).

## 3.7 References

[1] Mishra, D. K.; Dhote, V.; Bhargava, A.; Jain, D. K.; Mishra, P. K. Amorphous Solid Dispersion Technique for Improved Drug Delivery: Basics to Clinical Applications. *Drug Delivery and Translational Research* **2015**, *5* (6), 552–565.
[2] Baghel, S.; Cathcart, H.; O'Reilly, N. J. Polymeric Amorphous Solid Dispersions: A Review of Amorphization, Crystallization, Stabilization, Solid-State Characterization, and Aqueous Solubilization of Biopharmaceutical Classification System Class II Drugs. *Journal of Pharmaceutical Sciences* **2016**, *105* (9), 2527–2544.
[3] He, Y.; Ho, C. Amorphous Solid Dispersions: Utilization and Challenges in Drug Discovery and Development. *Journal of Pharmaceutical Sciences* **2015**, *104* (10), 3237–3258.
[4] Murdande, S. B.; Pikal, M. J.; Shanker, R. M.; Bogner, R. H. Solubility Advantage of Amorphous Pharmaceuticals: I. A Thermodynamic Analysis. *Journal of Pharmaceutical Sciences* **2010**, *99* (3), 1254–1264.
[5] Babu, N. J.; Nangia, A. Solubility Advantage of Amorphous Drugs and Pharmaceutical Cocrystals. *Crystal Growth & Design* **2011**, *11* (7), 2662–2679.
[6] Chawla, G.; Bansal, A. K. A Comparative Assessment of Solubility Advantage from Glassy and Crystalline Forms of a Water-Insoluble Drug. *European Journal of Pharmaceutical Sciences* **2007**, *32* (1), 45–57.
[7] Hancock, B. C.; Parks, M. What Is the True Solubility Advantage for Amorphous Pharmaceuticals? *Pharmaceutical Research* **2000**, *17* (4), 397–404.
[8] Newman, A.; Knipp, G.; Zografi, G. Assessing the Performance of Amorphous Solid Dispersions. *Journal of Pharmaceutical Sciences* **2012**, *101* (4), 1355–1377.
[9] Shah, N.; Iyer, R. M.; Mair, H.-J.; Choi, D.; Tian, H.; Diodone, R.; Fahnrich, K.; Pabst-Ravot, A.; Tang, K.; Scheubel, E.; Grippo, J. F.; Moreira, S. A.; Go, Z.; Mouskountakis, J.; Louie, T.; Ibrahim, P. N.; Sandhu, H.; Rubia, L.; Chokshi, H.; Singhal, D. Improved Human Bioavailability of Vemurafenib, a Practically Insoluble Drug, Using an Amorphous Polymer-Stabilized Solid Dispersion Prepared by a Solvent-Controlled Coprecipitation Process. *Journal of Pharmaceutical Sciences* **2013**, *102* (3), 967–981.
[10] Gui, Y.; McCann, E. C.; Yao, X.; Li, Y.; Jones, K. J.; Yu, L. Amorphous Drug–Polymer Salt with High Stability under Tropical Conditions and Fast Dissolution: The Case of Clofazimine and Poly(Acrylic Acid). *Molecular Pharmaceutics* **2021**, *18* (3), 1364–1372.
[11] Yao, X.; Kim, S.; Gui, Y.; Chen, Z.; Yu, J.; Jones, K. J.; Yu, L. Amorphous Drug–Polymer Salt with High Stability under Tropical Conditions and Fast Dissolution: The Challenging Case of Lumefantrine-PAA. *Journal of Pharmaceutical Sciences* **2021**, *110* (11), 3670–3677.
[12] Yao, X.; Neusaenger, A. L.; Yu, L. Amorphous Drug-Polymer Salts. *Pharmaceutics* **2021**, *13* (8), 1271.
[13] Hiew, T. N.; Zemlyanov, D. Y.; Taylor, L. S. Balancing Solid-State Stability and Dissolution Performance of Lumefantrine Amorphous Solid Dispersions: The Role of Polymer Choice and Drug–Polymer Interactions. *Molecular Pharmaceutics* **2021**, *19* (2), 392-413.
[14] Kelsall, K. N., Foroughi, L. M., Frank, D. S., Schenck, L., LaBuda, A., & Matzger, A. J. (2023). Structural Modifications of Polyethylenimine to Control Drug Loading and Release Characteristics of Amorphous Solid Dispersions. *Molecular Pharmaceutics*, 20 (*3)*, 1779–1787.
[15] Kelsall, K. N., Schubiner, R. O., Schenck, L., Frank, D. S., & Matzger, A. J. (2024). Enhancing the Acidity of Polymers for Improved Stabilization of Amorphous Solid Dispersions: Protonation of Weakly Basic Compounds. *ACS Applied Polymer Materials*, (6) *3*, 1592–1598.
[16] Song, Y.; Zemlyanov, D.; Chen, X.; Su, Z.; Nie, H.; Lubach, J. W.; Smith, D.; Byrn, S.; Pinal, R. Acid-Base Interactions in Amorphous Solid Dispersions of Lumefantrine Prepared by Spray-Drying and Hot-Melt Extrusion Using X-Ray Photoelectron Spectroscopy. *International Journal of Pharmaceutics* **2016**, *514* (2), 456–464.

[17] Amy Lan Neusaenger; Yao, X.; Yu, J.; Kim, S.; Hui, H.-W.; Huang, L.; Que, C.; Yu, L. Amorphous Drug–Polymer Salts: Maximizing Proton Transfer to Enhance Stability and Release. *Molecular Pharmaceutics* **2023**, *20* (2), 1347–1356.
[18] Jain, J.P.; Leong, F.J.; Chen, L.; Kalluri, S.; Koradia, V.; Stein, D.S.; Wolf, M.C.; Sunkara, G.; Kota, J. Bioavailability of lumefantrine is significantly enhanced with a novel formulation approach, an outcome from a randomized, open-label pharmacokinetic study in healthy volunteers. *Antimicrob. Agents Chemother.* **2017**. *61*(9).
[19] Evonik. (**2022**). *Eudragit*®, [Technical Literature] Evonik Industries AG.
[20] Yu, J.; Li, Y.; Yao, X.; Que, C.; Huang, L.; Hui, H.-W.; Gong, Y.; Qian, F.; Yu, L. Surface Enrichment of Surfactants in Amorphous Drugs: An X-Ray Photoelectron Spectroscopy Study. *Molecular Pharmaceutics* **2022**, *19* (2), 654–660.
[21] Marion Maclean Davis. *Acid-Base Behavior in Aprotic Organic Solvents*; U.S. Department of Commerce - National Bureau of Standards, 1968.
[22] Shen, X.; Wang, S.; Qian Lü; Guo, Y.; Li, Q. Translating Cancer Exosomes Detection into the Color Change of Phenol Red Based on Target-Responsive DNA Microcapsules. *Analytica Chimica Acta* **2022**, *1192*, 339357–339357.
[23] He, H., Hu, Y., Chen, S. *et al.* Preparation and Properties of a Hyperbranch-Structured Polyamine adsorbent for Carbon Dioxide Capture. *Sci Rep* **2017***, 7*, 3913.
[24] Amirdehi, M. A.; Pousti, M.; Asayesh, F.; Gharib, F.; Greener, J. Solvent Effects on Acid–Base Equilibria of Propranolol and Atenolol in Aqueous Solutions of Methanol: UV-Spectrophotometric Titration and Theory. *Journal of Solution Chemistry 2017*, *46*, 720–733.
[25] Sappidi, P., & Natarajan, U. (2016). Polyelectrolyte conformational transition in aqueous solvent mixture influenced by hydrophobic interactions and hydrogen bonding effects: PAA–water–ethanol. *Journal of Molecular Graphics and Modelling*, *64*, 60–74. https://doi.org/10.1016/j.jmgm.2015.12.004
[26] Ashland. (**2016**). *AquaSolve™ hydroxypropylmethylcellulose acetate succinate: Physical and chemical properties handbook,* [Technical Literature] Ashland Global.
[27] Trasi, N. S.; Bhujbal, S. V.; Zemlyanov, D. Y.; Zhou, Q. T.; Taylor, L. S. Physical stability and release properties of lumefantrine amorphous solid dispersion granules prepared by a simple solvent evaporation approach. *International Journal of Pharmaceutics: X* **2020**, *2*, 100052.

# Chapter 4. Slurry conversion: A general method for formulating amorphous solid dispersions and fully integrating drug and polymer components

Amy Lan Neusaenger, Caroline Fatina, Yichun Shen,
Junguang Yu, and Lian Yu

As submitted to
*Molecular Pharmaceutics* **2025**

## 4.1. Abstract

A solvent-sparing method, called “slurry conversion”, has been tested as a general approach to preparing amorphous solid dispersions (ASDs). In this method, a solid mixture of a drug and a polymer is stirred in the presence of a small quantity of a solvent, which is subsequently removed. In previous work, the method enabled more complete salt formation between lumefantrine (LMF), a basic antimalarial, with acidic polymers, than the common methods of hot melt extrusion and spray drying, leading to improved physical stability and release. Here we apply this method to 18 poorly soluble drugs formulated as binary and ternary ASDs. For a rigorous test, these drugs were formulated with a single polymer, poly(acrylic acid) (PAA), under the same condition: room temperature stirring in 1:1 ethanol-dichloromethane at 4:1 solvent/solid ratio. ASDs were prepared for 16 of the 18 drugs at 25% drug loading and 11 at 50% drug loading. The drugs that were not fully amorphized did not dissolve in the default solvent or crystallized during drying. For most drugs, an abrupt “clearing” of the slurry was observed during stirring, indicating complete dissolution and amorphization before drying. While clearing did not occur for some drugs (e.g., clofazimine), the product was still fully amorphous, through solvent-mediated conversion. For a basic drug, the degree of protonation by PAA increases smoothly with PAA concentration and is ordered by its basic strength, supporting the conclusion that the method allows the system to reach thermodynamic equilibrium. In addition to binary ASDs, ternary ASDs containing two drugs (LMF and artemether or LMF and artesunate) were successfully prepared, laying the foundation for applications in combination therapies. In these ternary formulations, the protonation of LMF follows the trend established for binary systems. We also find that slurry conversion can be scaled up at least 60-fold without any difficulties or adverse effect on the structure and properties of the product. Overall, our results demonstrate that slurry conversion is a general, low-cost, and green alternative to conventional methods for manufacturing ASDs where the components are fully integrated.

## 4.2. Introduction

Solid oral dosage forms are traditionally formulated with the crystals of the active ingredients. Recent decades have seen significant growth in the development of amorphous solid dispersions (ASDs)[1,2,3,4] to increase the bioavailability of poorly soluble drugs.[5,6] Among the factors that account for this increased bioavailability are the higher solubility of an amorphous drug than its crystalline counterpart[7,8] and the release of drug-containing nanoparticles that could facilitate absorption through a "reservoir" or "shuttle" effect.[9,10,11]

An ASD is a multicomponent formulation, typically containing a drug, a polymer, and a surfactant, and can be manufactured in many ways.[12] Hot melt extrusion (HME),[13,14] spray drying (SD),[15] and freeze drying[16] are commercially important methods. In addition, ASDs can be prepared by mechanical activation,[17] rotary evaporation (RE),[18] antisolvent precipitation (AP),[19,20,21] and spray-freeze drying.[22] These methods differ in solvent usage, processing temperature, equipment cost, and energy consumption. Since 2021, this laboratory has experimented with a simple method, called slurry conversion (SC), for ASD preparations,[23,24,25,26] where solid ingredients are stirred in the presence of a small volume of a solvent, which is subsequently removed.

Given the many ways to prepare an ASD, many have investigated whether they produce the same product in terms of internal structure and performance characteristics.[27,28,29,30] Despite work in this area, the current understanding remains limited. We illustrate this situation using lumefantrine (LMF), a poorly soluble antimalarial, which has

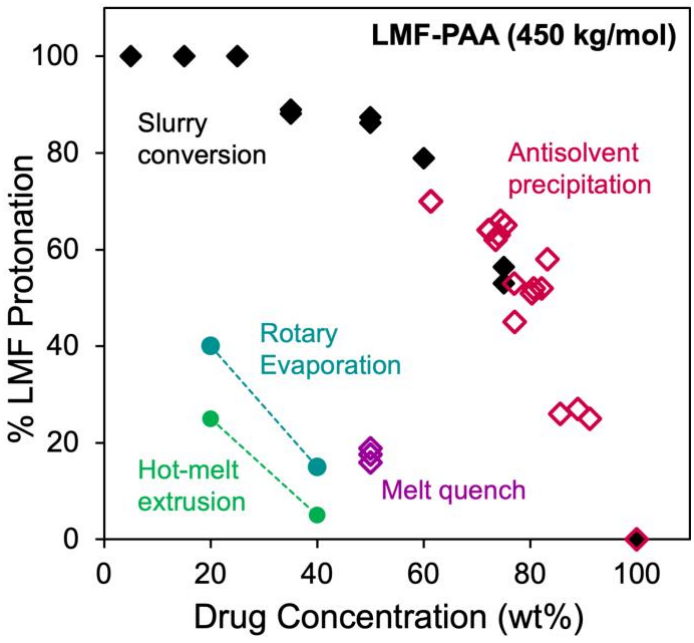


**Figure 1.** Degree of LMF protonation by PAA in formulations prepared by different methods. At a fixed drug concentration, the different methods reached very different degrees of protonation. Adapted from Figures 5 and 6 in Ref 25.

been formulated as ASDs by many groups in recent years.[31,50,51,32,25,26,33,34] LMF is a basic drug, and Figure 1 shows its degree of protonation when formulated with an acidic polymer, poly(acrylic acid) (PAA), by various methods.[25] The degree of protonation is a direct probe of how well the drug has been mixed and reacted with the polymer. We observe a large difference between the ASDs prepared by the different methods. At 40% drug loading, the degree of protonation ranges from near zero for an ASD prepared by HME[31] to 85% for that prepared by SC.[25] For this drug, the degree of protonation directly impacts its physical stability and dissolution performance. The large difference shown in Figure 1 is also observed for LMF formulated with other acidic polymers,[26] highlighting the common occurrence of a potentially widespread problem.

In this work, we evaluate the generality of the slurry conversion method for formulating ASDs, both binary and ternary, and its ability to control drug-polymer salt formation. In previous work,[26] LMF was formulated with different polymers, and here we investigate various drugs (Scheme 1) formulated with the same polymer PAA. All drugs selected are poorly water soluble (BCS Class II or IV)[35,36] and have varying basic strengths for testing the completion of their salt formation with the acidic polymer PAA. For a strong test of the method, a single synthesis condition[25,26] was employed for the different drugs at fixed temperature, solvent, and solvent/solid ratio. We find that slurry conversion can prepare ASDs for most drugs tested (16/18 at 25% drug loading and 11/18 at 50% drug loading). For a given drug, the degree of salt formation varies smoothly with the PAA concentration and correlates with its basic strength, supporting the conclusion that slurry conversion enables full interaction between the drug and the polymer. In addition to binary formulations, ternary ASDs containing multiple drugs were investigated to test the ability to prepare combination therapies, an increasingly utilized approach for treating infections.[37] We find that LMF can be formulated as ternary ASDs with artemether and artesunate – standard combinations treating malaria, where LMF is protonated to a degree expected from the trend for binary ASDs. These findings demonstrate that slurry conversion is a versatile, low-cost, and green alternative to the conventional methods for ASD manufacturing.

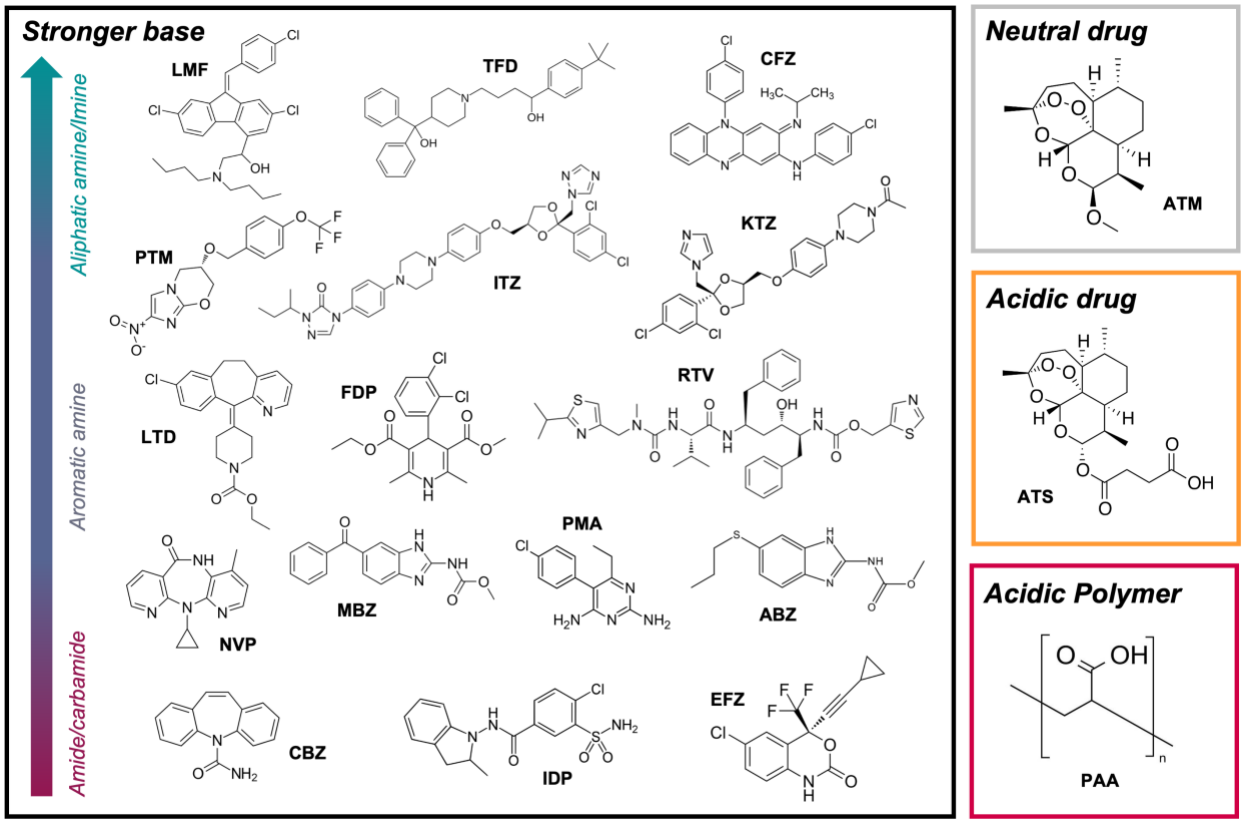


**Scheme 1.** Structures of poly(acrylic acid) (PAA) and the drugs used in this work: lumefantrine (LMF), terfenadine (TFD), clofazimine (CFZ), pretomanid (PTM), itraconazole (ITZ), ketoconazole (KTZ), loratadine (LTD), felodipine (FDP), ritonavir (RTV), nevirapine (NVP), mebendazole (MBZ), pyrimethamine (PMA), albendazole (ABZ), carbamazepine (CBZ), indapamide (IDP), and efavirenz (EFZ), the neutral drug artemether (ATM) and the acidic drug artesunate (ATS).

## 4.3. Materials & Methods

### Materials

Poly(acrylic acid) (MW = 450,000 g/mol), albendazole, clofazimine, erythromycin, indapamide, loratadine, mebendazole, and terfenadine were purchased from Sigma-Aldrich (St. Louis, MO), nevirapine from Ambeed, Inc. (Arlington Heights, IL), carbamazepine from Alfa Aesar (Haverhill, MA), felodipine from J&K Scientific (San Jose, CA), and pyrimethamine from MP Biomedicals

(Solon, OH). Itraconazole, ketoconazole, and lumefantrine were purchased from VWR International (Radnor, PA). Pretomanid was gifted by TB Alliance (Pretoria, South Africa) and artemether and artesunate by Nanjing Bilatchem Industrial Co., Ltd. (Nanjing, China). Dichloromethane (DCM) (ChromAR grade) was purchased from Thermo Fisher Scientific (Fair Lawn, NJ), and ethanol from Decon Laboratories (King of Prussia, PA). All materials were used as received.

**Slurry Synthesis**

The condition for slurry synthesis of ASDs has been described previously.[26] In brief, the drug and polymer powders were mixed at 25 or 50 wt% drug loading and dichloromethane (DCM) and ethanol (EtOH) at 1:1 volume ratio were added in sequence to reach a 1:4 (w/w) solid/solvent ratio in the slurry. Each mixture was stirred with a magnetic stir bar at room temperature for up to 30 minutes and was dried under vacuum at room temperature for one day. During drying, the rapid loss of solvent caused the viscous solution to boil and rise, forming a brittle, glassy foam that was ground in an agate mortar with a pestle to a powder.

To investigate the ability to scale up slurry synthesis, the batch size was enlarged from the standard size of 0.4 g of total solids (drug and polymer) up to 25 g. The scale-up process employed the same solvent, solid/solvent ratio, and drying condition as described above. A 20 mL glass vial was used to house the reaction mixture at the 0.4 g scale; a 500 mL glass bottle was used at the 25 g scale. To facilitate mixing at a larger scale, a Polytron PT 1200 E Handled Homogenizer was used in place of a magnetic stirrer.

**Powder X-Ray Diffraction (PXRD)**

PXRD was performed with a Bruker D8 Advance X-ray diffractometer with a Cu Kα source operating at a tube load of 40 kV and 40 mA. A powder sample of approximately 10 mg was spread and flattened on a Si (510) zero-background holder and scanned between 3° and 40° (2θ) at a step size of 0.02° and a scan rate of 1 s/step. For a partially crystalline sample, % crystallinity was calculated by dividing the area of the crystalline peaks by the total area of the crystalline peaks and the amorphous halo, treating the amorphous halo as a broad peak. Peak integration was performed using the program EVA from Bruker-AXS. This procedure provides an estimate of the crystalline fraction in a sample. A more accurate determination could be made using a calibration

curve constructed from the PXRD patterns of known crystalline fractions, but this was not pursued in this work.

**X-ray Photoelectron Spectroscopy (XPS)**

The details of XPS measurement and data analysis have been described previously.[38] For each pure drug reference and ASD prepared, approximately 5 mg of powder was pressed onto a carbon tape fixed to the XPS sample holder. The high-resolution spectrum of the N atom was used to measure the protonated fraction of an amine drug. For drugs containing a single nitrogen, a simple two-Gaussian fitting was performed using the program Origin following smart baseline subtraction. For drugs containing multiple nitrogen atoms, the protonated fraction was obtained using a curve subtraction method (see Results & Discussion). For each sample, spectra were recorded in duplicate (two separate regions) and averaged.

## 4.4. Results and Discussion

We first describe the results on binary ASDs to highlight the success rate of amorphization and trends in salt formation and then the findings on ternary ASDs containing multiple drugs.

***Slurry Synthesis Amorphization Success Rate and Clearing Transition***. In this work, different drugs (Scheme 1) were formulated with PAA at 25% and 50% drug loading (DL) under the same condition (room temperature stirring in 1:1 DCM-EtOH at 4:1 solvent/solid ratio). Table 1 summarizes the systems investigated and the success rate for slurry conversion to prepare amorphous solid dispersions. In this table, the crystallinity of the dried formulations is shown where zero signifies an amorphous product and a non-zero value indicates the crystalline fraction of the drug determined by PXRD (Figure 2). For comparison, Figure 2 also shows the PXRD patterns of the crystalline raw materials and the reference patterns generated from single-crystal structures to demonstrate their phase purity.[39-56]

**Table 1.** Amorphization success rates of binary drug-PAA ASDs by slurry conversion. Crystallinity of each dried formulation is given with zero signifying an amorphous product. DL: drug loading.

| *Drug* | *MW (g/mol)* | *Crystallinity of dried formulation* | |
|---|---|---|---|
| | | *25% DL* | *50% DL* |
| Clofazimine (CFZ) | 473.4 | 0 | 0 |
| Lumefantrine (LMF) | 528.9 | 0 | 0 |
| Terfenadine (TFD) | 471.7 | 0 | 0 |
| Carbamazepine (CBZ) | 236.3 | 0 | 0 |
| Efavirenz (EFZ) | 315.7 | 0 | 0 |
| Indapamide (IDP) | 365.8 | 0 | 0 |
| Albendazole (ABZ) | 265.3 | 12% | 15% |
| Felodipine (FDP) | 383.1 | 0 | 0 |
| Itraconazole (ITZ) | 705.6 | 0 | 0 |
| Ketoconazole (KTZ) | 531.4 | 0 | 6% |
| Loratadine (LTD) | 382.9 | 0 | 0 |
| Mebendazole (MBZ) | 295.3 | 16% | 25% |
| Nevirapine (NVP) | 266.3 | 0 | 26% |
| Pyrimethamine (PMA) | 248.7 | 0 | 10% |
| Pretomanid (PTM) | 359.3 | 0 | 31% |
| Ritonavir (RTV) | 720.9 | 0 | 0 |
| Artemether (ATM) | 298.4 | 0 | 93% |
| Artesunate (ATS) | 384.4 | 0 | 0 |

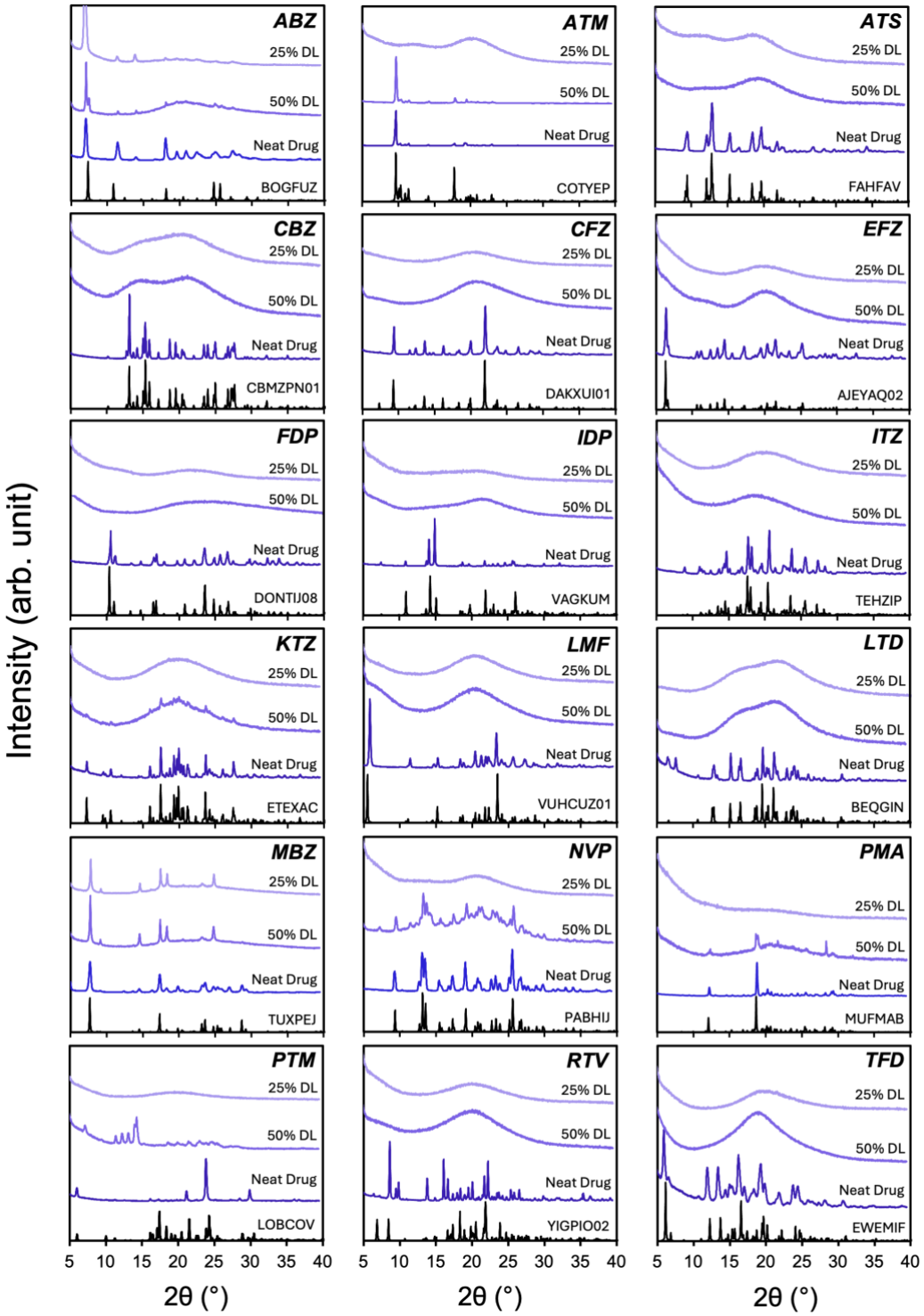


**Figure 2.** PXRD patterns of binary drug-PAA formulations prepared using the slurry method at 25 and 50% drug loading (DL), along with the patterns for the pure crystalline drugs as starting materials and their reference patterns generated from the single-crystal structures deposited in CCDC under the refcode supplied.[38-55] Most formulations were fully amorphous and a few partially crystalline.

Table 1 and Figure 2 show that for most drugs investigated, the slurry method successfully rendered the initially crystalline drug amorphous (zero crystallinity). Of the 18 drugs, 16 were amorphized at 25% DL and 11 at 50% DL. The decrease of the amorphization rate with DL is expected since less polymer is available to interact with the drug and prevent its crystallization. The drugs tested cover a wide range of structures and therapeutic classes, indicating a wide applicability of the slurry conversion method for formulating ASDs.

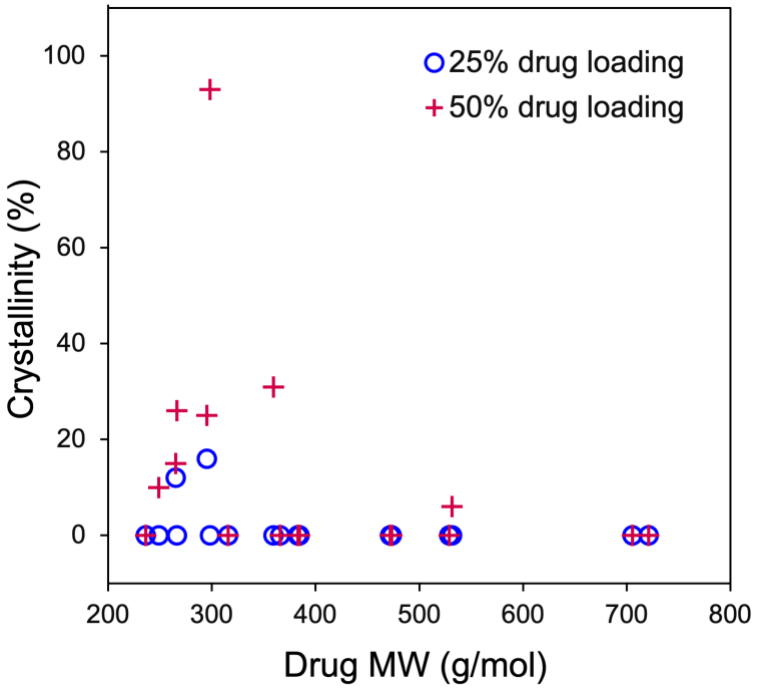


**Figure 3.** Crystallinity of dried formulations at 25% and 50% DL plotted against the drug's molecular weight. Zero crystallinity indicates an amorphous formulation. Low molecular-weight drugs tend to remain partially crystalline in the dried product.

Our survey of the 18 drugs indicate that the drugs of higher molecular weights (MW) are more likely to be amorphized. We can see this result by examining Table 1; Figure 3 shows the result more clearly by plotting the crystallinity of each dried formulation against the MW of the drug. The partially crystalline formulations are mainly associated with the drugs of lower MW. At MW > 350 g/mol, amorphization was successful in all but one case (ketoconazole at 50% DL, with 6% crystallinity). This result is not surprising because smaller molecules tend to crystallize faster than larger ones. In addition, at a fixed drug loading, a lower-MW drug has higher mole fraction and higher chemical potential (assuming ideal mixing), leading to higher a driving force of crystallization. Crystallization could occur in the drying step even if the drug was fully dissolved in the solvent with the polymer (see below).

A notable feature of the slurry synthesis is that for most drugs investigated, the initially turbid slurry abruptly "cleared" after a few minutes of stirring, forming a transparent, viscous solution. This transition was a useful visual indicator of complete dissolution and amorphization of the initially crystalline drug, before the drying step to lock in the amorphous structure. Figure 4a illustrates this clearing transition using LMF-PAA as an example. The slurry remained turbid for several minutes and suddenly cleared with an increase of viscosity, sometimes halting the rotation of the stir bar. This transition provides an efficient screening tool for identifying drug-polymer combinations suitable for slurry conversion, but as we show below with CFZ, complete clearing is not a necessary condition for amorphization.

Of the drugs tested, three did not show the clearing transition: CFZ, ABZ, and MBZ. As Figure 4b shows, the CFZ slurry remained opaque during stirring and contained residual solids, but a pronounced color change occurred from red to black, indicating the reaction between CFZ and PAA (salt formation).[23] Despite the lack of clearing, subsequent drying of the CFZ slurry yielded a fully amorphous solid (Figure 2). This example illustrates that even without full clearing (dissolution), the drug and the polymer could still interact, transforming the initially crystalline drug to an amorphous solid dispersion, as in a solution-mediated polymorphic transformation. The red-to-black color change of the CFZ slurry is a result of the protonation of CFZ's imine group and its effect on the π-electron system.[23]

Similar to CFZ, the slurries of ABZ and MBZ did not clear, but unlike CFZ, their dried slurries were partially crystalline (Table 1). This was the result of the low solubility of these drugs in the default solvent and their relatively low basicity to react with PAA. It was possible to fully dissolve ABZ and MBZ in an alternative solvent (DMSO) at an elevated temperature of 75°C, but the high boiling point of DMSO made the subsequent drying difficult. It is of interest to further optimize the method to prepare ASDs of these challenging drugs.

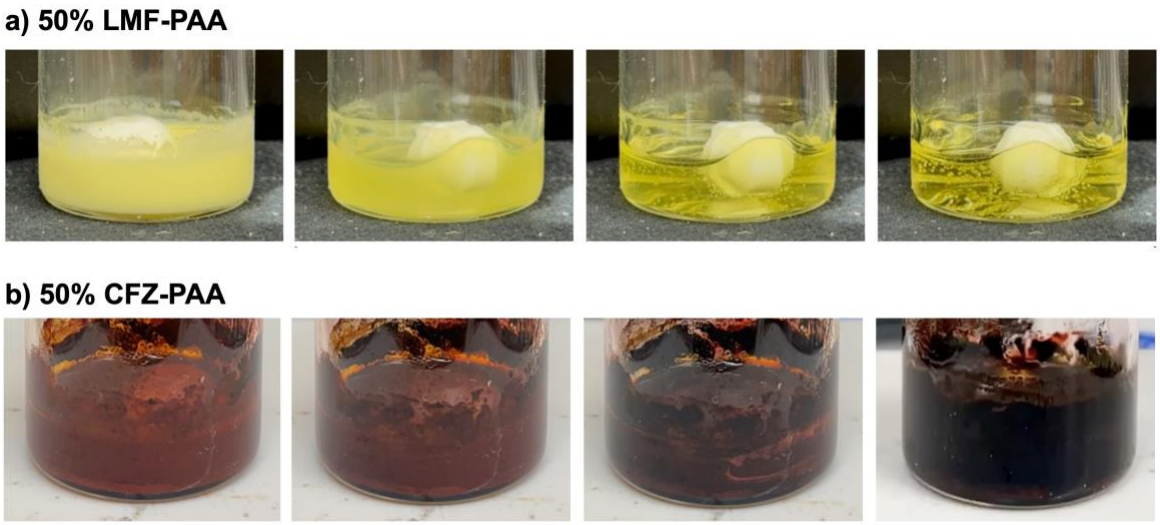


**Figure 4.** Clearing transition during slurry conversion. (a) Typical progression illustrated with LMF-PAA, where a turbid slurry turns into a clear solution and dries to an amorphous solid. (b) Atypical behavior illustrated with CFZ-PAA, where the slurry did not fully clear. Despite this, the CFZ-PAA slurry dried to an amorphous product.

***Salt Formation***

Previous work has shown that for an ASD of lumefantrine and an acidic polymer, the degree of salt formation depends strongly on the method of manufacturing, and in turn, influences its physical stability and release kinetics.[50,25,26] Following the previous work, we use the degree of salt formation here as a probe of the internal structure of an ASD and a metric for comparing different formulation methods. Figure 5 shows the XPS N spectra collected for this purpose. For the drugs of this study, the potential salt formation involves the protonation of a nitrogenous base by PAA, thus altering its XPS N spectrum. In Figure 5, the top two panels correspond to the two aliphatic amines (TFD and LMF), the next three panels to the aromatic amines (LTD, NVP, and FDP), and the bottom panel to an amide (CBZ). In this order, the drug's basic strength decreases, and so should the degree of protonation by PAA. For the weakest bases, little or no protonation is expected, but there could be spectral change due to the formation of stronger hydrogen bonds between the drug and PAA than between the drug molecules. These expectations are

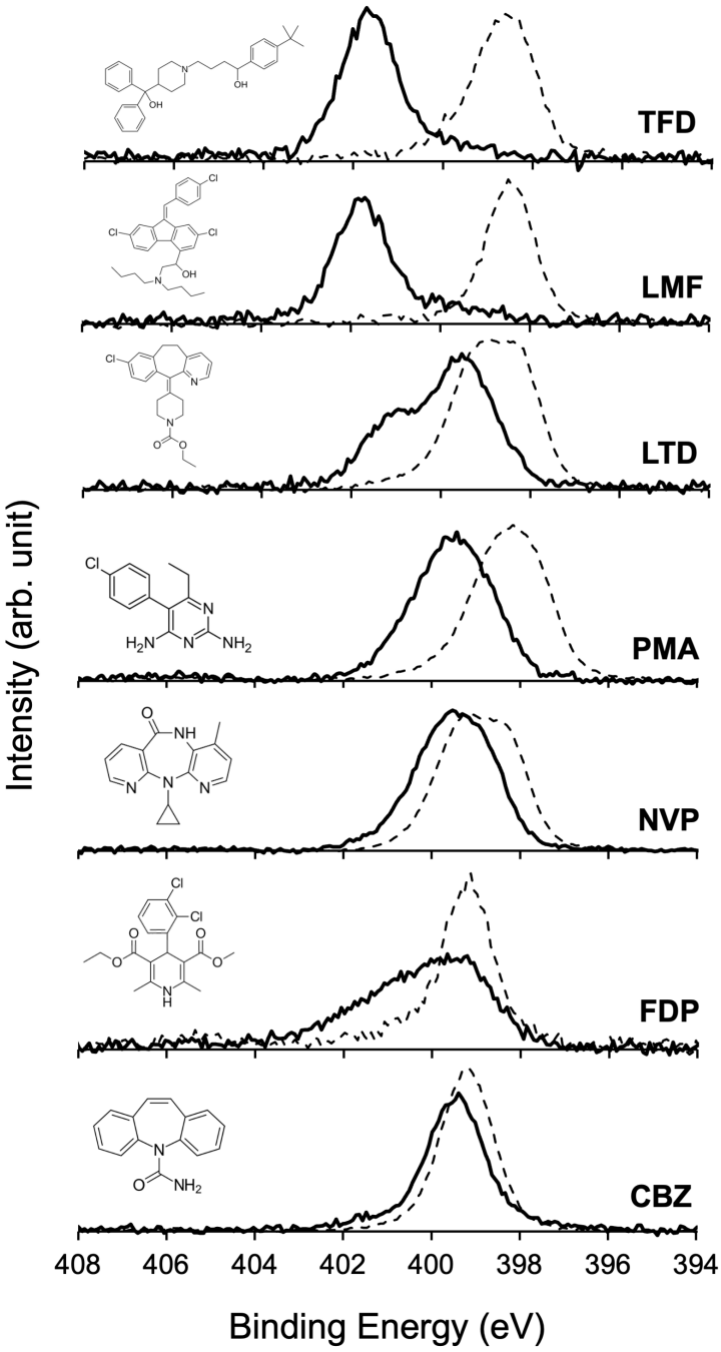


**Figure 5.** XPS N spectra of drug-PAA ASDs prepared by slurry synthesis (solid curves) and the corresponding pure drugs (dashed curves). 25 wt% drug loading for all ASDs.

broadly confirmed by the observed spectra. For LMF and TFD, the N spectrum shifts to higher binding energy (BE), by about 2 eV, indicating the protonation of the aliphatic amine by PAA.[25] For the other drugs, the peak shifts are smaller. For CBZ, the shift is barely visible, consistent with its lack of basicity and the peak shift could be a result of stronger hydrogen bonds between CBZ and PAA than between CBZ molecules, without proton exchange.

Figure 6 shows the degree of protonation for a given drug as a function of DL. The data on LMF[25] and CFZ[23] are from the previous work in this lab and the other data are from this work. If the drug has a single basic nitrogen atom (e.g., LMF, TFD, and FDP), the observed spectrum is fitted as a sum of two Gaussian functions that represent the unprotonated and the protonated N atoms and their relative areas yield the degree of protonation.[25] For LTD, NVP, and CBZ, there are multiple nitrogen atoms in the molecule and only one of them is expected to interact strongly with PAA (the amide N, for example, is expected to be inert). For these drugs, a subtraction method was used. As illustrated in Figure 7 for LTD, the spectrum of the pure drug is first scaled to have the same area $A_0$ as that of the ASD spectrum and then subtracted from the ASD spectrum. The positive area DA in the subtracted spectrum corresponds to the increase of protonated nitrogen atoms and the negative area to the loss of unprotonated nitrogen atoms. Dividing DA by the area that represents one nitrogen atom ($A_0/2$, where 2 is the number of nitrogen atoms per LTD molecule) gives the fraction of protonation. The subtraction procedure removes the signal from the non-reactive nitrogen atom (amide) and isolates the change due to salt formation. This method avoids the otherwise complex peak fitting process to account for both reactive and non-reactive nitrogen atoms.

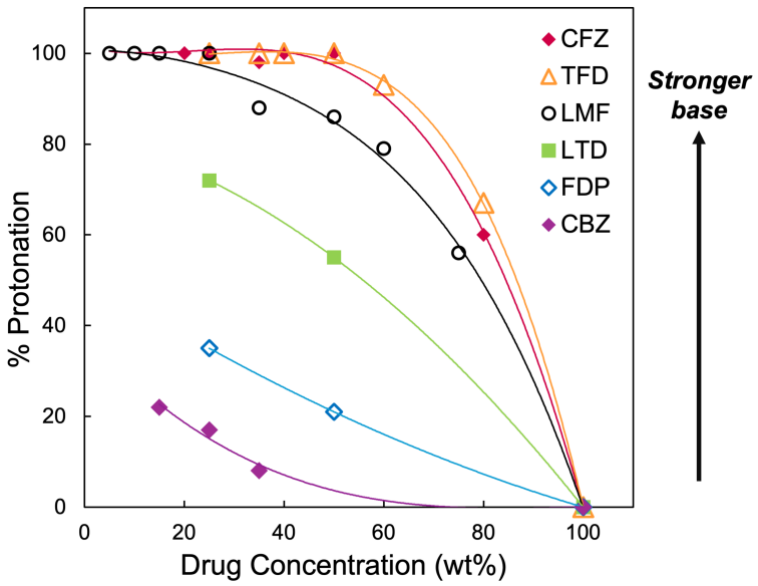


**Figure 6.** Degree of protonation as a function of drug loading for 6 drugs formulated with PAA. The degree of protonation increases with decreasing drug loading (increasing PAA concentration) and basic strength.

Figure 6 shows that for each drug, the extent of drug-polymer salt formation smoothly decreases with DL. This is sensible because as the drug concentration increases, more drug molecules compete for the same reaction site on PAA, leading to lower probability of success. When compared at the same DL, the different drugs show different degrees of interaction and the overall ranking agrees with that of their basic strengths: aliphatic amine (LMF and TFD) and imine (CFZ) > aromatic amine (LTD, NVP, and FDP) > amide (CBZ). LMF and TFD are similar ternary aliphatic amines, and it is sensible that they are similarly protonated by PAA at the same DL. For the weaker bases CBZ and FDP, the N atom peak shift observed during XPS analysis may have large contributions from hydrogen bonding between the drug and PAA, and the precise breakdown between proton transfer and hydrogen bonding requires further analysis.

The salt-formation results observed here (Figure 6) are not surprising from the standpoint of acid-base equilibrium, but noteworthy given the known difficulty to complete salt formation in a drug-polymer ASD (Figure 1). For LMF, the degree of salt formation with an acidic polymer varies significantly with the method of preparation.[50,51,25,26] This variability can be attributed to the difficulty of a sluggish macromolecule to fully react with a small molecule. Of the various methods compared in Figure 1, slurry conversion outperforms the others in completing the salt formation (Figure 1),[26] and the result of this study supports this conclusion. If the method had difficulty in completing the drug-polymer reaction, the data in Figure 6 would not form the smooth

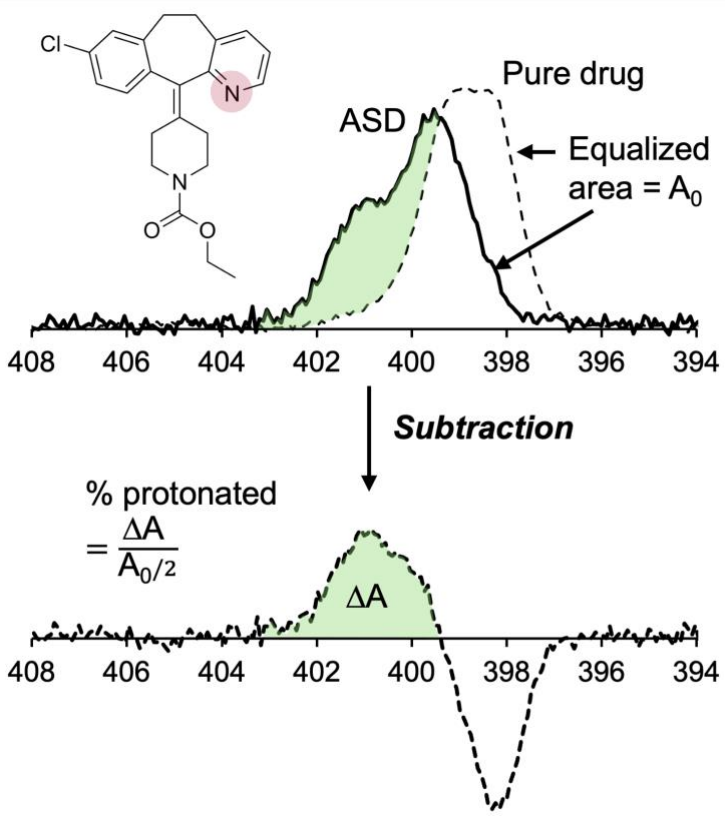


**Figure 7.** Subtraction method for determining the degree of protonation when non-reactive N atoms are present, illustrated for LTD.

trends that are expected based on acid-base equilibrium.

***Ternary Formulations***

Of the 48 ASD products FDA-approved between 2012 and 2023, 18 were fixed-dose combinations (FDCs) to facilitate patient compliance and synergy between drugs.[56] Coartem® (lumefantrine-artemether) exemplifies an FDC for malaria[57] and Kaletra® (lopinavir-ritonavir) an FDC for AIDS. We investigated whether slurry conversion can prepare multi-drug ASDs for applications in this area. We used lumefantrine-artemether (LMF-ATM) and lumefantrine-artesunate (LMF-ATS) as models, and to connect with the results on binary systems, used PAA as the formulation polymer. Table 2 summarizes the ternary formulations prepared and the success rate of amorphization. These formulations contained LMF and a partner drug (ATM or ATS) at different ratios (1:1 and 6:1) and were prepared at two DLss (25 and 50%). The 6:1 drug ratio was chosen because the clinically important Coartem contains LMF and ATM at this ratio. For these ternary systems, the DL refers to the total amount of the drugs in the formulation.

**Table 2**. Amorphization success rate of ternary ASDs prepared by slurry conversion. PAA is the dispersion polymer. The 6:1 ratio was chosen to match the composition in Coartem®.

| *Drug A* | *Drug B* | *A:B Ratio (w/w)* | *Crystallinity of dried formulation* | |
|---|---|---|---|---|
| | | | *25% DL (A+B)* | *50% DL (A+B)* |
| Lumefantrine (LMF) | Artemether (ATM) | 1:0 | 0 | 0 |
| | | 6:1 | 0 | 0 |
| | | 1:1 | 0 | 0 |
| | | 0:1 | 0 | 93% |
| Lumefantrine (LMF) | Artesunate (ATS) | 1:0 | 0 | 0 |
| | | 6:1 | 0 | 0 |
| | | 1:1 | 0 | 0 |
| | | 0:1 | 0 | 0 |

Table 2 indicates that all the ternary formulations prepared were amorphous (zero crystallinity) and the PXRD patterns that support this conclusion are collected in Figure 8. All the ternary

formulations showed broad and featureless PXRD patterns, without the sharp crystalline diffraction peaks present in the raw starting materials (bottom of Figure 8), indicating their amorphous nature. At the bottom of Figure 8 are also given the PXRD patterns generated from the single-crystal structures deposited in CCDC, which verify the phase purity of each crystalline starting material. Between ATM and ATS, ATM is the faster crystallizer since in the binary formulation with PAA (50% DL), ATM is partially crystalline (93%), but ATS is fully amorphous. However, in the ternary formulations of ATM, LMF, and PAA, ATM is fully amorphous (Table 2). This highlights that the presence of LMF helps inhibit the crystallization of ATM.

As in the case of most binary ASDs prepared, all ternary formulations tested exhibited an abrupt clearing transition where the turbid slurry became transparent (Figure 4a), indicating dissolution of the crystalline drug before the drying step. The inclusion of a secondary drug had no significant effect on the clearing behavior observed for the binary formulations. This suggests that the clearing transition is a generic feature of slurry conversion independent of the number of chemical components present and can be used as a general screening tool for systems suitable for this approach.

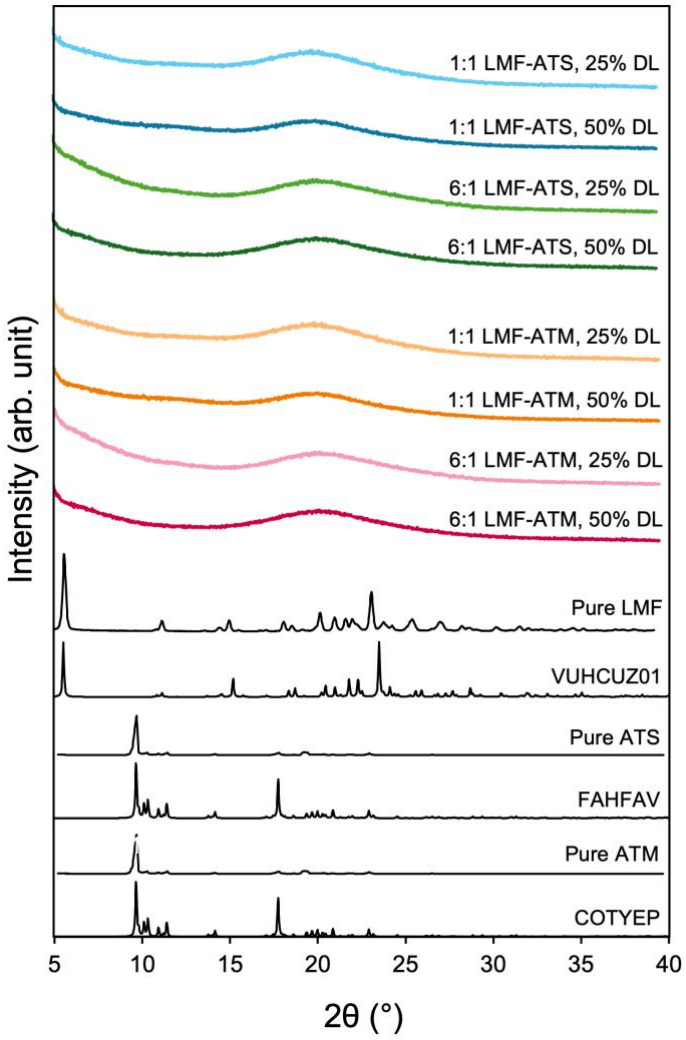


**Figure 8**. PXRD patterns of ternary ASDs prepared by slurry conversion, along with those of the crystalline drugs and the reference patterns generated from the single-crystal structures deposited in CCDC under the refcode supplied. All ternary ASDs prepared were amorphous.

XPS was used to determine the degree of salt formation between LMF and PAA in the ternary formulations, for comparison with the trend observed with the binary formulations (Figure 1). Figure 9 shows the XPS N spectra for the ternary ASDs prepared. Each of these spectra features a strong peak corresponding to protonated N atoms, and a small peak at lower BE corresponding to unprotonated N atoms is visible with only two formulations with high LMF concentrations (50% DL). This indicates complete or nearly complete protonation of LMF by PAA in these ternary ASDs.

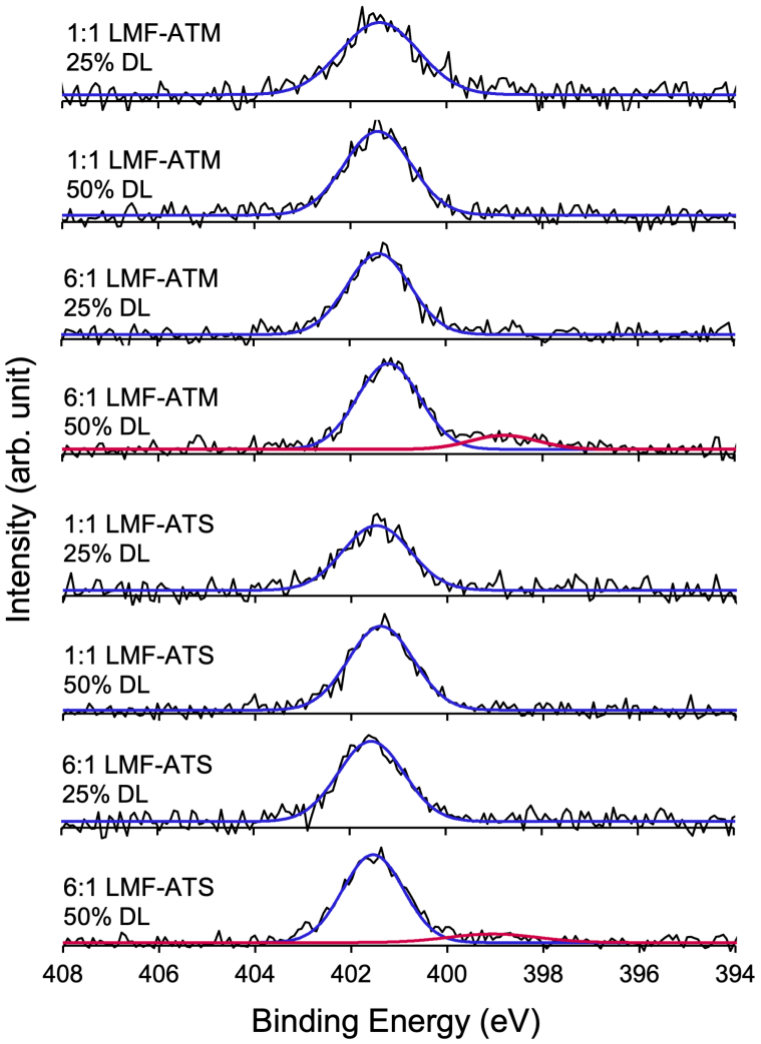


**Figure 9**. XPS N spectra of ternary ASDs. The peak at higher BE corresponds to the protonated N atom of LMF; the peak at lower BE to the unprotonated N atom.

Figure 10 shows the degree of protonation of LMF in the ternary ASDs calculated from the XPS spectra in Figure 9 using the same method described above for the binary ASDs. For comparison, the previous results on the binary ASDs composed of LMF and PAA are also included in Figure 10. In this plot, the degree of protonation of LMF is plotted against its concentration in the ASD, be it binary or ternary. We find that the data points for the ternary ASDs conform well with the trend for the binary ASDs. This result indicates that the second drug (ATM or ATS), at the concentration used, has a minor effect on the acid-base reaction between LMF and PAA. Of the two partner drugs with LMF, ATM is neutral and ATS is acidic (Scheme 1), and the fact that there is little difference in their effect on the LMF-PAA reaction indicates that they are mostly inert bystanders, perhaps because PAA has far higher acidic group density than ATS in the formulations prepared. This result may be useful for predicting the degree of salt formation in multicomponent ASDs if the polymer supplies most of the reaction sites.

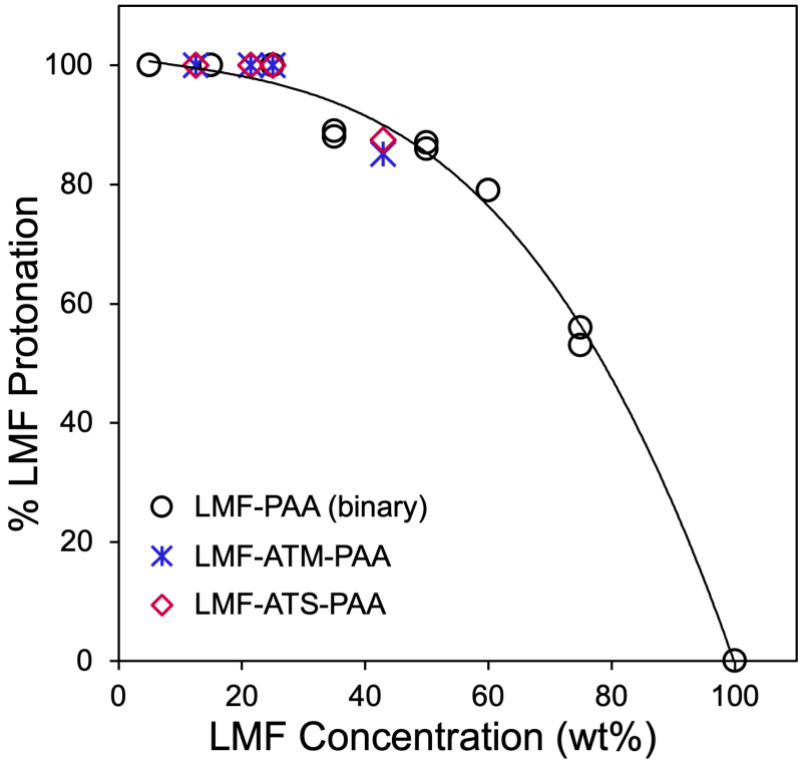


**Figure 10.** Degree of protonation of LMF by PAA in binary (circles) and ternary (other symbols) ASDs vs % LMF in the formulation. The data on binary and ternary ASDs fall on a common trend.

***Scale-Up of Slurry Conversion***

To assess the ability to scale up slurry synthesis, we used the LMF-PAA formulation as a model and increased the batch size from the standard 0.4 g up to 25 g. The process at larger scale employed the same solvent, solvent/solid ratio, and drying condition as the standard process. To facilitate mixing, a handheld homogenizer was used in place of a magnetic stirrer. We found that the process could be scaled up without any difficulties or any adverse effect on the structure and properties of the product. At the larger scale, the same clearing transition was observed where the initially turbid slurry abruptly became a transparent and viscous solution during mixing; see the picture in Figure 11a for a cleared slurry at the 25 g scale. Figure 11a compares the PXRD patterns of the dried products obtained by slurry synthesis at the 0.4 g and 25 g scales. Both materials are amorphous, showing no crystalline diffraction peaks. Figure 11b shows the XPS nitrogen spectra of the two formulations. These spectra indicate that LMF was highly protonated in the ASDs and the degrees of protonation were both at 87%. These results demonstrate that the slurry synthesis can be readily performed at increased scales. This work has successfully increased the batch size

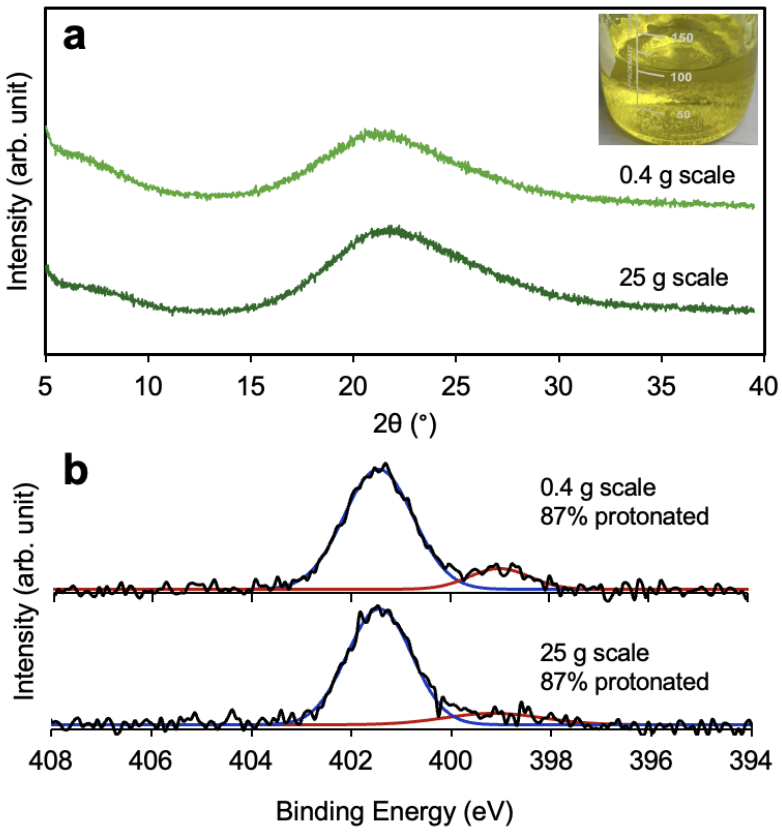


**Figure 11.** (a) PXRD patterns of LMF-PAA formulations at 50% drug loading prepared by slurry conversion at two batch sizes: 0.4 g (top) and 25 g (bottom). The inset shows the 25 g scale slurry after clearing, before drying to a solid product. (b) XPS N spectra of the two formulations in (a). The peak at higher BE corresponds to the protonated N atom of LMF; the peak at lower BE to the unprotonated N atom. Both formulations show 87% protonation.

60-fold, and further work is warranted to explore further scale up on industrial processing equipment.

## 4.5. Conclusions

This study investigated the generality of slurry conversion (SC) as a low-cost, solvent-sparing method to synthesize amorphous solid dispersions (ASDs) of poorly soluble drugs. To complement a previous study where the method was used to formulate the same drug (lumefantrine) with different polymers,[26] here it is applied to formulate multiple drugs with the same polymer (PAA). For a rigorous test, 18 drugs (Scheme 1) were formulated under a single condition: room temperature stirring and 1:1 ethanol-DCM as solvent at 1:4 solid/solvent ratio. We find a high success rate of amorphization (ASD formation): 16/18 at 25% drug loading and 11/18 at 50% drug loading. Of the 18 drugs, only ABZ and MBZ failed outright, for their insolubility in the default solvent and fast crystallization. Overall, the high success rate of this simple method is encouraging. Using LMF as a model, this work has shown that the slurry synthesis can be scaled up 60-fold without encountering any difficulties or any adverse effect on the structure and properties of the product. We highlight that the method has very low equipment cost, lower solvent usage than other solvent-based methods, and low energy consumption, and that there is room for further improvement in these metrics. This method permits rapid screening of candidate formulations in early development and has the potential to be a general platform for ASD manufacturing.

Using XPS, we have characterized the degree of salt formation between a drug and PAA in an ASD. The strongest bases (CFZ, an imine, and LMF and TFD, two aliphatic amines) were protonated to the greatest extent, followed by LTD and FDP (aromatic amines) and by CBZ (amide). For each drug, the degree of protonation smoothly decreases with increasing drug loading, a consequence of more molecules competing for the same reaction site at lower probability of success. Both results are expected for an acid-base reaction at equilibrium and support the conclusion that slurry conversion allows the ASD ingredients to fully mix and react. Had it failed to do so, we would expect erratic results of salt formation as illustrated in Figure 1, without smooth and meaningful trends. Although slurry conversion was first used to synthesize amorphous drug-

polymer salts,[62,63] its success with basic drugs of different strengths (even an acidic drug, ATS) indicates its applicability for synthesizing neutral ASDs.

The physical state of the drug and the polymer in the slurry deserves attention as it influences how the components interact during synthesis and the ASD structure after drying. The often observed clearing transition (Figure 4a) indicates full dissolution of the components in the slurry solvent and amorphization of the initially crystalline drug. For salt-forming systems, the drug and the polymer are likely organized as ion pairs in the organic slurry solvent and remain as such during drying to a solid. Unlike water, an organic solvent is less capable of stabilizing isolated ions by solvation. Elucidating the state of the drug and the polymer in the slurry could help understand and control the resulting ASD structures.

## 4.6. Acknowledgements

This work was supported by the Bill and Melinda Gates Foundation (OPP1160408) and we acknowledge the helpful discussions with Niya Bowers, David Monteith, and Paco Alvarez. Under the grant conditions of the Foundation, a Creative Commons Attribution 4.0 Generic License has already been assigned to the Author Accepted Manuscript version that might arise from this submission. The data that support the findings of this study are openly available in Mendeley Data at doi: 10.17632/gtft43t4fn.1. The authors acknowledge the use of the characterization facility of the NSF-supported University of Wisconsin Materials Research Science and Engineering Center (DMR- 2309000).

## 4.7. References

[1] Chiou, W. L.; Riegelman, S. Pharmaceutical Applications of Solid Dispersion Systems. *Journal of Pharmaceutical Sciences* **1971**, *60*(9), 1281–1302. https://doi.org/10.1002/jps.2600600902.
[2] Serajuddin, A. T. M. Solid Dispersion of Poorly Water-Soluble Drugs: Early Promises, Subsequent Problems, and Recent Breakthroughs. *Journal of Pharmaceutical Sciences* **1999**, *88* (10), 1058–1066. https://doi.org/10.1021/js9804031.
[3] Van den Mooter, G. The Use of Amorphous Solid Dispersions: A Formulation Strategy to Overcome Poor Solubility and Dissolution Rate. *Drug Discovery Today: Technologies* **2012**, *9* (2), e79–e85. https://doi.org/10.1016/j.ddtec.2011.10.002.
[4] He, Y.; Ho, C. Amorphous Solid Dispersions: Utilization and Challenges in Drug Discovery and Development. *Journal of Pharmaceutical Sciences* **2015**, *104* (10), 3237–3258. https://doi.org/10.1002/jps.24541.
[5] Law, D.; Schmitt, E. A.; Marsh, K. C.; Everitt, E. A.; Wang, W.; Fort, J. J.; Krill, S. L.; Qiu, Y. Ritonavir–PEG 8000Amorphous Solid Dispersions: In Vitro and in Vivo Evaluations. *Journal of Pharmaceutical Sciences* **2004**, *93* (3), 563–570. https://doi.org/10.1002/jps.10566.
[6] Jain, J. P.; Leong, F. J.; Chen, L.; Kalluri, S.; Koradia, V.; Stein, D. S.; Wolf, M.-C.; Sunkara, G.; Kota, J. Bioavailability of Lumefantrine Is Significantly Enhanced with a Novel Formulation Approach, an Outcome from a Randomized, Open-Label Pharmacokinetic Study in Healthy Volunteers. *Antimicrobial Agents and Chemotherapy* **2017**, *61* (9). https://doi.org/10.1128/aac.00868-17.
[7] Babu, N. J.; Nangia, A. Solubility Advantage of Amorphous Drugs and Pharmaceutical Cocrystals. *Crystal Growth & Design* **2011**, *11*(7), 2662–2679. https://doi.org/10.1021/cg200492w.
[8] Murdande, S. B.; Pikal, M. J.; Shanker, R. M.; Bogner, R. H. Solubility Advantage of Amorphous Pharmaceuticals: I. A Thermodynamic Analysis. *Journal of Pharmaceutical Sciences* **2010**, *99*(3), 1254–1264. https://doi.org/10.1002/jps.21903.
[9] Harmon, P.; Galipeau, K.; Xu, W.; Brown, C.; Wuelfing, W. P. Mechanism of Dissolution-Induced Nanoparticle Formation from a Copovidone-Based Amorphous Solid Dispersion. *Molecular Pharmaceutics* **2016**, *13* (5), 1467–1481. https://doi.org/10.1021/acs.molpharmaceut.5b00863.
[10] Kesisoglou, F.; Wang, M.; Galipeau, K.; Harmon, P.; Okoh, G.; Xu, W. Effect of Amorphous Nanoparticle Size on Bioavailability of Anacetrapib in Dogs. *Journal of Pharmaceutical Sciences* **2019**, *108* (9), 2917–2925. https://doi.org/10.1016/j.xphs.2019.04.006.
[11] Qian, K.; Stella, L.; Jones, D. S.; Andrews, G.; Du, H. Drug-Rich Phases Induced by Amorphous Solid Dispersion: Arbitrary or Intentional Goal in Oral Drug Delivery? *Pharmaceutics* **2021**, *13* (6), 889–889. https://doi.org/10.3390/pharmaceutics13060889.
[12] Bhujbal, S. V.; Mitra, B.; Jain, U.; Gong, Y.; Agrawal, A.; Karki, S.; Taylor, L. S.; Kumar, S.; Zhou, Q. Pharmaceutical Amorphous Solid Dispersion: A Review of Manufacturing Strategies. *Acta Pharmaceutica Sinica B* **2021**, *11* (8), 2505–2536. https://doi.org/10.1016/j.apsb.2021.05.014.
[13] Repka, M. A.; Majumdar, S.; Kumar Battu, S.; Srirangam, R.; Upadhye, S. B. Applications of Hot-Melt Extrusion for Drug Delivery. *Expert Opinion on Drug Delivery* **2008**, *5* (12), 1357–1376. https://doi.org/10.1517/17425240802583421.
[14] Repka, M. A.; Shah, S.; Lu, J.; Maddineni, S.; Morott, J.; Patwardhan, K.; Mohammed, N. N. Melt Extrusion: Process to Product. *Expert Opinion on Drug Delivery* **2011**, *9* (1), 105–125. https://doi.org/10.1517/17425247.2012.642365.
[15] Paudel, A.; Worku, Z. A.; Meeus, J.; Guns, S.; Van den Mooter, G. Manufacturing of Solid Dispersions of Poorly Water Soluble Drugs by Spray Drying: Formulation and Process Considerations. *International Journal of Pharmaceutics* **2013**, *453* (1), 253–284. https://doi.org/10.1016/j.ijpharm.2012.07.015.
[16] Tang, X. (Charlie); Pikal, M. J. Design of Freeze-Drying Processes for Pharmaceuticals: Practical Advice. *Pharmaceutical Research* **2004**, *21* (2), 191–200. https://doi.org/10.1023/b:pham.0000016234.73023.75.

[17] Crowley, K. J.; Zografi, G. Cryogenic Grinding of Indomethacin Polymorphs and Solvates: Assessment of Amorphous Phase Formation and Amorphous Phase Physical Stability. *Journal of Pharmaceutical Sciences* **2002**, *91* (2), 492–507. https://doi.org/10.1002/jps.10028.
[18] Hiew, T. N.; Zemlyanov, D. Y.; Taylor, L. S. Balancing Solid-State Stability and Dissolution Performance of Lumefantrine Amorphous Solid Dispersions: The Role of Polymer Choice and Drug–Polymer Interactions. *Molecular Pharmaceutics* **2021**. https://doi.org/10.1021/acs.molpharmaceut.1c00481.
[19] Bhujbal, S. V.; Pathak, V.; Zemlyanov, D. Y.; Taylor, L. S.; Zhou, Q. (Tony). Physical Stability and Dissolution of Lumefantrine Amorphous Solid Dispersions Produced by Spray Anti-Solvent Precipitation. *Journal of Pharmaceutical Sciences* **2020**. https://doi.org/10.1016/j.xphs.2020.12.033.
[20] Strotman, N. A.; Schenck, L. Coprecipitated Amorphous Dispersions as Drug Substance: Opportunities and Challenges. *Organic Process Research & Development* **2021**, *26* (1), 10–13. https://doi.org/10.1021/acs.oprd.1c00380.
[21] Armstrong, M.; Wang, L.; Ristroph, K.; Tian, C.; Yang, J.; Ma, L.; Santipharp Panmai; Zhang, D.; Karthik Nagapudi; Prud'homme, R. K. Formulation and Scale-up of Fast-Dissolving Lumefantrine Nanoparticles for Oral Malaria Therapy. *Journal of Pharmaceutical Sciences* **2023**, *112*(8), 2267–2275. https://doi.org/10.1016/j.xphs.2023.04.003.
[22] Adeli, E. The Use of Spray Freeze Drying for Dissolution and Oral Bioavailability Improvement of Azithromycin. *Powder Technology* **2017**, *319*, 323–331. https://doi.org/10.1016/j.powtec.2017.06.043.
[23] Gui, Y.; McCann, E. C.; Yao, X.; Li, Y.; Jones, K. J.; Yu, L. Amorphous Drug–Polymer Salt with High Stability under Tropical Conditions and Fast Dissolution: The Case of Clofazimine and Poly(Acrylic Acid). *Molecular Pharmaceutics* **2021**, *18* (3), 1364–1372. https://doi.org/10.1021/acs.molpharmaceut.0c01180.
[24] Yao, X.; Kim, S.; Gui, Y.; Chen, Z.; Yu, J.; Jones, K. J.; Yu, L. Amorphous Drug–Polymer Salt with High Stability under Tropical Conditions and Fast Dissolution: The Challenging Case of Lumefantrine-PAA. *Journal of Pharmaceutical Sciences* **2021**, *110* (11), 3670–3677. https://doi.org/10.1016/j.xphs.2021.07.018.
[25] Amy Lan Neusaenger; Yao, X.; Yu, J.; Kim, S.; Hui, H.-W.; Huang, L.; Que, C.; Yu, L. Amorphous Drug–Polymer Salts: Maximizing Proton Transfer to Enhance Stability and Release. *Molecular Pharmaceutics* **2023**, *20* (2), 1347–1356. https://doi.org/10.1021/acs.molpharmaceut.2c00942.
[26] Neusaenger, A. L.; Fatina, C.; Yu, J.; Yu, L. Effect of Polymer Architecture and Acidic Group Density on the Degree of Salt Formation in Amorphous Solid Dispersions. *Molecular Pharmaceutics* **2024**, *21* (7), 3375–3382. https://doi.org/10.1021/acs.molpharmaceut.4c00089.
[27] Haser, A.; Cao, T.; Lubach, J.; Listro, T.; Acquarulo, L.; Zhang, F. Melt Extrusion vs. Spray Drying: The Effect of Processing Methods on Crystalline Content of Naproxen-Povidone Formulations. *European Journal of Pharmaceutical Sciences* **2017**, *102*, 115–125. https://doi.org/10.1016/j.ejps.2017.02.038.
[28] Tau, R.; Ong, C. K.; Cheng, S.; Ng, W. K. Amorphization of Crystalline Active Pharmaceutical Ingredients via Formulation Technologies. *Powder Technology* **2017**, *311*, 175–184. https://doi.org/10.1016/j.powtec.2017.01.004.
[29] Dedroog, S.; Huygens, C.; Van den Mooter, G. Chemically Identical but Physically Different: A Comparison of Spray Drying, Hot Melt Extrusion and Cryo-Milling for the Formulation of High Drug Loaded Amorphous Solid Dispersions of Naproxen. *European Journal of Pharmaceutics and Biopharmaceutics* **2019**, *135*, 1–12. https://doi.org/10.1016/j.ejpb.2018.12.002.
[30] Martynek, D.; Ridvan, L.; Sivén, M.; Šoóš, M. Stability and recrystallization of amorphous solid dispersions prepared by hot-melt extrusion and spray drying. *International Journal of Pharmaceutics* **2025**, journal pre-proof. doi: https://doi.org/10.1016/j.ijpharm.2025.125331
[31] Song, Y.; Zemlyanov, D.; Chen, X.; Su, Z.; Nie, H.; Lubach, J. W.; Smith, D.; Byrn, S.; Pinal, R. Acid-Base Interactions in Amorphous Solid Dispersions of Lumefantrine Prepared by Spray-Drying and Hot-Melt Extrusion Using X-Ray Photoelectron Spectroscopy. *International Journal of Pharmaceutics* **2016**, *514* (2), 456–464. https://doi.org/10.1016/j.ijpharm.2016.06.126.

[32] Frank, D. S.; Prasad, P.; Iuzzolino, L.; Schenck, L. Dissolution Behavior of Weakly Basic Pharmaceuticals from Amorphous Dispersions Stabilized by a Poly(Dimethylaminoethyl Methacrylate) Copolymer. *Molecular Pharmaceutics* **2022**, *19* (9), 3304–3313. https://doi.org/10.1021/acs.molpharmaceut.2c00456.
[33] Armstrong, M.; Wang, L.; Ristroph, K.; Tian, C.; Yang, J.; Ma, L.; Santipharp Panmai; Zhang, D.; Karthik Nagapudi; Prud'homme, R. K. Formulation and Scale-up of Fast-Dissolving Lumefantrine Nanoparticles for Oral Malaria Therapy. *Journal of Pharmaceutical Sciences* **2023**, *112*(8), 2267–2275. https://doi.org/10.1016/j.xphs.2023.04.003.
[34] Li, S.; Zhang, Z.; Gu, W.; Gallas, M.; Jones, D.; Boulet, P.; Johnson, L. M.; Victoire de Margerie; Andrews, G. P. Hot Melt Extruded High-Dose Amorphous Solid Dispersions Containing Lumefantrine and Soluplus. *International Journal of Pharmaceutics* **2024**, *665*, 124676–124676. https://doi.org/10.1016/j.ijpharm.2024.124676.
[35] Wu, C.-Y.; Benet, L. Z. Predicting Drug Disposition via Application of BCS: Transport/Absorption/ Elimination Interplay and Development of a Biopharmaceutics Drug Disposition Classification System. *Pharmaceutical Research* **2005**, *22* (1), 11–23. https://doi.org/10.1007/s11095-004-9004-4.
[36] Lindenberg, M.; Kopp, S.; Dressman, J. B. Classification of Orally Administered Drugs on the World Health Organization Model List of Essential Medicines according to the Biopharmaceutics Classification System. *European Journal of Pharmaceutics and Biopharmaceutics* **2004**, *58* (2), 265–278. https://doi.org/10.1016/j.ejpb.2004.03.001.
[37] Organization WH. *The Selection and Use of Essential Medicines*. World Health Organization; 2024.
[38] Yu, J.; Li, Y.; Yao, X.; Que, C.; Huang, L.; Hui, H.-W.; Gong, Y.; Qian, F.; Yu, L. Surface Enrichment of Surfactants in Amorphous Drugs: An X-Ray Photoelectron Spectroscopy Study. *Molecular Pharmaceutics***2022**, *19* (2), 654–660. https://doi.org/10.1021/acs.molpharmaceut.1c00786.
[39] A. Alhalaweh; Lou, B.; Bostrom, D.; S.P. Velaga. CCDC 668711: Experimental Crystal Structure Determination. *The Cambridge Structural Database* **2008**. https://doi.org/10.5517/ccqfvb9.
[40] Luo, X.; Herman; Brossi, A.; Flippen-Anderson, J. L.; Gillardi, R. The Chemistry of Drugs Part IV, Configurations of Antimalarials Derived from Qinghaosu: Dihydroqingyhaosu, Artemether, and Artesunic Acid. *Helvetica Chimica Acta* **1984**, *67* (6), 1515–1522. https://doi.org/10.1002/hlca.19840670615.
[41] Liang Li, Dong Yicheng, Zhu Naijue, *Jiegou Huaxue*, 1986, 5, 73
[42] Reboul, J. P.; B. Cristau; Soyfer, J. C.; Astier, J. P. 5H-Dibenz[B,F]Azépinecarboxamide-5 (Carbamazépine). *Acta Crystallographica Section B* **1981**, *37* (10), 1844–1848. https://doi.org/10.1107/s0567740881007383.
[43] Urszula Rychlewska; Humphrey, B.; Eggleston, D. S.; Hodgson, D. J. Antileprosy Dihydrophenazines. Structural Characterization of Two Crystal Forms of Clofazimine and of Isoclofazimine, B.3857. *Journal of the American Chemical Society* **1985**, *107* (16), 4768–4772. https://doi.org/10.1021/ja00302a027.
[44] Mahapatra, S.; Thakur, T. S.; Joseph, S.; Varughese, S.; Desiraju, G. R. New Solid State Forms of the Anti-HIV Drug Efavirenz. Conformational Flexibility and High *Z'* Issues. *Crystal Growth & Design***2010**, *10* (7), 3191–3202. https://doi.org/10.1021/cg100342k.
[45] Ou, X.; Li, X.; Rong, H.; Yu, L.; Lu, M. A General Method for Cultivating Single Crystals from Melt Microdroplets. *Chemical Communications* **2020**, *56* (69), 9950–9953. https://doi.org/10.1039/d0cc03157g.
[46] Bojarska, J.; Fruziński, A.; Maniukiewicz, W. Quantifying Intermolecular Interactions in Solid State Indapamide and Other Popular Diuretic Drugs: Insights from Hirshfeld Surface Study. *Journal of Molecular Structure* **2016**, *1116*, 22–29. https://doi.org/10.1016/j.molstruc.2016.03.006.
[47] Peeters, O. M.; Blaton, N. M.; De, J. Cis-2-Sec-Butyl-4-{4-[4-(4-{[2-(2,4-Dichlorophenyl)-2-(1H-1,2,4-Triazol-1-Ylmethyl)-1,3-Dioxolan-4-Yl]Methoxy}Phenyl)-1-Piperazinyl]Phenyl}-2,4-Dihydro-3H-1,2,4-Triazol-3-One (Itraconazole). *Acta Crystallographica Section C Crystal Structure Communications* **1996**, *52* (9), 2225–2229. https://doi.org/10.1107/s0108270196004180.
[48] Peeters, O. M.; Blaton, N. M.; Gerber, J. G.; Gal, J. (+)-*Cis*-1-Acetyl-4-(4-{[(2*R*,4*S*)-2-(2,4-Dichlorophenyl)-2-(1*H*-Imidazol-1-Ylmethyl)-1,3-Dioxolan-4-Yl]Methoxy}Phenyl)Piperazine [(2*R*,4*S*)-

(+)-Ketoconazole]. *Acta Crystallographica Section E Structure Reports Online* **2004**, *60* (3), o367–o369. https://doi.org/10.1107/s1600536804003046.
[49] de Freitas-Marques, M.; Yoshida, M. I.; Fernandes, C.; Rodrigues, B. L.; Mussel, W. N. Lumefantrine Comparative Study: Single Crystal, Powder X-Ray Diffraction, Hirshfeld Surface, and Thermal Analysis. *Journal of Structural Chemistry* **2020**, *61* (1), 151–159. https://doi.org/10.1134/s0022476620010175.
[50] Kaminski, J. J.; Carruthers, N. I.; Wong, S.-C.; Chan, T.-M.; Billah, M. M.; Tozzi, S.; McPhail, A. T. Conformational Considerations in the Design of Dual Antagonists of Platelet-Activating Factor (PAF) and Histamine. *Bioorganic & Medicinal Chemistry* **1999**, *7* (7), 1413–1423. https://doi.org/10.1016/s0968-0896(99)00075-9.
[51] Mui, P. W.; Jacober, S. P.; Hargrave, K. D.; Adams, J. Crystal Structure of Nevirapine, a Non-Nucleoside Inhibitor of HIV-1 Reverse Transcriptase, and Computational Alignment with a Structurally Diverse Inhibitor. *Journal of Medicinal Chemistry* **1992**, *35* (1), 201–202. https://doi.org/10.1021/jm00079a029.
[52] Sethuraman, V.; Thomas Muthiah, P. Hydrogen-Bonded Supramolecular Ribbons in the Antifolate Drug Pyrimethamine. *Acta Crystallographica Section E Structure Reports Online* **2002**, *58* (8), o817–o818. https://doi.org/10.1107/s1600536802011133.
[53] Li, X.; Manjunatha, U. H.; Goodwin, M. B.; Knox, J. E.; Lipinski, C. A.; Keller, T. H.; Barry, C. E.; Dowd, C. S. Synthesis and Antitubercular Activity of 7-(R)- and 7-(S)-Methyl-2-Nitro-6-(S)-(4-(Trifluoromethoxy)Benzyloxy)-6,7-Dihydro-5H-Imidazo[2,1-b][1,3]Oxazines, Analogues of PA-824. *Bioorganic & Medicinal Chemistry Letters* **2008**, *18* (7), 2256–2262. https://doi.org/10.1016/j.bmcl.2008.03.011.824. *Bioorganic & Medicinal Chemistry Letters*. 2008;(7):2256-2262. doi:10.1016/j.bmcl.2008.03.011
[54] Bauer, J.; Spanton, S.; Henry, R.; Quick, J.; Dziki, W.; Porter, W.; Morris, J. Ritonavir: An Extraordinary Example of Conformational Polymorphism. *Pharmaceutical Research* **2001**, *18* (6), 859–866. https://doi.org/10.1023/a:1011052932607.
[55] Mustafa Bookwala; Ashwini Gumireddy; Aitken, J. A.; Peter. Single Crystal Structure of Terfenadine Form I. *Journal of Chemical Crystallography* **2021**, *52* (1), 81–88. https://doi.org/10.1007/s10870-021-00892-3.
[56] Moseson, D. E.; Tran, T. B.; Karunakaran, B.; Rohan Ambardekar; Tze Ning Hiew. Trends in Amorphous Solid Dispersion Drug Products Approved by the U.S. Food and Drug Administration between 2012 and 2023. *International Journal of Pharmaceutics X* **2024**, *7*, 100259–100259. https://doi.org/10.1016/j.ijpx.2024.100259.
[57] Lemma, H.; Löfgren, C.; San Sebastian, M. Adherence to a Six-Dose Regimen of Artemether-Lumefantrine among Uncomplicated Plasmodium Falciparum Patients in the Tigray Region, Ethiopia. *Malaria Journal* **2011**, *10* (1). https://doi.org/10.1186/1475-2875-10-349.

# Chapter 5. Optimizing drug nanoparticle release from amorphous solid dispersions: exceptional performance of poly(acrylic acid) for releasing lumefantrine

Amy Lan Neusaenger, Yichun Shen, Caroline Fatina, Lian Yu

As submitted to
*The International Journal of Pharmaceutics* **2025**

## 5.1. Abstract

Amorphous solid dispersions of lumefantrine have been prepared with 10 polymers and their drug release has been measured in 0.1% sodium dodecyl sulfate. Poly(acrylic acid) (PAA) significantly outperforms the other polymers in reaching the highest apparent solubility through a 0.2 mm filter, and its outperformance persists as drug loading increases from 25% to 50%, without the sudden decline of release reported for some formulations. The PAA formulation releases its drug cargo as nanoparticles that are stable for at least 8 hours, sufficient for transit through the gastrointestinal tract. The nanoparticles released by PAA are the smallest (~10 nm) of the formulations tested. The exceptional performance of PAA is likely due to its high aqueous solubility, high acidic group density, and ability to interact with ionic species during dissolution. Our finding motivates further studies of PAA as a promising and presently underutilized polymer for amorphous formulations.

## 5.2. Introduction

Amorphous solid dispersions (ASDs) are the focus of active ongoing research for enhancing the delivery of poorly soluble drugs.[1,2] An ASD typically contains a hydrophobic drug, a hydrophilic polymer, and a surfactant, and can be prepared by both solvent-based and solvent-free methods. While the common motivation for developing an ASD is the higher solubility of an amorphous drug than its crystalline counterpart,[3,4] there has been recent attention to the ability of an ASD to release its drug cargo as nanoparticles, leading to an apparent solubility that substantially exceeds the true solubility with potential benefits for drug absorption.[5,6,7,8,9,10] Apart from *in situ* generation, nanoparticles can be preloaded in a solid formulation and subsequently released by reconstitution.[11] To the extent that drug-rich nanoparticles can facilitate drug delivery, optimizing their formation and stability is a key component of ASD development.

For some medicines, formulations with high drug loading are desirable for reducing the pill burden. A notable observation in this context is that drug release from an ASD can suddenly decline as drug loading increases.[12,13,14] For ASDs prepared with polyvinylpyrrolidone/vinyl acetate copolymer (PVPVA), the maximal drug loading before the decline of release is 30% for ritonavir,[12] 35% for lumefantrine (LMF),[13] and 5% for ledipasvir.[14] Given these reports, it is of interest to investigate alternative formulations and release conditions to help achieve good release at high drug loading.

Apart from the broad context described above, the present study was motivated by our previous work on ASDs based on polyacrylic acid (PAA). PAA is a water-soluble polymer with a high acidic-group density. Our initial interest was to take advantage of the abundant acidic groups to form salts with basic drugs, thus preventing their crystallization in hot and humid climates. In this role, PAA excels, producing ASDs with extensive salt formation and high stability against crystallization at 40 °C/75% RH, the harshest condition for drug stability testing.[15,16,17,18] A curious result from this work is that the high stability of these ASDs should cause low solubility, but the PAA formulations show excellent release in biorelevant media.[15,17] For the drugs tested to date, clofazimine[15] and LMF,[16] high apparent solubility was observed in the Simulated Gastric Fluid (SGF) and the Simulated Intestinal Fluid (SIF), even at a high drug loading of 75% and 50%, respectively. This result is counterintuitive, especially in light of a study by Hiew et al., who report

that LMF dispersed in an acidic, salt-forming polymer shows good physical stability but poor release, whereas LMF dispersed in the neutral polymer PVPVA has the opposite combination of properties.[13] It is noteworthy that PAA was not included in their study.

A possible solution to this puzzle lies in the distinction between true solubility and apparent solubility. The thermodynamic connection between stability and solubility applies only to true solubility (molecularly dissolved drug), not to apparent solubility, which may include dispersed nanoparticles. To test this hypothesis, in this work, we dispersed amorphous LMF in 10 polymers including PAA and measured its release in an aqueous medium. The apparent solubility of each ASD was measured through a 0.2 mm filter, a common filter for solubility measurements, and Dynamic Light Scattering (DLS) was used to monitor drug dissolution as nanoparticles. The 10 polymers include: poly(acrylic acid) (PAA), Eudragit® L100, Eudragit® L100-55, hypromellose phthalate (HPMCP), cellulose acetate phthalate (CAP), hypromellose acetate succinate (HPMCAS, in grades HF, MF, and LF), polyvinylpyrrolidone K-30 (PVP), and polyvinylpyrrolidone/vinyl acetate copolymer (PVPVA). See Scheme 1 for the structures of the polymers and other compounds of this study. Of these polymers, PVP and PVPVA are neutral and the rest are acidic, able to form salts with LMF.[18] ASDs were prepared at 25 and 50% drug loading using a simple slurry conversion method.[16,17] The aqueous medium of this study was 0.1% sodium dodecyl sulfate (SDS), which is below the critical micelle concentration of SDS. It was chosen because (1) 0.1% SDS is the surfactant component of SGF, (2) an ASD often contains and dissolves in the presence of a surfactant, and (3) as an ionic surfactant, SDS may better differentiate the different ASDs of this study than a neutral surfactant.

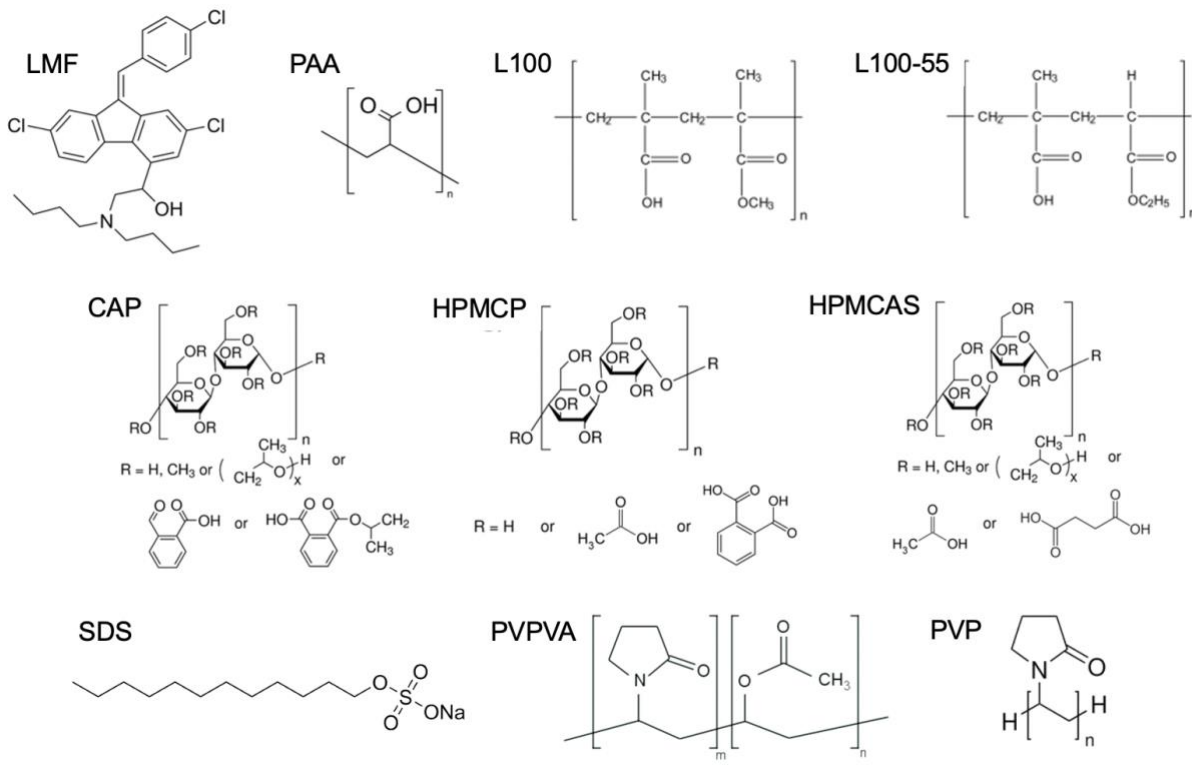


**Scheme 1.** Structures of lumefantrine (LMF), sodium dodecyl sulfate (SDS) and the dispersion polymers of this work: poly(acrylic acid) (PAA), Eudragit L100, Eudragit L100-55, cellulose acetate phthalate (CAP), hypromellose phthalate (HPMCP), hypromellose acetate succinate (HPMCAS), polyvinylpyrrolidone (PVP), and polyvinylpyrrolidone/vinyl acetate copolymer (PVPVA). The three grades of HPMCAS used (HF, MF, LF) had different succinyl contents. Eudragit L100 and L100-55 are random copolymers where the ratio of the two segments is close to 1, and PVPVA is a random copolymer whose m:n ratio is approximately 6:4.

We report that of the 10 polymers tested, PAA outperforms the others in reaching the highest apparent solubility and this advantage persists even at the higher drug loading (50%). In contrast, the ASD prepared with the neutral polymer PVPVA shows reasonably good release at 25% drug loading but virtually no release at 50%. Both visual observation and DLS indicate the formation of nanoparticles during dissolution, accounting for the high apparent solubility relative to the true solubility. The nanoparticles released from the PAA formulation are the smallest and the most abundant. Our findings show that PAA is a promising dispersion polymer for preparing high drug loading ASDs with good release. Since the drug is released as nanoparticles, not dissolved molecules, there is no conflict with the thermodynamic relation between stability and solubility.

## 5.3. Materials & Methods

***Materials***

Poly(acrylic acid) (PAA, MW = 450,000 g/mol), cellulose acetate phthalate (CAP, MW = 2,500 g/mol), polyvinylpyrrolidone K30 (PVP), polyvinylpyrrolidone/vinyl acetate copolymer (PVPVA), and sodium dodecyl sulfate (SDS) were purchased from Sigma-Aldrich (St. Louis, MO). Eudragit L100 (MW = 125,000 g/mol) and L100-55 (MW = 320,000 g/mol) were purchased from Evonik Industries (Essen, Germany). Hypromellose phthalate (HPMCP-55, MW = 45,600 g/mol) and hypromellose acetate succinate (HPMCAS-LF, HPMCAS-MF, HPMCAS-HF; MW = 17,000 – 20,000 g/mol) were purchased from Shin-Etsu Chemical Company Ltd. (Tokyo, Japan). Lumefantrine was purchased from VWR International (Radnor, PA), dichloromethane (ChromAR grade) from Thermo Fisher Scientific (Fair Lawn, NJ), and ethanol from Decon Laboratories (King of Prussia, PA). All materials were used as received. Water was purified using a Milli-Q Lab Water Purification System.

***Slurry Synthesis***

The slurry synthesis of amorphous LMF-polymer salts has been previously described.[15,16,17] The powders of LMF and a polymer were mixed at a 1:1 or 1:3 ratio (50 or 25% drug loading) and a mixed solvent of dichloromethane (DCM) and ethanol (1:1 v/v) was added at a solid/liquid ratio of 1:4 (w/w). Each formulation batch contained 400 mg in solid mass and its slurry was stirred magnetically at 25 °C for up to 20 min. During stirring, an abrupt “clearing transition” occurred,

yielding a transparent viscous solution. This solution was dried under vacuum and ground in an agate mortar and pestle to obtain a free-flowing amorphous powder.

***Apparent Solubility (AS)***

20 mg of an ASD at 25 or 50% drug loading was added into 20 mL 0.1% SDS. If fully dissolved, the dissolved solids' concentration would be 1 mg/mL and the drug concentration would be [LMF] = 0.25 mg/mL for the 25% drug loading ASD and 0.5 mg/mL for the 50% drug loading ASD. After stirring at 37 °C for 1 hour, a 3 mL aliquot was drawn and filtered through a 0.2 mm syringe filter. 0.2 mL of a filtered solution was pipetted in a well of a UV-transparent Corning® 96-well plate and its absorbance at 340 nm was measured with a Clariostar® Plus plate reader. If necessary, the sample solution was diluted with a 10 mg/mL SDS solution before measurement. The LMF concentration was calculated against a calibration curve constructed for the same plate reader using LMF solutions in 10 mg/mL SDS of known concentrations. LMF concentration in each solution was calculated using a standard calibration curve.

***Dynamic Light Scattering (DLS)***

DLS measurements were performed with a Malvern Zetasizer Nano ZS instrument (Southborough, MA) with a back scattering detector (173°). Prior to measurement, each solution was centrifuged to settle any undissolved solid material and to avoid filtration disturbance to the "native" particle size distribution. Centrifugation was performed at 25 °C and 5000 RPM for 5 minutes. 1 mL of each solution was added to a disposable cuvette without dilution and measured after 2 minutes of equilibration at 25 °C. In the analysis setting, water was chosen as dispersant (viscosity = 0.9 cP, RI = 1.330) and the drug nanoparticles were assumed to have an RI value of 1.5, which is typical for organic solids.[19] All measurements were made in duplicate.

***Nanoparticle Size Stability***

20 mg of any ASD of interest was dissolved into 20 mL 0.1% SDS. After stirring at 37 °C for 1 hour, 2 mL of each solution was withdrawn and filtered through a 0.45 mm syringe filter. A filtered solution was added to a disposable cuvette with a lid for DLS measurement as described above as a function of time on the instrument up to 96 hours. Between measurements, the cuvettes were stored at 25 °C.

## 5.4. Results

### *Apparent Solubility*

Figure 1 shows the apparent solubility of the ASDs of LMF in various polymers at 25% and 50% drug loading in 0.1% SDS. The numerical values are collected in Table 1. In each measurement, an ASD was dispersed in the dissolution medium at a total concentration of 1 mg/mL; that is, if fully dissolved, [LMF] would be 0.25 mg/mL for an ASD at 25% drug loading and 0.5 mg/mL for an ASD at 50% drug loading (horizontal lines in Figure 1). After equilibration at 37 °C for one hour, an aliquot of the solution was withdrawn and passed through a 0.2 mm filter and its drug concentration was determined. The one hour time was chosen because previous dissolution measurements had shown that steady-state drug concentration was reached at this time.[16] When the various solutions were sampled, the solution from dissolving the PAA formulation contained no residual solids by visual observation, whereas those from dissolving the other polymer formulations did. This suggests that the PAA formulation had the highest apparent solubility, which was confirmed by quantitative measurements.

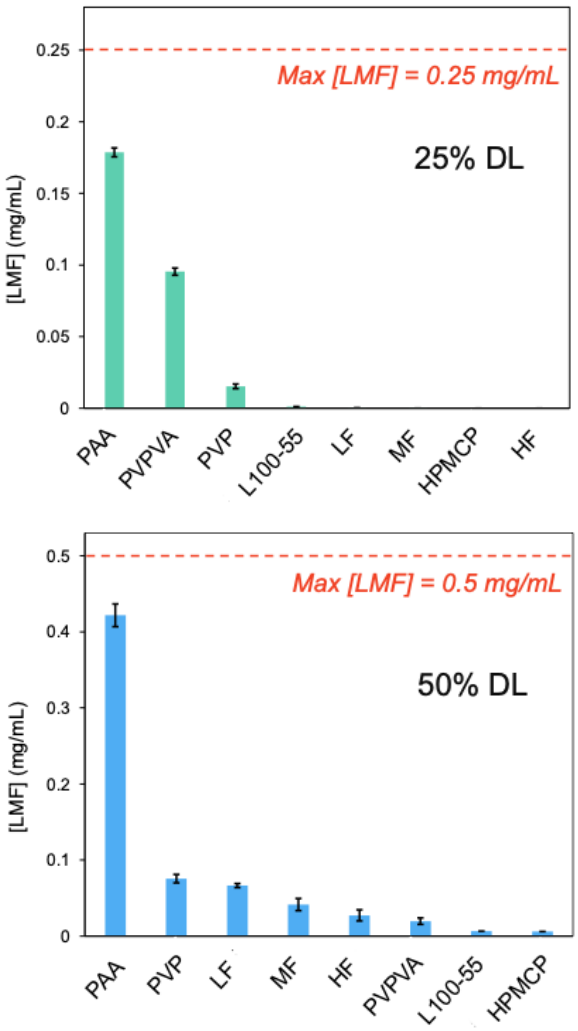


**Figure 1.** Apparent solubility of the ASDs of LMF in various polymers at 25% and 50% drug loading in 0.1% SDS. PAA outperforms the other dispersion polymers by this measure.

Consistent with the visual observation, Figure 1 shows that the PAA formulation had the highest apparent solubility, and the measured value approached the maximal concentration for complete dissolution. The difference between the apparent solubility and the maximal value could result from the rejection of the larger particles by the filter and/or drug absorption by the filter regardless of particle size.

For the ASDs at 25% drug loading, the second-best polymer in terms of drug release was PVPVA, followed by PVP, and little release was observed from the ASDs prepared with the other polymers. For the ASDs at 50% drug loading, the second-best polymer was PVP, followed by HPMCAS-LF, HPMCAS-MF, HPMCAS-HF, PVPVA, L100-55, and HPMCP. The outperformance of PAA relative to the second-best polymer increased at the higher drug loading. It is noteworthy that with increasing drug loading, the runner-up polymer changed from PVPVA to PVP, while PAA remained the best performer. For the three HPMCAS grades (LF, MF, and HF), the relative performance followed the order LF > MF > HF, which is the descending order for their acidic-group densities and the degrees of salt formation with LMF in the respective ASDs.[18]

**Table 1.** Apparent solubilities and % release of LMF dispersed in different polymers.[a]

| Drug loading → | 25% | | 50% | |
|---|---|---|---|---|
| Polymer ↓ | [LMF], mg/mL | % release | [LMF], mg/mL | % release |
| PAA | 0.190 (5) | 76 (2) | 0.43 (2) | 86 (3) |
| L100 | ND | ND | ND | ND |
| L100-55 | ND | ND | 0.009 (7) | 2 (1) |
| HPMCP | ND | ND | 0.008 (6) | 2 (1) |
| CAP | ND | ND | ND | ND |
| LF | ND | ND | 0.068 (3) | 14 (1) |
| MF | ND | ND | 0.043 (8) | 9 (2) |
| HF | ND | ND | 0.029 (8) | 6 (2) |
| PVPVA | 0.105 (1) | 42 (1) | 0.020 (1) | 4 (1) |
| PVP | 0.025 (1) | 10 (1) | 0.074 (10) | 15 (2) |

[a] The value in parathesis is the standard deviation of the preceding value in the last digit(s).
ND: Not detected.

A point of reference for the apparent solubilities in Figure 1 and Table 1 is the amorphous solubility of LMF, 0.007 mg/mL (measured in the pH 6.8 phosphate buffer).[13] Several ASDs prepared in this work have apparent solubilities that exceed the amorphous solubility, suggesting the formation of nanoparticles that could pass through the filter (0.2 mm) and contribute to the measured drug concentration. These nanoparticles were confirmed by visual observation and DLS (see below).

Figure 2 shows the effect of increasing drug loading on the percentage of drug release from each ASD. This quantity is calculated by dividing the apparent solubility by the maximal drug concentration for complete dissolution (Figure 1). Except for PVPVA, all the polymers tested show slightly improved release performance with increasing drug loading. PAA is the best performer at both 25% and 50% drug loading, releasing 76% and 86% of the drug, respectively. For the PVPVA formulation, increasing the drug loading significantly reduces the fraction of the drug released, from 42% to 4%. The formulations with HPMCAS (3 grades) show improved drug release with increasing drug loading, from almost no release to several percent. Of the three grades of HPMCAS, the LF formulation gains the most in this regard, followed by MF and HF. For the PVP formulation, the increase of drug loading causes the released fraction of the drug to increase, from 10% to 15%. Later we will discuss these results in comparison with the release profiles reported in the literature.

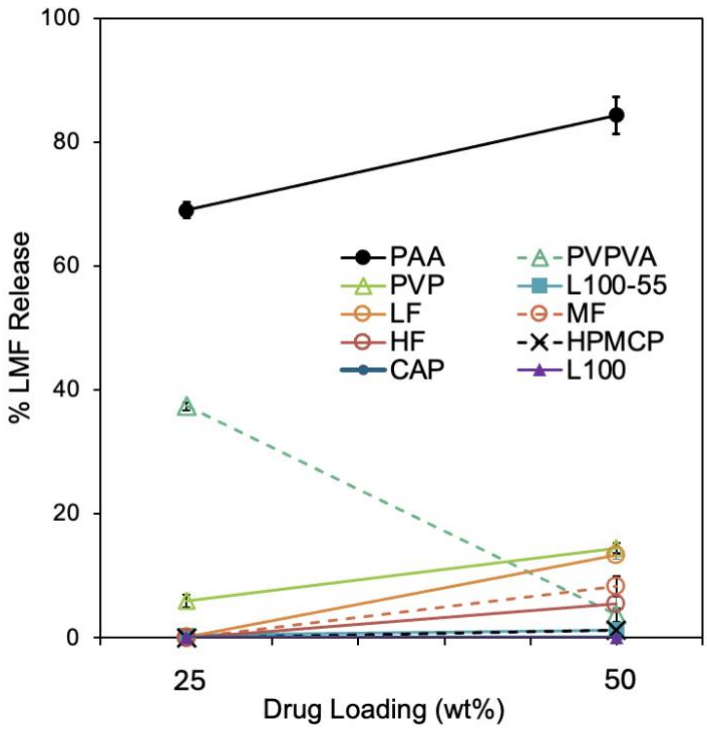


Figure 2. Percentage of LMF released from ASDs at 25 and 50% drug loading. LMF dispersed in PAA is the most completely released at both levels of drug loading. The PVPVA formulation performs well at 25% drug loading but poorly at 50% drug loading.

***Nanoparticles Released by ASD Dissolution***

Both visual observation and DLS indicate the release of nanoparticles by the dissolution of the ASDs. In this section, we present the characterization of these nanoparticles to help understand the high apparent solubility observed. Note that this characterization only probes the portion of the drug that had been released into solution, *not the undissolved solid*, which contained most of the drug for some ASDs. Figure 3 shows the visual appearance of the filtered solutions (through 0.2 mm filters) used for solubility measurements. These solutions were obtained by dissolving the ASDs at 50% drug loading; similar results were observed for the ASDs at 25% drug loading and are not shown. Except for the ASDs prepared with L100 and CAP, all ASDs dissolved in 0.1% SDS to yield solutions with a blue tinge caused by light scattering (the Tyndall effect), indicating the presence of colloidal particles. The solutions from dissolving the ASDs of PAA, PVP, and PVPVA showed the strongest Tyndall effect.

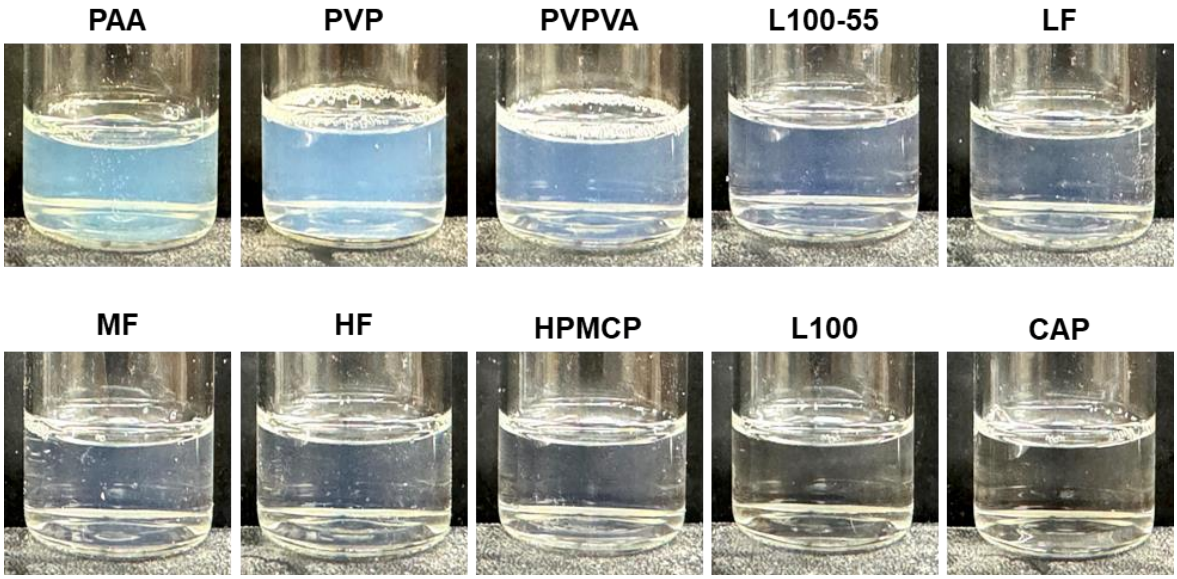


**Figure 3.** Appearance of filtered solutions obtained by dissolving various LMF-polymer ASDs in 0.1% SDS, arranged in descending order of the Tyndall effect.

The strength of the Tyndall effect has an approximate but imperfect correlation with the apparent solubility (Figure 1). The ASD prepared with PAA has the highest apparent solubility, but its Tyndall effect by eye is comparable to that of the ASDs prepared with PVP and PVPVA. This

likely reflects the fact that light scattering intensity is sensitive to particle size and larger particles cause stronger scattering. The solution from dissolving The PAA formulation has higher apparent solubility and its solution must contain a larger quantity of particles, and its lack of stronger scattering suggests that its particles are smaller. To confirm this, DLS data were collected and are presented below.

Figures 4 and 5 show the DLS data of the solutions obtained by dissolving the various ASDs in 0.1% SDS. To probe the native particle sizes, the solutions were not filtered and only gently centrifuged to settle undissolved solids. The data on the CAP and L100 ASDs are excluded because they did not generate significant nanoparticles during dissolution. In these figures, particle size profiles are presented in both intensity and volume representations. DLS measures the fluctuation of scattering intensity caused by moving particles and the data are analyzed to determine the diffusion coefficient of the particles and through the Stokes-Einstein relation, their size. For a polydisperse sample, larger particles cause stronger scattering, and the intensity-based size is biased toward larger particles. For our purpose, the volume-based size is more important, corresponding to the size of the particles that occupy the largest volume fraction. The latter is obtained by further processing the DLS data under additional assumptions. The two representations of the DLS data differ significantly for some samples, indicating their polydispersity. For the PAA formulation, the intensity-based distribution has a maximum above 100 nm and weaker peaks at smaller sizes; in the volumed-based distribution, the maximum occurs near 10 nm. This indicates that most of the nanoparticles by volume fraction are ~10 nm in size, but there are also larger particles that are responsible for much of the measured scattering intensity. Below, we will focus on the volume-based distributions.

Figures 4 and 5 show that the particles released by the PAA formulation are significantly smaller than those by the other formulations, and the average size of these particles, ~10 nm, would allow them to pass through a 0.2 mm filter. Given the visual observation that the PAA formulation is fully dispersed in the aqueous medium, leaving no residual solids, the particle-size result explains the high apparent solubility of the formulation (Figure 1) and why it approaches the maximal concentration for complete dissolution. In essence, the solid formulation is fully dispersed in the aqueous medium as nanoparticles, most of which can pass through the filter.

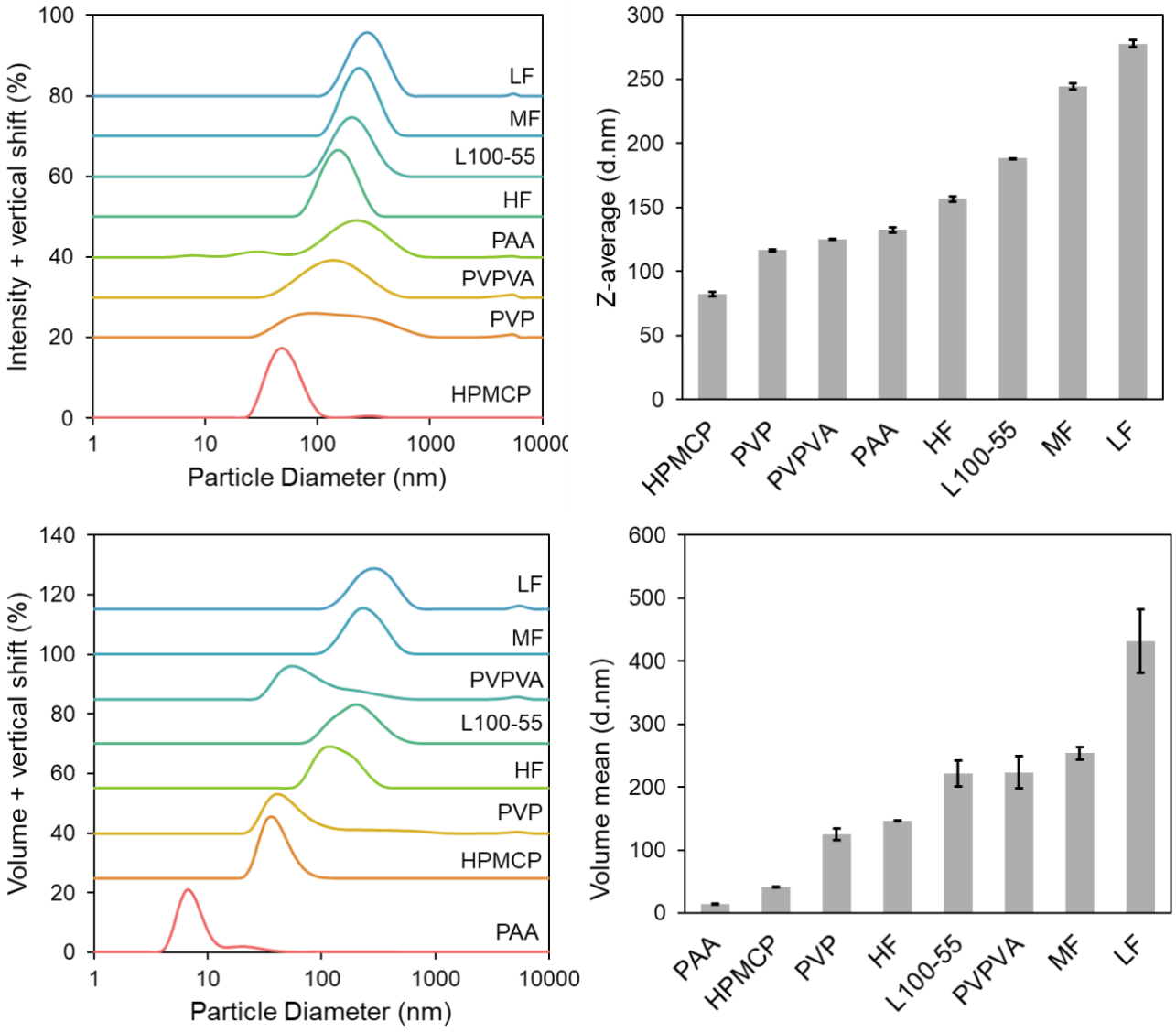


**Figure 4.** Intensity-based (top) and volume-based (bottom) particle size distributions in the solutions produced by dissolving 25% drug-loading ASDs in 0.1% SDS at 1 mg/mL. Left: Distribution curves. Right: Average sizes.

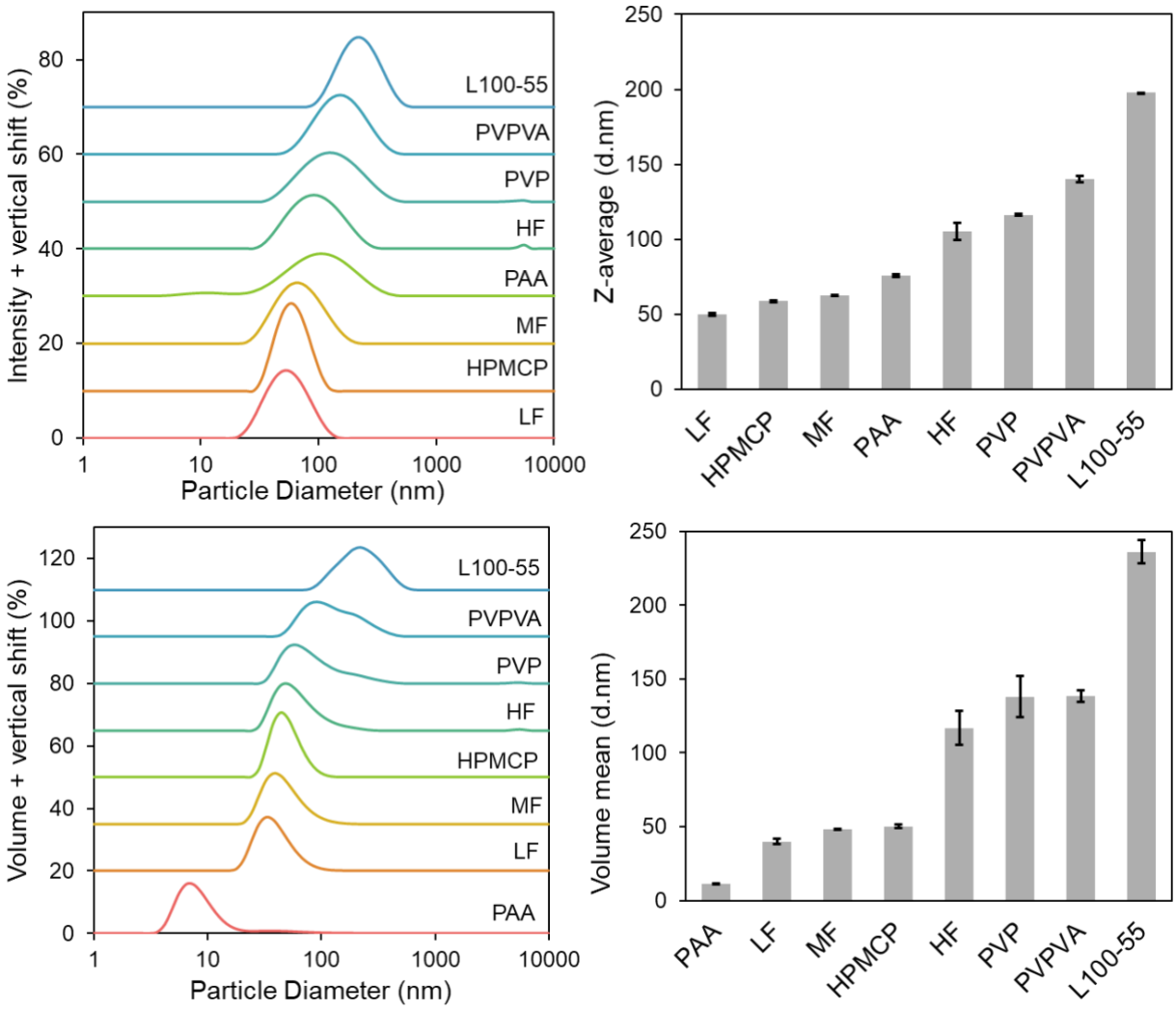


**Figure 5.** Intensity-based (top) and volume-based (bottom) particle size distributions in the solutions produced by dissolving 50% drug-loading ASDs in 0.1% SDS at 1 mg/mL. Left: Distribution curves. Right: Average sizes.

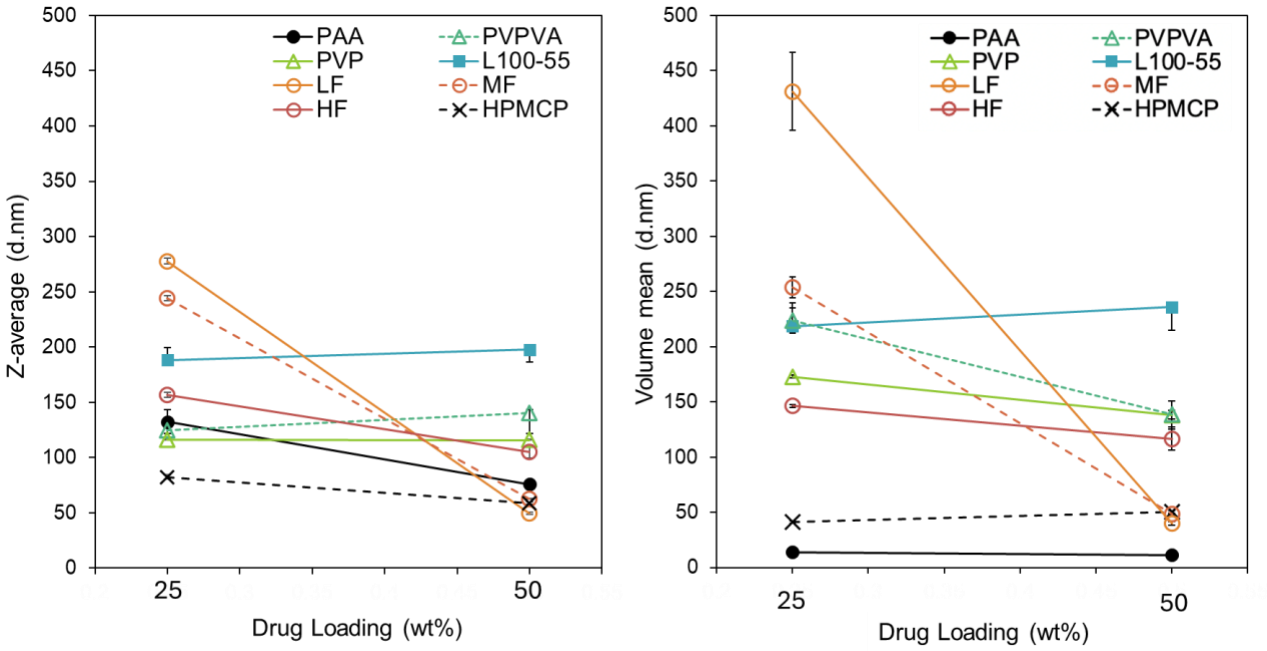


**Figure 6**. Average size of particles released by dissolving each ASD plotted against its drug loading. Left: Intensity-based average size (Z-average). Right: Volume-based average size (volume mean).

Figure 6 plots the average size of the particles released by dissolving each ASD against its drug loading. Both the intensity-based and the volume-based sizes are shown, but we focus on the latter. We find that the average size of the particles released by the PAA formulation is the smallest at both drug loadings and is insensitive to the change of drug loading. This suggests that PAA outperforms the other polymers by consistently releasing the smallest particles. Figure 7 plots the fraction of drug release (Figure 2) against the size of particles produced during dissolution (Figures 4 and 5). In this format, we can test whether the formulation with higher apparent solubility also releases smaller particles. Although the data show significant scattering, a negative trend is evident. This trend suggests that the ability to rapidly generate very small nanoparticles is a key factor responsible for the good release of an ASD. It directs attention to the formation and stabilization of small particles in optimizing drug release by the nanoparticle mechanism.

***Nanoparticle stability.*** For their pharmaceutical applications, the nanoparticles released from an ASD must be sufficiently stable over time. We evaluated this property by monitoring the apparent solubility and the particle size distribution as a function of time. Figure 8 shows the apparent solubility of the three best-performing ASDs identified above, namely, those containing PAA, PVP,

and PVPVA, as a function of time. For this evaluation, each ASD was dispersed in 0.1% SDS at 1 mg/mL; the solution was stirred at 37 °C and aliquots were drawn at different times to determine the apparent solubility.

Figure 8 shows that during the 8 hours of measurement, the three ASDs maintained their apparent solubility. The PAA formulation had the highest apparent solubility initially and its advantage persisted over time. This indicates that during the time of observation, the nanoparticles were stable, without significant aggregation and growth. The 8 hours of stability is sufficient for the transit of an orally administered drug through the gastrointestinal tract.

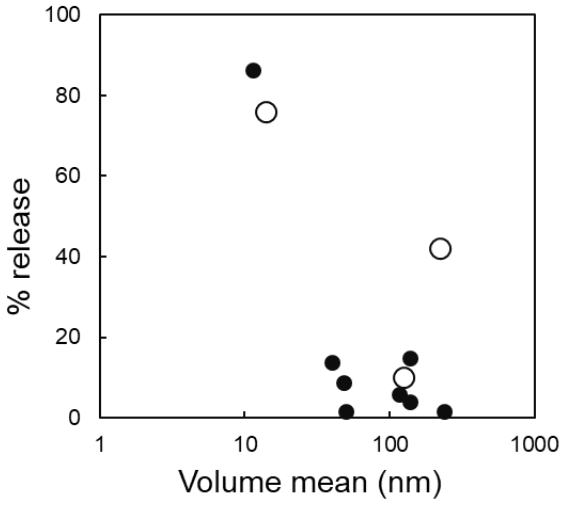


**Figure 7.** Fraction of drug release from an ASD vs. average size of particles generated by dissolution. Open circles: 25% drug loading. Solid circles: 50% drug loading.

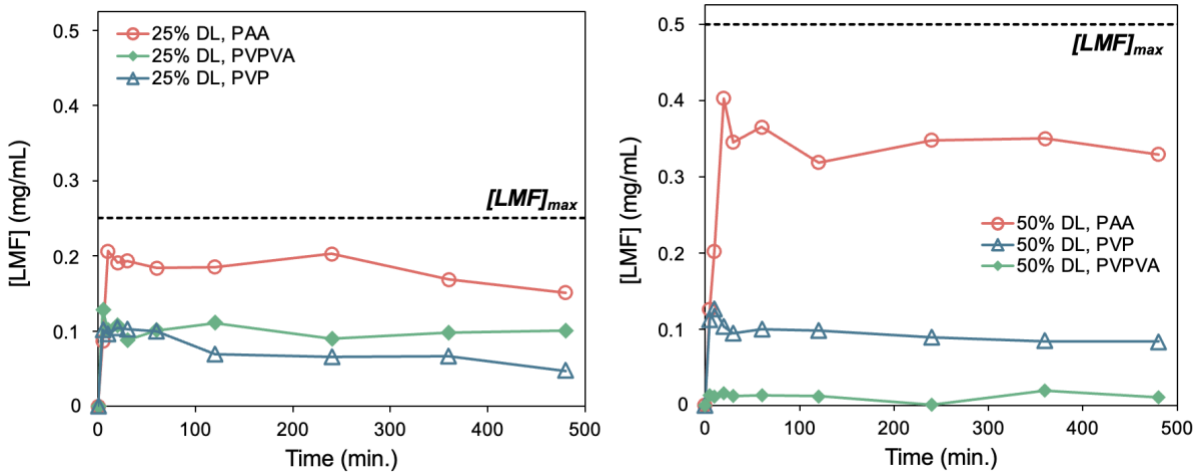


**Figure 8.** Apparent solubility of the ASDs of LMF formulated with PAA, PVP and PVPVA in 0.1% SDS as a function of time. Results are shown for ASDs at 25% drug loading (left) and 50% drug loading (right).

Figure 9 shows the DLS data to characterize the size stability of the nanoparticles released by each ASD. Since we are mainly interested in the relative changes, only the intensity-based size distributions ("raw data") are shown. We find that the nanoparticles released from all three ASDs are stable for at least 8 hours. This is seen from the distribution curves on the left and the Z-averages on the right. These results are consistent with the constant apparent solubility shown in Figure 8. If the nanoparticles grew over time, the apparent solubility would decrease. In comparing the three ASDs, it is noteworthy that the PAA formulation has the highest apparent solubility (Figure 8) and thus the highest particle concentration. A higher particle concentration provides a larger driving force for the aggregation and growth of the particles, and yet the nanoparticles released by the PAA formulation are as stable as those released by the other formulations.

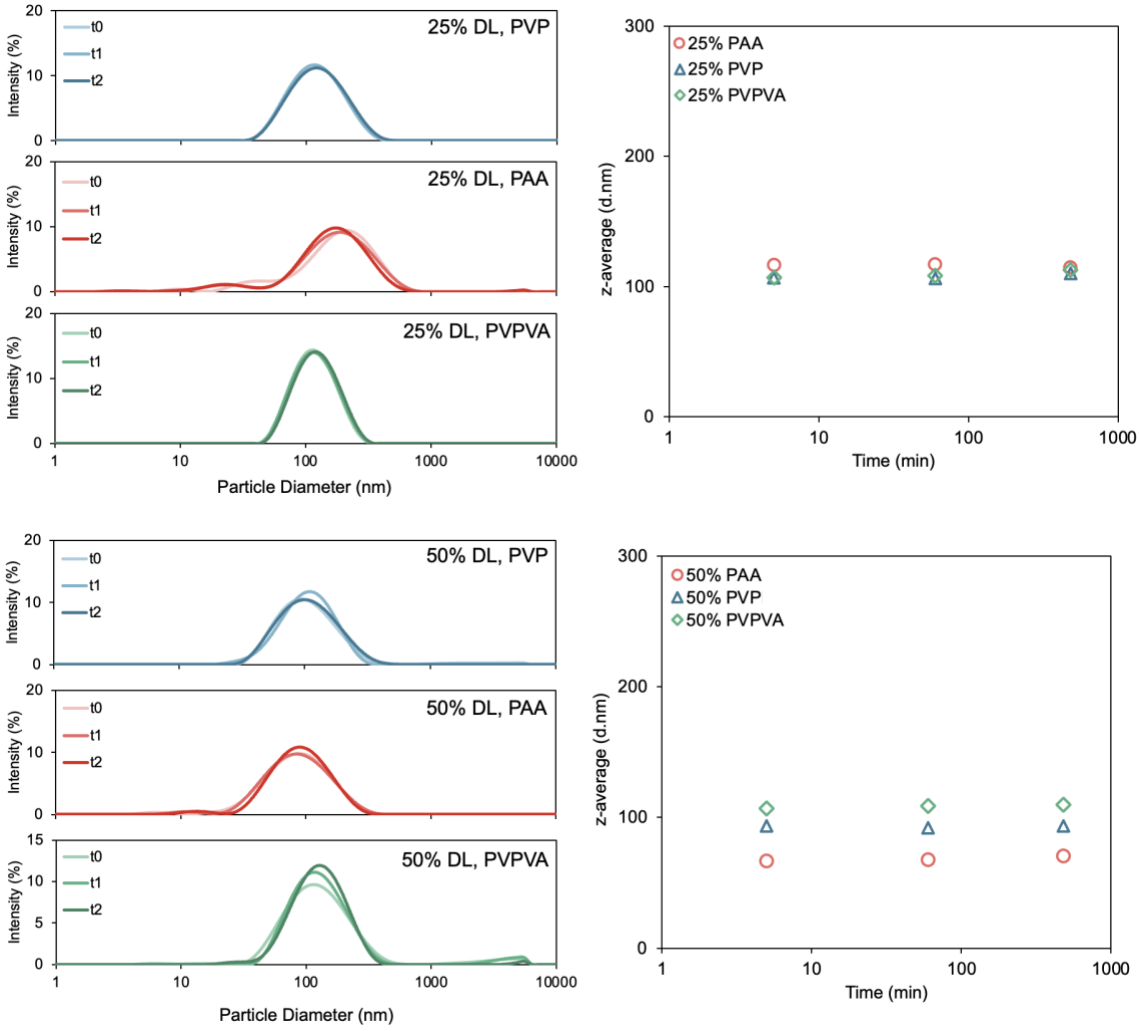


Figure 9. Size stability of nanoparticles released by ASD dissolution. Top: ASDs at 25% drug loading. Bottom: ASDs at 50% drug loading. t0: freshly prepared (5 min). t1: 60 min. t3: 480 min.

## 5.5. Discussion

This work has compared the performance of 10 dispersion polymers for releasing their amorphous LMF cargo as drug-rich nanoparticles in 0.1% SDS. We find that PAA significantly outperforms the other polymers, even at a relatively high drug loading of 50% (Figure 1). This enables the LMF-PAA ASD to be physically stable against crystallization and have high apparent solubility,[16,17] a puzzling combination of properties that had motivated this work. In addition, we find that the release performance is not harmed (in fact slightly improved) by the increase of drug loading from 25% to 50% for all the polymers except for PVPVA (Figure 2). Below we discuss these results.

**Can an Amorphous Formulation Be Physically Stable and Provide Efficient Release?**

One motivation for this work was the combination of physical stability and apparent solubility of the amorphous LMF-PAA formulation.[50,23,16] According to thermodynamics, a more stable solid phase is less soluble. The extensive salt formation between LMF and PAA[17] decreases the drug's chemical potential and its driving force to crystallize. This is consistent with the high physical stability of the amorphous formulation, but contradicts its high solubility.[16] The key to resolve this puzzle is to realize that the thermodynamic relation refers to true solubility, not apparent solubility. We have shown that the high apparent solubility of the LMF-PAA formulation is due to the efficient drug release as nanoparticles, not to the enhanced true solubility. The particles can pass through a fine filter (0.2 mm) commonly used for solubility measurements and contribute to the measured "solubility". Thus, there is no conflict with thermodynamics. To the extent that drug-rich nanoparticles benefit drug absorption, it is possible for an amorphous formulation to be both physically stable and "highly soluble".

The amorphous formulations of LMF with the three grades of HPMCAS (LF, MF, and HF) provide further understanding of the balance between stability and release. For the ASDs at 50% drug loading, the relative release performance is LF > MF > HF (Figure 1). This is the order in which the acidic-group densities in these polymers decrease and the degrees of salt formation in the corresponding ASDs fall.[18] By the thermodynamic reasoning above, the true solubility of the formulation should increase in the same order since there are fewer ionic interactions to lower the drug's chemical potential in the solid state. Superficially, this contracts the trend of worsening

release in the same order, but this puzzle resolves itself once we realize that the thermodynamic argument applies to the true solubility, not the apparent solubility that reflects mainly the dispersed nanoparticles.

**Is PAA a Special Polymer?**

This work has shown that PAA outperforms the other polymers for releasing its drug cargo as nanoparticles, even at the relatively high drug loading of 50% (Figures 1 and 2). Visual observations indicate the PAA formulation is almost fully dispersed as nanoparticles, leaving no residual solids, and DLS indicates that the nanoparticles released by this formulation are the smallest (~10 nm) and are stable over time. At present, PAA is not a standard dispersion polymer for preparing ASDs, and our findings suggest that PAA could be promising polymer for future applications.

Compared to the other polymers of this study, PAA is among the most water-soluble and has the highest acidic-group density. Since the drug in an ASD is generally hydrophobic, the high aqueous solubility of the dispersion polymer would enable its quick release from the solid, driving local phase separation and generation of drug-rich particles. The high acidic-group density of PAA enables extensive salt formation with a basic drug like LMF. In the solid state, these ionic interactions help prevent drug crystallization, even under hot and humid conditions; during dissolution, the ionized drug and polymer can interact with ionic species in solution and such interactions would be less important for neutral or less extensively ionized drugs and polymers. For example, NaCl and other inorganic salts can trigger drug release from the ionic complex between a basic polymer and an acidic drug.[20] The SDS in our dissolution medium can interact with an ionized drug or polymer[21,22,23,24,25] through mechanisms that might be negligible for neutral molecules. While such interactions can cause precipitation,[23] this need not be a negative effect as the goal is to release the drug as nanoparticles, so long as the nanoparticles are efficiently generated and stabilized on the timescale of drug absorption (hours).

**Effect of Drug Loading on Release**

For all the polymers tested here except for PVPVA, the drug release performance improves slightly as drug loading increases from 25% to 50%. For PVPVA, the opposite is observed, making it the second-best performing polymer at 25% drug loading and one of the worst at 50% drug loading.

This pattern of drug release is both similar and different from that reported by Hiew et al.[13] and below we compare the two studies.

Hiew et al. have dispersed LMF in various polymers and measured their release in a phosphate buffer (pH 6.8). For the ASD prepared with PVPVA, they observe an abrupt decline of drug release above 35% drug loading, fully consistent with our result. Quantitatively, the apparent solubility of their ASD at 25% drug loading, 100 mg/mL, agrees with our value of 95 mg/mL. For the acidic polymers (L100, HPMCP, CAP, HPMCAS-MF), however, Hiew et al. observe significantly worse release with increasing drug loading, with the effect being noticeable even at 5% drug loading, whereas we find improved drug release as drug loading increases from 25% to 50%.

We speculate that a major cause for the divergent conclusions is the difference in the ASDs prepared in the two studies and the conditions of their testing. Hiew et al. used rotary evaporation to prepare ASDs, and we used slurry conversion. These two methods both involve drying solutions and should in principle yield the same product, but this is not the case: as Table 2 shows, for the acidic polymers, Hiew et al.'s ASDs had consistently less extensive salt formation than those of this work. For example, when dispersed in HPMCAS-MF, LMF is 41% protonated in our product and 19% in theirs. It should not be surprising if ASDs of such different internal structures show different release behaviors. In addition, Hiew et al. measured the surface-area-normalized release rate of a tablet in a pH 6.8 phosphate buffer, and we measured the release from a powder dispersed in 0.1% SDS. Prior to measurements, their solutions were centrifuged and ours were passed through a 0.2 mm filter. It is reassuring that for the PVPVA formulation, both studies observed decline of drug release near 35% drug loading. For the ASDs prepared with acidic polymers, the different release behaviors could reflect the different degrees of ionization in the solid state and the interactions with different ionic species in the solution. Taken together, the results of the two studies argue that the worsening of drug release with increasing drug loading could be avoidable by employing different dispersion polymers[26] and testing conditions, and for the same dispersion polymer, even by modifying the synthesis conditions.

Table 2. Degrees of protonation (%) of LMF in ASDs with different polymers.[18]

| Polymer | 25% drug loading, this work | 25% drug loading, Hiew et al.[12] | 50% drug loading, this work |
|---|---|---|---|
| PAA | 91 | - | 87 |
| L100 | 78 | 49 | 55 |
| L100-55 | 79 | - | 60 |
| HPMCP | 79 | 46 | 67 |
| CAP | 80 | 55 | 70 |
| LF | 58 | - | 40 |
| MF | 41 | 19 | 23 |
| HF | 33 | - | 20 |
| PVPVA | 0 | - | 0 |
| PVP | 0 | - | 0 |

## 5.6 Conclusions

Lumefantrine (LMF) is a highly hydrophobic, poorly water-soluble drug. In this work, we have dispersed amorphous LMF in 10 different polymers and tested its release in 0.1% sodium dodecyl sulfate (SDS), a common medium for dissolution testing. We find that poly(acrylic acid) (PAA) outperforms the other polymers in releasing LMF as nanoparticles, reaching the highest apparent solubility (measured through a 0.2 mm filter). The excellent release performance of PAA persists as drug loading increases from 25% to 50%. DLS measurements showed that of the 10 polymers tested, PAA releases the drug cargo as the smallest particles (~10 nm in size) and we find an approximate correlation between smaller particle size and more complete drug release across the polymers. The nanoparticles released from the PAA formulation are stable for at least 8 hours, sufficient for their transit through the gastrointestinal tract. The efficient release of nanoparticles from the PAA formulation answers the question that had motivated this work, namely, how this formulation can have high stability and good release, in apparent violation of thermodynamics. Since the drug is released mainly as particles, not dissolved molecules, there is no conflict with thermodynamics. If the solubility of a formulation is defined to include both true solubility and apparent solubility (of dispersed nanoparticles), an amorphous drug-polymer salt can be simultaneously stable and soluble.

At present, PAA is not a standard polymer for preparing amorphous solid dispersions, and our finding motivates further work to explore its applications in this area, especially for ASDs of high drug loading. Relative to the other polymers studied, PAA is among the most water-soluble and has the highest acidic-group density, enabling extensive salt formation and ionic interactions with a basic drug like LMF. A remarkable result from this work is the release of very small particles (~10 nm) from the PAA formulation, which remain stable against aggregation and growth for at least 8 hours. Whether this is a general feature for an amorphous dispersion in PAA is a worthy question for future studies.

## 5.7 Acknowledgements

This work was supported by the Bill and Melinda Gates Foundation (OPP1160408) and we acknowledge the helpful discussions with Niya Bowers, David Monteith, and Paco Alvarez. Under the grant conditions of the Foundation, a Creative Commons Attribution 4.0 Generic License has already been assigned to the Author Accepted Manuscript version that might arise from this submission.

## 5.8. References

[1] Mishra, D. K.; Dhote, V.; Bhargava, A.; Jain, D. K.; Mishra, P. K. Amorphous Solid Dispersion Technique for Improved Drug Delivery: Basics to Clinical Applications. *Drug Delivery and Translational Research* **2015**, *5* (6), 552–565.
[2] Baghel, S.; Cathcart, H.; O'Reilly, N. J. Polymeric Amorphous Solid Dispersions: A Review of Amorphization, Crystallization, Stabilization, Solid-State Characterization, and Aqueous Solubilization of Biopharmaceutical Classification System Class II Drugs. *Journal of Pharmaceutical Sciences* **2016**, *105* (9), 2527–2544.
[3] Babu, N. J.; Nangia, A. Solubility Advantage of Amorphous Drugs and Pharmaceutical Cocrystals. *Crystal Growth & Design* **2011**, *11*(7), 2662–2679. https://doi.org/10.1021/cg200492w.
[4] Murdande, S. B.; Pikal, M. J.; Shanker, R. M.; Bogner, R. H. Solubility Advantage of Amorphous Pharmaceuticals: I. A Thermodynamic Analysis. *Journal of Pharmaceutical Sciences* **2010**, *99*(3), 1254–1264. https://doi.org/10.1002/jps.21903.
[5] Tho, I.; Liepold, B.; Rosenberg, J.; Maegerlein, M.; Brandl, M.; Fricker, G. Formation of nano/micro-dispersions with improved dissolution properties upon dispersion of ritonavir melt extrudate in aqueous media. *European Journal of Pharmaceutical Sciences* 2010, *40*(1), 25-32. doi:10.1016/j.ejps.2010.02.003
[6] Harmon, P.; Galipeau, K.; Xu, W.; Brown, C.; Wuelfing, W. P. Mechanism of Dissolution-Induced Nanoparticle Formation from a Copovidone-Based Amorphous Solid Dispersion. *Molecular Pharmaceutics* **2016**, *13* (5), 1467–1481. https://doi.org/10.1021/acs.molpharmaceut.5b00863.
[7] Taylor, L. S.; Zhang, G. G. Z. Physical Chemistry of Supersaturated Solutions and Implications for Oral Absorption. *Advanced Drug Delivery Reviews* **2016**, *101*, 122–142. https://doi.org/10.1016/j.addr.2016.03.006.
[8] Kesisoglou, F.; Wang, M.; Galipeau, K.; Harmon, P.; Okoh, G.; Xu, W. Effect of Amorphous Nanoparticle Size on Bioavailability of Anacetrapib in Dogs. *Journal of Pharmaceutical Sciences* **2019**, *108* (9), 2917–2925. https://doi.org/10.1016/j.xphs.2019.04.006.
[9] Stewart, A. M.; Grass, M. E. Practical Approach to Modeling the Impact of Amorphous Drug Nanoparticles on the Oral Absorption of Poorly Soluble Drugs. *Mol. Pharmaceutics* **2020**, *17*, 180−189
[10] Qian, K.; Stella, L.; Jones, D. S.; Andrews, G.; Du, H. Drug-Rich Phases Induced by Amorphous Solid Dispersion: Arbitrary or Intentional Goal in Oral Drug Delivery? *Pharmaceutics* **2021**, *13* (6), 889–889. https://doi.org/10.3390/pharmaceutics13060889.
[11] Armstrong, M.; Wang, L.; Ristroph, K.; Tian, C.; Yang, J.; Ma, L.; Panmai, S.; Zhang, D.; Nagapudi, K.; Prud'homme; R.K. Formulation and scale-up of fast-dissolving lumefantrine nanoparticles for oral malaria therapy. *Journal of Pharmaceutical Sciences* 2023, *112*(8), pp.2267-2275.
[12] Indulkar, A.S.; Lou, X.; Zhang, G.G.; Taylor, L.S. Insights into the dissolution mechanism of ritonavir–copovidone amorphous solid dispersions: importance of congruent release for enhanced performance. *Molecular pharmaceutics* 2019, *16*(3), pp.1327-1339.
[13] Hiew, T. N.; Zemlyanov, D. Y.; Taylor, L. S. Balancing Solid-State Stability and Dissolution Performance of Lumefantrine Amorphous Solid Dispersions: The Role of Polymer Choice and Drug–Polymer Interactions. *Molecular Pharmaceutics* **2021**, *19*(2), 392-413. https://doi.org/10.1021/acs.molpharmaceut.1c00481.
[14] Que, C.; Lou, X.; Dmitry Zemlyanov; Mo, H.; Indulkar, A. S.; Gao, Y.; Zhang, Z.; Taylor, L. S. Insights into the Dissolution Behavior of Ledipasvir–Copovidone Amorphous Solid Dispersions: Role of Drug Loading and Intermolecular Interactions. *Molecular Pharmaceutics* **2019**, *16* (12), 5054–5067. https://doi.org/10.1021/acs.molpharmaceut.9b01025.
[15] Gui, Y.; McCann, E. C.; Yao, X.; Li, Y.; Jones, K. J.; Yu, L. Amorphous Drug–Polymer Salt with High Stability under Tropical Conditions and Fast Dissolution: The Case of Clofazimine and Poly(Acrylic Acid). *Molecular Pharmaceutics* **2021**, *18* (3), 1364–1372. https://doi.org/10.1021/acs.molpharmaceut.0c01180.
[16] Yao, X.; Kim, S.; Gui, Y.; Chen, Z.; Yu, J.; Jones, K. J.; Yu, L. Amorphous Drug–Polymer Salt with High Stability under Tropical Conditions and Fast Dissolution: The Challenging Case of Lumefantrine-PAA. *Journal of Pharmaceutical Sciences* **2021**, *110* (11), 3670–3677. https://doi.org/10.1016/j.xphs.2021.07.018.

[17] Neusaenger, A.; Yao, X.; Yu, J.; Kim, S.; Hui, H.-W.; Huang, L.; Que, C.; Yu, L. Amorphous Drug-Polymer Salts: Maximizing proton transfer to enhance stability and release. *Mol. Pharmaceutics* **2023**, *20*, 1347–1356.
[18] Neusaenger, Amy; Fatina, Caroline; Yu, Junguang; Yu, Lian. Effect of polymer architecture and acidic group density on the degree of salt formation in amorphous solid dispersions. *Mol. Pharm.* **2024**, *21*, 3375–3382. doi.org/10.1021/acs.molpharmaceut.4c00089.
[19] Winchell, A. N., *The Optical Properties of Organic Compounds*. 2nd ed.; Academic Press: New York, 1954; p 487.
[20] Kindermann, C.; Matthée, K.; Strohmeyer, J.; Sievert, F.; Breitkreutz, J. Tailor-made release triggering from hot-melt extruded complexes of basic polyelectrolyte and poorly water-soluble drugs. *European journal of pharmaceutics and biopharmaceutics* 2011, *79*(2), 372-381.
[21] Chen, Y.; Wang, S.; Wang, S.; Liu, C.; Su, C.; Hageman, M.; Hussain, M.; Haskell, R.; Stefanski, K.; Qian, F. Sodium Lauryl Sulfate Competitively Interacts with HPMC-as and Consequently Reduces Oral Bioavailability of Posaconazole/HPMC-as Amorphous Solid Dispersion. *Molecular Pharmaceutics* **2016**, *13* (8), 2787–2795. https://doi.org/10.1021/acs.molpharmaceut.6b00391.
[22] Bhattachar, S. N.; Risley, D. S.; Werawatganone, P.; Aburub, A. Weak Bases and Formation of a Less Soluble Lauryl Sulfate Salt/Complex in Sodium Lauryl Sulfate (SLS) Containing Media. *International Journal of Pharmaceutics* **2011**, *412* (1-2), 95–98. https://doi.org/10.1016/j.ijpharm.2011.04.018.
[23] Guo, Y.; Mishra, M. K.; Wang, C.; Sun, C. C. Crystallographic and Energetic Insights into Reduced Dissolution and Physical Stability of a Drug–Surfactant Salt: The Case of Norfloxacin Lauryl Sulfate. *Molecular Pharmaceutics* **2019**. https://doi.org/10.1021/acs.molpharmaceut.9b01015.
[24] Helgeson ME. Colloidal behavior of nanoemulsions: Interactions, structure, and rheology. *Current Opinion in Colloid & Interface Science*. Published online October 2016:39-50.
[25] Qi S, Roser S, Edler KJ, et al. Insights into the Role of Polymer-Surfactant Complexes in Drug Solubilisation/Stabilisation During Drug Release from Solid Dispersions. *Pharmaceutical Research*. **2012**, (1):290-302.
[26] Sugandha Saboo; Moseson, D. E.; Kestur, U. S.; Taylor, L. S. Patterns of Drug Release as a Function of Drug Loading from Amorphous Solid Dispersions: A Comparison of Five Different Polymers. *European Journal of Pharmaceutical Sciences* **2020**, *155*, 105514–105514. https://doi.org/10.1016/j.ejps.2020.105514.

# Chapter 6. Conclusions and Future Work

Amy Lan Neusaenger

This thesis considered the preparation of effective amorphous solid dispersions (ASDs), particularly the effect of processing conditions and dispersion polymer on the stability and solubility behavior of the formulation with an emphasis on the degree of salt formation between the drug and dispersion polymer. In Chapter 2 and 3, we investigated salt formation in and performance of lumefantrine (LMF) ASDs. In Chapter 4, we show the versatility of our synthesis approach (slurry conversion) in amorphizing a wide variety of basic drugs dispersed in poly(acrylic acid) (PAA). In Chapter 5, we turn our attention to the solution state, identifying PAA as a promising formulation polymer for the dispersion of drug-rich nanoparticles to improve drug release.

## 6.1. Synthesis and characterization of amorphous drug-polymer salts

Chapter 2 examined the role of processing conditions on the degree of LMF protonation in LMF-PAA ASDs and their subsequent stability under accelerated storage conditions (40 C/75% RH) and release in Simulated Gastric Fluid (SGF). This work compared slurry conversion (SC) and antisolvent precipitation (AP) to the more conventional ASD synthesis methods of hot-melt extrusion (HME) and rotary evaporation (RE). It was found that SC and AP were able to achieve reaction equilibrium for LMF-PAA salt formation while HME and RE did not, with SC distinct from AP in its drug loading (DL) tunability. This degree of salt formation is a critical attribute due to its demonstrated ability to enhance both stability and release of an LMF-PAA ASD.

In Chapter 2 and 3, we consider the formulation of lumefantrine (LMF) amorphous solid dispersions (ASDs) formulated with alternative acidic polymers. In Chapter 3, we show that the outperformance of SC over other synthetic methods persists for these other LMF-polymer systems, indicating that the ability of SC to effectively facilitate intimate component mixing and subsequent equilibrium reaction behavior is not unique to LMF-PAA dispersions. Similarly, we demonstrate in Chapter 4 that the versatility of SC holds for a variety of poorly soluble basic drugs dispersed in PAA. In addition to the previously described LMF, 17 additional poorly soluble drugs including 15 basic, 1 neutral, and 1 acidic drug were formulated with PAA using the standard SC synthesis. Fully amorphous dispersions were successfully prepared under these synthesis conditions for 16 of the 18 drugs at 25% DL and 11 at 50% DL, with most

formulations undergoing an observable “clearing” during stirring, indicating complete dissolution and amorphization prior to drying. Furthermore, it was shown that SC could be used to prepare ternary ASDs (two drugs dispersed in PAA) and could also be scaled up at least 60-fold for LMF-PAA at 50% DL with only minor modifications to the stirring method. This demonstrated versatility of the slurry method is encouraging given its very low equipment cost, lower solvent usage than other solvent-based methods, and low energy consumption.

**Fig. 1.** Contribution by mass percentage to materials of concern outlined by Glaxo-Smith-Kline (GSK). Dichloromethane (DCM) corresponds to over 75% of this mass. Adapted from Ref. 2.

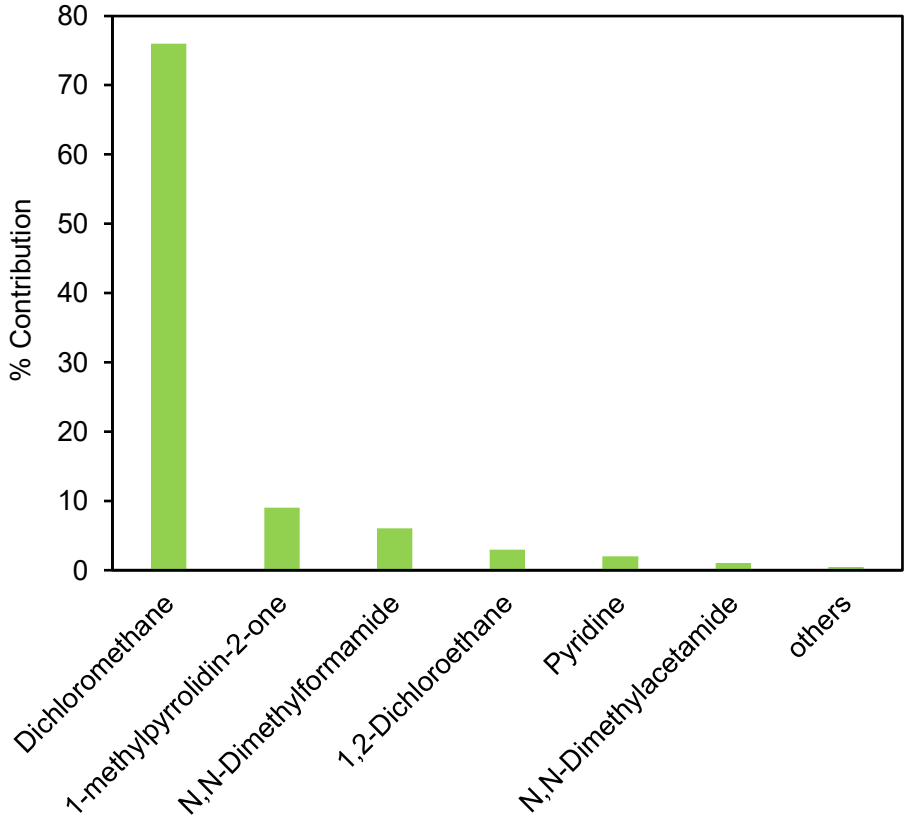


While these results are highly promising, it is important to anticipate potential scale-up challenges and points that could benefit from further optimization. While EtOH is considered a low-risk (Class 3) residual solvent in finished pharmaceutical products according to the FDA, DCM has a very low threshold for safety and is suggested to be present in finished pharmaceutical products at no more than 600 ppm.[1] Recent years have seen increasing efforts of industrial leaders to reduce the quantity of DCM used in pharmaceutical processes; DCM is by

far the largest contributor to materials of concern (Fig. 1).[2] To ensure that translation of SC to manufacturing scale remains viable, reliable analysis of residual DCM in dried slurry products is necessary. If DCM is shown to be inconsistently removed to a sufficient extent, alternative solvents that do not negatively affect the versatility of SC should be investigated to ease further scale-up and late-stage development.

Head-space gas chromatography with a flame ionization detector (GC-FID) has been shown to be a reliable method to determine DCM content in both liquid and solid samples due to its high volatility.[3] The LMF-PAA system should be studied first, given its demonstrated compatibility with SC at a variety of DLs and its well-characterized performance under optimal conditions. LMF-PAA should be prepared using standard SC synthesis at a range of DLs (5 – 75 wt%) at regular intervals and dried at room temperature under vacuum as previously described. Dried ASDs can then be ground into a fine powder to ensure sufficient exposed surface area for solvent evaporation. Known masses of each ground formulation may then be added to head-space GC vials of sufficient volume and held above the DCM boiling point (> 40C) to allow removal of residual DCM and subsequent quantification via head-space air sampler after a standard calibration of samples with known DCM content. Should this test demonstrate that sufficient DCM is removed (regardless of DL) for these LMF-PAA ASDs, additional LMF-based ASDs dispersed in different polymers should be analyzed using the same procedure. Due to the highly varied solubility and gelling behavior of different polymers in organic solvent, it is important to ensure that the removal of DCM from SC products is not strongly dependent on the ASD components.

Should the removal of DCM be exceedingly difficult or unreliable, alternative solvents may be explored. Preliminary work has identified acetone as a candidate for DCM substitution, particularly given its status as a Class 3 solvent with an acceptable limit in finished pharmaceutical products that is approximately 10 times that of DCM. For LMF-PAA prepared using SC at 75C with acetone as a substitute for DCM during synthesis, 25 and 50% DL ASDs can be successfully formulated (Fig. 2). The use of mild heating in this preliminary experiment was due to the relatively lower solubility of LMF in acetone compared to DCM, but it is likely that this temperature could be lowered if needed for more favorable processing should these

conditions be scaled up. Due to LMF-PAA's well-characterized and previously described apparent solubility benchmarks, the effect of acetone substitution should first be examined in the LMF-PAA system. The dispersion behavior of LMF-PAA at both 25 and 50% DL (both successful in amorphization using acetone/ethanol as shown in Fig. 2) in 0.1% SDS can first be quickly assessed and compared to the results presented in Chapter 6 for a DCM/ethanol

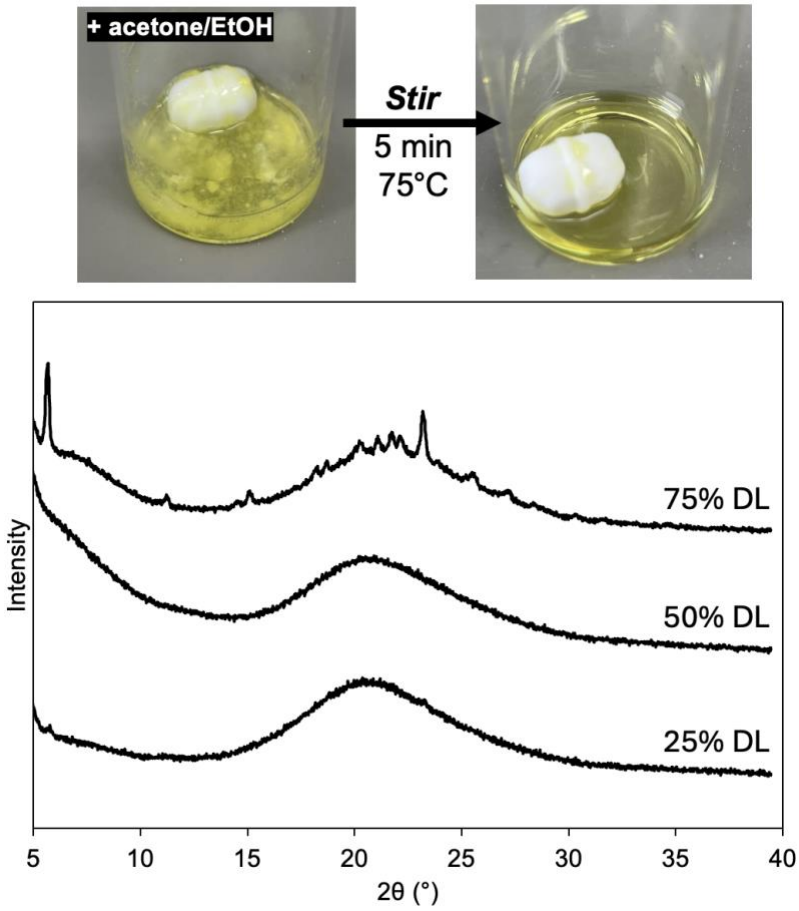


**Fig. 2.** The appearance before and after stirring at 75C for 50% LMF-PAA synthesized with an acetone/EtOH solvent (top) and the PXRD patterns for dried slurries after synthesis. Sharp peaks for 75% DL indicate that acetone cannot successfully replace DCM at very high DLs but is sufficient up to at least 50% DL.

synthesis. Should these ASDs show comparable performance under these conditions, longer-scale dissolution in biorelevant media like SGF may then be performed to ensure equivalent apparent solubility. If promising, other previously investigated drug-polymer systems may be tested using an acetone/ethanol slurry solvent, however it should be noted that highly detailed

dissolution data for all of these systems is not yet available for direct comparison as in the case of LMF-PAA.

As shown in Chapters 2 and 4, the ability of SC to facilitate reaction equilibrium for a variety of basic drugs prepared with PAA is a promising result, particularly given the range of basic strengths represented. Interestingly, even for a stronger base like LMF (pKa ~9), most DLs have a population of unprotonated LMF molecules that are still amorphous and remain so even after long-term storage under high temperature and humidity. CFZ-PAA is the exception to this rule, where 100% protonation is required for full amorphization; a partially neutral CFZ-PAA formulation will also be partially crystalline. This raises the question: what is the mechanism underlying LMF stabilization even in the absence of salt formation with PAA? It is possible that these "extra" LMF molecules are able to access weaker, less rigid interactions with PAA (i.e. hydrogen bonding) or they may simply be kinetically immobilized in the polymer matrix as in the case of a more conventional ASD based on a neutral polymer like PVP. To probe this, an analytical method capable of elemental mapping with high resolution may be employed. While XPS has been previously used under the assumption of a uniform sample obtained after grinding, the high sensitivity and resolution of XPS has been used in other cases to perform 2D mapping of sample surfaces with detailed binding state information.[4] This technique may permit a better understanding of the solid amorphous material generated after drying. Rather than directly dried in bulk as a solution immediately after "clearing," this clear solution should instead be spread on a suitable substrate as a thin film and dried in this state to generate a flat surface that represents the "natural" state of the glassy solid generally produced after vacuum drying. 2D mapping using XPS can then be performed on this dried film to 1) spatially and visually assess the distribution of protonated LMF molecules and 2) determine the binding state of non-protonated LMF molecules based on their binding energy shift: a lesser extent relative to protonated LMF suggesting hydrogen bonding, and a lack of shift indicating fully neutral LMF molecules.

The nature of the drug-polymer interaction present in drug-PAA dispersions with weak basicity is also of interest for further study. Unlike an aliphatic amine like LMF, an amide such as carbamazepine is expected to be minimally protonated, if at all. However, N spectra obtained from XPS for CBZ-PAA ASDs show a degree of peak shift, indicating a population of N atoms at a higher binding energy. Whether or not this corresponds to true protonation is uncertain, as

amides are known to be very weak bases. To better understand the nature of this interaction, CBZ can instead be prepared as an ASD with a nonionic polymer with hydrogen bonding capabilities. CBZ-PVPVA is a promising candidate for this purpose, due to the demonstrated compatibility of PVPVA with SC. These CBZ-PVPVA ASDs may then be compared (at an identical DL) to CBZ-PAA, using XPS to generate high-resolution N spectra for both. Should the two ASDs show peak shift of a similar magnitude, drug-polymer interaction limited to hydrogen bonding is likely. If the degree of peak shift is different (i.e. + 2 eV for CBZ-PAA and + 1 eV for CBZ-PVPVA), this raises the possibility of a low degree of protonation facilitated by SC.

## 6.2 Modified release of amorphous drug-polymer salts

In Chapter 5, we focus on the release behavior in 0.1% sodium dodecyl sulfate (SDS) in water from a variety of LMF-based ASDs. We find that PAA outperforms other polymers in releasing LMF as nanoparticles and reaching a high apparent solubility (AS), measured after filtration through a 0.2 μm filter. This outperformance of PAA over 9 other dispersion polymers (7 acidic and 2 neutral) persists from 25 to 50% DL, both releasing the greatest amount of LMF and producing the largest volume fraction of small-size (~10 nm) particles. These findings are especially notable considering the high degree of solid-state stability of these same LMF-PAA formulations, showing that if the solubility of a formulation is defined to include both true solubility and apparent solubility (of dispersed nanoparticles), an amorphous drug-polymer salt can be simultaneously stable and soluble. PAA's superior performance in this study suggests its potential viability as a new dispersion polymer and motivates further exploration of its dispersion capabilities.

Polyelectrolyte formulations have been shown to be both ionic strength and pH-responsive, increasing drug release rate in response to targeted sections of the GI tract or through the use of salt and pH modifiers within the formulation itself. This suggests that PAA's particle formation behavior can be influenced by excipients in the chosen aqueous medium and may even be tunable. Previous work has shown that PAA can induce changes in drug release from polyvinylidene fluoride (PVDF) depending on the local ionic strength,[5] suggesting that amorphous salts prepared with PAA may also display ionic strength-dependent drug release. This

can be first tested in SGF, as it is already formulated with sodium chloride (NaCl) as a component (2.5 g/L) which can be easily adjusted to modify the ionic strength of the solution. In normal SGF, the ionic concentrations of the included species (NaCl, sodium dodecyl sulfate (SDS, HCl) yield an ionic strength of approximately 0.05 mol/L. To test the effect of ionic strength on LMF-PAA dissolution in SGF, the ionic strength may be increased to approximately 0.075 and 0.1 mol/L by adding an additional 1.5 g and 3 g NaCl, respectively. The resulting colloids or solutions generated under each of these conditions may then be analyzed for a) [LMF] using UV-Vis, b) particle formation and particle size via DLS as described in Chapter 5, and c) if formed, particle stability against aggregation. Should the adjustment of ionic strength prove beneficial, this can inform the design of more potent formulations through the inclusion of inorganic salts to ensure maximized release via a target ionic strength.

Similar to the influence of ionic strength, pH is also known to affect the behavior of polyelectrolytes like PAA in solution. This may be capitalized on instead of or in addition to ionic strength modulation. Basic APIs like LMF are expected to show decreased solubility in neutral-pH environments like the intestinal tract, and thus may benefit from locally modified pH to enhance release. The formation of LMF-PAA particles can first be evaluated as a function of pH with testing conditions that encompass the full biological range (pH ~2 to pH~8), with tests for both particle size and [LMF] performed as described above. Should a significant effect be identified at low pH, these LMF-PAA formulations can then be evaluated in the presence of a dissolved acidic pH modifier like citric acid, with the performance compared to that observed in the absence of this species. If promising, these pH-modifiers may be explored as an excipient included in the solid formulation, but it is important to note that this may interfere with LMF-PAA salt formation and thus negatively affect solid-state stability, observable via a decrease in $T_g$ measured via DSC and/or more rapid LMF crystallization over time.

The LMF-PAA dispersion behavior is also highly notable due to the large volume fraction of particles generated at very small size (~10 nm). This result is intriguing and deserving of further study to enhance our understanding of these unique particles and their ability to provide exceptional LMF release. To better visualize these particles and help verify their size, nanoparticle tracking analysis (NTA) could be used to observe these particles in their native solution state. If unsuitable or ineffective for this purpose, cryogenic transmission electron

microscopy (cryo-TEM) may instead be employed.[6] Zeta potential measurements could also be used to obtain additional chemical information about the particles, as the assembly of surfactants and/or dissolved polymer is detectable as a change in the zeta potential.[7]

## 6.3. References

[1] Guidance for Industry, Q3C Impurities: Residual Solvents, U.S. Food and Drug Administration, Rockville, Maryland, December 1997.
[2] Constable, D. J. C.; Jimenez-Gonzalez, C.; Henderson, R. K. Perspective on Solvent Use in the Pharmaceutical Industry. *Organic Process Research & Development* **2007**, *11* (1), 133–137. https://doi.org/10.1021/op060170h.
[3] Sakai, T.; Morita, Y.; Wakui, C. Biological Monitoring of Workers Exposed to Dichloromethane, Using Head-Space Gas Chromatography. *Journal of Chromatography B* **2002**, *778* (1-2), 245–250.
[4] Friedman, A. K.; Shi, W.-Q.; Losovyj, Y. B.; Siedle, A. R.; Baker, L. A. Mapping Microscale Chemical Heterogeneity in Nafion Membranes with X-Ray Photoelectron Spectroscopy. **2018**, *165*(11), H733–H741. https://doi.org/10.1149/2.0771811jes.
[5] Järvinen, K., Åkerman, S., Svarfvar, B. et al. Drug Release from pH and Ionic Strength Responsive Poly(acrylic acid) Grafted Poly(vinylidenefluoride) Membrane Bags In Vitro. *Pharm Res* **1998**, 15, 802–805.
[6] Jara, M. O.; Warnken, Z. N.; Sahakijpijarn, S.; Thakkar, R.; Kulkarni, V. R.; Christensen, D. J.; Koleng, J. J.; Williams, R. O. Oral Delivery of Niclosamide as an Amorphous Solid Dispersion That Generates Amorphous Nanoparticles during Dissolution. *Pharmaceutics* **2022**, *14* (12), 2568. https://doi.org/10.3390/pharmaceutics14122568.
[7] Correa, C. E.; Gao, Y.; Indulkar, A. S.; Ueda, K.; Zhang, Z.; Taylor, L. S. Impact of Surfactants on the Performance of Clopidogrel-Copovidone Amorphous Solid Dispersions: Increased Drug Loading and Stabilization of Nanodroplets. *Pharmaceutical Research* **2022**, *39* (1), 167–188. https://doi.org/10.1007/s11095-021-03159-w.